USGS
science for a changing world

Occurrence Model for Magmatic Sulfide-Rich Nickel-Copper-(Platinum-Group Element) Deposits Related to Mafic and Ultramafic Dike-Sill Complexes

Scientific Investigations Report 2010–5070–I

U.S. Department of the Interior
U.S. Geological Survey

COVER. Ferrar dikes and sills intruding Beacon sandstones, Finger Mountain, Dry Valleys, Antarctica. Photograph by Dean Peterson, Duluth Metals Limited.

Occurrence Model for Magmatic Sulfide-Rich Nickel-Copper-(Platinum-Group Element) Deposits Related to Mafic and Ultramafic Dike-Sill Complexes

By Klaus J. Schulz, Laurel G. Woodruff, Suzanne W. Nicholson, Robert R. Seal II, Nadine M. Piatak, Val W. Chandler, and John L. Mars

Chapter I of
Mineral Deposit Models for Resource Assessment

Scientific Investigations Report 2010–5070–I

U.S. Department of the Interior
U.S. Geological Survey

U.S. Department of the Interior
SALLY JEWELL, Secretary

U.S. Geological Survey
Suzette Kimball, Acting Director

U.S. Geological Survey, Reston, Virginia: 2014

Suggested citation:
Schulz, K.J., Woodruff, L.G., Nicholson, S.W., Seal, R.R., II, Piatak, N.M., Chandler, V.W., and Mars, J.L., 2014, Occurrence model for magmatic sulfide-rich nickel-copper-(platinum-group element) deposits related to mafic and ultramafic dike-sill complexes: U.S. Geological Survey Scientific Investigations Report 2010–5070–I, 80 p., *http://dx.doi.org/10.3133/sir20105070I*.

ISSN 2328-0328 (online)

Contents

Figures

Tables

Conversion Factors

SI to Inch/Pound

Multiply	By	To obtain
	Length	
centimeter (cm)	0.3937	inch (in.)
millimeter (mm	0.03937	inch (in.)
meter (m)	3.281	foot (ft)
kilometer (km)	0.6214	mile (mi)
	Area	
square kilometer (km^2)	247.1	acre
square kilometer (km^2)	0.3861	square mile (mi^2)
	Volume	
liter (L)	33.82	ounce, fluid (oz)
liter (L)	2.113	pint (pt)
liter (L)	1.057	quart (qt)
liter (L)	0.2642	gallon (gal)
cubic kilometer (km^3)	0.2399	cubic mile (mi^3)
	Mass	
gram (g)	0.03527	ounce, avoirdupois (oz)
milligram (mg)	3.527×10^{-5}	ounce, avoirdupois (oz)
kilogram (kg)	2.205	pound avoirdupois (lb)

Abbreviations Used in This Report

g/L	gram per liter
$\mu g/L$	microgram per liter
mg/L	milligram per liter
mg/kg	milligrams per kilogram
%	percent
‰	per mil
ε_{Nd}	epsilon neodymium
ε_{Sr}	epsilon strontium
$\delta^{18}0$	delta O-18
$\delta^{34}S$	delta S-34
γ_{Os}	gamma osmium
Al	aluminum
Ag	silver
As	arsenic
Au	gold
Ba	barium
Bi	bismuth
Cd	cadmium
Co	cobalt
Cr	chromium
Cu	copper
Fe	iron
Ga	Giga-annum; age in billions of years
Hg	mercury
Ir	iridium
IPGE	iridium-group PGEs (Os-Ir-Ru)
K	potassium
km	kilometers
La	lanthanum
LIP	large igneous province
m	meters
Mg	magnesium
MgO	magnesium oxide
MORB	mid-ocean ridge basalt
Ma	Mega-annum; age in millions of years
Mt	million metric tons
My	million years
Mkm^2	million square kilometers
Mkm^3	million cubic kilometers
NAP	net acidizing potential
Nb	niobium
Nd	neodymium
Ni	nickel

NNP	net-neutralizing potential
O	oxygen
Os	osmium
P	phosphorus
Pb	lead
Pd	palladium
PGE	platinum-group elements
PPGE	platinum-group PGEs (Rh-Pt-Pd)
Pt	platinum
ppb	parts per billion
Re	rhenium
REE	rare earth elements
Rh	rhodium
Ru	ruthenium
S	sulfur
Sb	antimony
Se	selenium
Sm	samarium
Sr	strontium
t	metric tons
Ta	tantalum
Te	tellurium
Th	thorium
Ti	titanium
V	vanadium
Yb	ytterbium
Zn	zinc

Occurrence Model for Magmatic Sulfide-Rich Nickel-Copper-(Platinum-Group Element) Deposits Related to Mafic and Ultramafic Dike-Sill Complexes

By Klaus J. Schulz,[1] Laurel G. Woodruff,[2] Suzanne W. Nicholson,[1] Robert R. Seal II,[1] Nadine M. Piatak,[1] Val W. Chandler,[3] and John L. Mars[1]

1. Introduction

Overview

Magmatic sulfide deposits containing nickel (Ni) and copper (Cu), with or without (±) platinum-group elements (PGE), account for approximately 60 percent of the world's nickel production (Naldrett, 2004). Most of the remainder of the Ni production is derived from lateritic deposits, which form by weathering of ultramafic rocks in humid tropical conditions (Elias, 2002; Freyssinet and others, 2005). Magmatic Ni-Cu±PGE sulfide deposits are spatially and genetically related to bodies of mafic and/or ultramafic rocks. The sulfide deposits form when the mantle-derived mafic and/or ultramafic magmas become sulfide-saturated and segregate immiscible sulfide liquid, commonly following interaction with continental crustal rocks (Arndt and others, 2005).

Deposits of magmatic Ni-Cu sulfides occur with mafic and/or ultramafic bodies emplaced in diverse geologic settings. They range in age from Archean to Tertiary, but the largest number of deposits are Archean and Paleoproterozoic (Eckstrand and Hulbert, 2007). Although deposits occur on most continents, ore deposits (deposits of sufficient size and grade to be economic to mine) are relatively rare; major deposits are present in Russia, China, Australia, Canada, and southern Africa (fig. 1–1). Nickel-Cu sulfide ore deposits can occur as single or multiple sulfide lenses within mafic and/or ultramafic bodies with clusters of such deposits comprising a district or mining camp. Typically, deposits contain ore grades of between 0.5 and 3 percent Ni and between 0.2 and 2 percent Cu (Eckstrand and Hulbert, 2007). Tonnages of individual deposits range from a few tens of thousands to tens of millions of metric tons (Mt) bulk ore (Barnes and Lightfoot, 2005). Two giant Ni-Cu districts, with ≥10 Mt Ni, dominate world Ni sulfide resources and production (fig. 1–2). These are the Sudbury district, Ontario, Canada, where sulfide ore deposits are at the lower margins of a meteorite impact-generated igneous complex and contain 19.8 Mt Ni; and the Noril'sk-Talnakh district, Siberia, Russia, where the ore deposits are in subvolcanic mafic intrusions related to flood basalts and contain 23.1 Mt Ni (Eskstrand and Hulbert, 2007). In the United States, the Duluth Complex in Minnesota, comprised of a group of mafic intrusions related to the 1.1 Ga Midcontinent Rift system, represents a major Ni resource of 8 Mt Ni, but deposits generally exhibit low grades (0.2 percent Ni, 0.66 percent Cu) and remain in the process of being proven economic.

The sulfides in magmatic Ni-Cu deposits generally constitute a small volume of the host rock(s) and tend to be concentrated in the lower parts of the mafic and/or ultramafic bodies, often in physical depressions or areas marking changes in the geometry of the footwall topography (Barnes and Lightfoot, 2005). In most deposits, the sulfide mineralization can be divided into disseminated, matrix or net, and massive sulfide, depending on a combination of the sulfide content of the rock and the silicate texture. The major Ni-Cu sulfide mineralogy typically consists of an intergrowth of pyrrhotite (Fe_7S_8), pentlandite ($[Fe, Ni]_9S_8$), and chalcopyrite ($FeCuS_2$). Cobalt, PGE, and gold (Au) are extracted from most magmatic Ni-Cu ores as byproducts, although such elements can have a significant impact on the economics in some deposits, such as the Noril'sk-Talnakh deposits, which produce much of the world's palladium. In addition, deposits may contain between 1 and 15 percent magnetite associated with the sulfides (Barnes and Lightfoot, 2005).

Scope

A number of schemes have been used to subdivide magmatic Ni-Cu±PGE sulfide deposits, with most based on sulfide compositions, tectonic settings, and petrologic characteristics of

[1] U.S. Geological Survey, Reston, Virginia

[2] U.S. Geological Survey, Mounds View, Minnesota

[3] Minnesota Geological Survey, St. Paul, Minnesota

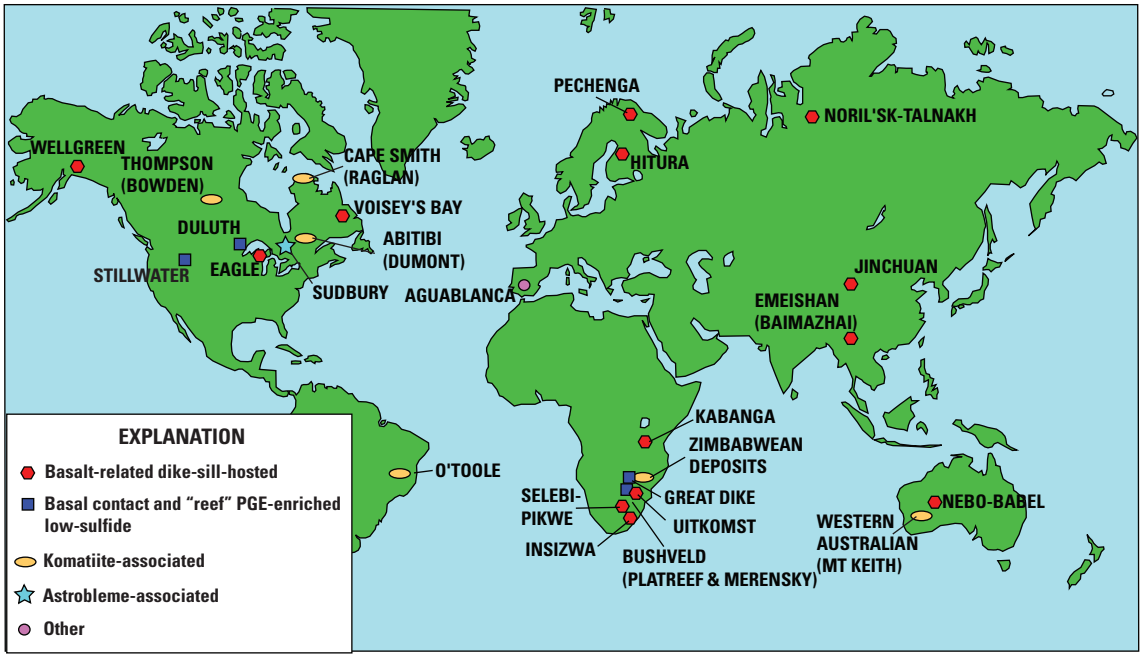

Figure 1–1. Locations of some of the world's major nickel and platinum-group element (PGE) mining camps and types of deposits.

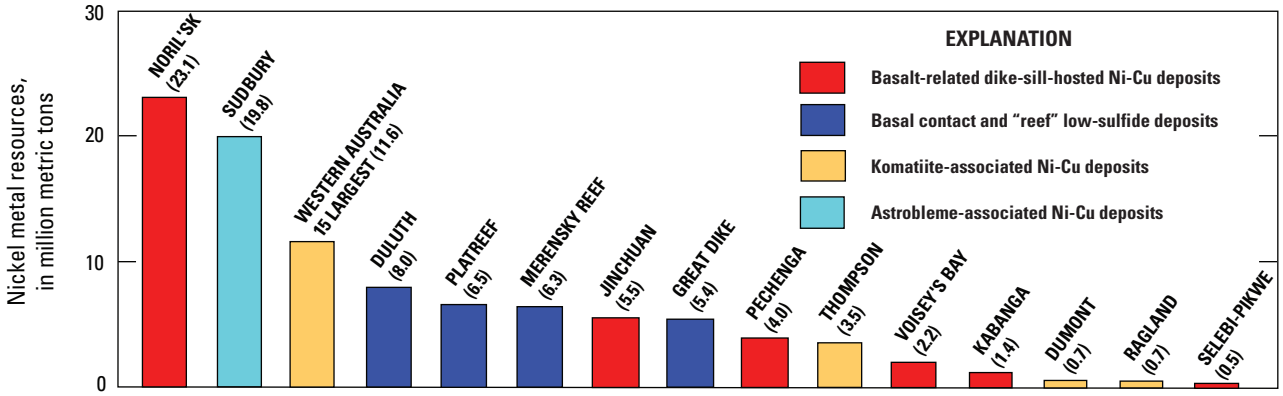

Figure 1–2. Histogram comparing the total nickel metal resources for the fifteen largest deposits worldwide. Numbers are in millions of metric tons. Figure modified from Hoatson and others (2006).

the mafic and/or ultramafic rocks that host the deposits (Page, 1986a–f; Naldrett, 1989, 1997, 2004; Eckstrand, 1995; Lesher and Keays, 2002; Lesher, 2004; Barnes and Lightfoot, 2005; Hoatson and others, 2006). Based on their principal metal production, however, magmatic sulfide deposits are best divided into two major types (Naldrett, 2004). The first are sulfide-rich, typically with 10 to 90 percent sulfide minerals, and which have economic value primarily because of their Ni and Cu content. Second are those that are sulfide-poor, typically with 0.5 to 5 percent sulfide minerals, and exploited principally for PGE.

The sulfide-rich Ni-Cu±PGE deposits can be further subdivided into two compositional groups on the basis of their Ni/Cu ratios (Barnes and Lightfoot, 2005). Deposits in the first subgroup have Ni/Cu ratios in the range of 0.8 to 2.5 and Ni concentrations (concentrations calculated in 100 percent sulfides) ranging from 1 to 6 percent (Barnes and Lightfoot, 2005). With the exception of the deposits in the Sudbury district, Canada, which are related to a meteorite-impact-generated melt sheet, these deposits are associated with small- to medium-sized differentiated mafic and/or ultramafic dikes and sills related mostly to tholeiitic basalt magmas emplaced in continental settings. In addition, most of the major Ni deposits in this subgroup, including the three largest producing Ni-Cu sulfide camps after Sudbury (Noril'sk-Talnakh, Russia; Jinchuan, China; and Voisey's Bay, Canada; Eckstrand and Hulbert, 2007) are related to dynamic magmatic systems and occur in intrusions that served as magma conduits (Naldrett,

1999; Maier and others, 2001). Deposits in the second subgroup have Ni/Cu ratios greater than 3 and Ni concentrations (in 100 percent sulfides) generally in the range of 6 to 18 percent (Barnes and Lightfoot, 2005). Those deposits mostly are hosted by komatiitic lava flows, dikes and sills (for example, Mt. Keith, Australia; Raglan and Dumont, Canada). The deposits in the Pechenga Camp in the Kola Peninsula, Russia, however, are hosted by ferropicrite-related intrusions (Brügmann and others, 2000; Barnes and others, 2001).

The sulfide-poor deposits generally occur as sparsely dispersed sulfide minerals in basal units or stratabound layers or reefs in very large to medium-sized, typically layered mafic/ultramafic intrusions (for example, Platreef and Merensky Reef, Bushveld Complex, South Africa; J-M Reef, Stillwater Complex, Montana, United States; Duluth Complex, Minnesota, United States). These low-sulfide PGE-enriched deposits are not included in this deposit model.

Purpose

This deposit model is intended primarily to provide the basis for assessing the occurrence of undiscovered, potentially economic magmatic sulfide-rich Ni-Cu±PGE deposits in the United States. The strategy employed by the U.S. Geological Survey (USGS) in quantitative mineral-resource assessments (Singer, 1993, 2007) consists of (1) delineating tracts permissive for the occurrence of undiscovered magmatic Ni- and Cu-bearing sulfide deposits, (2) estimating the amount of metal and some ore characteristics by means of appropriately selected grade and tonnage models, and (3) estimating the number of undiscovered deposits by deposit type. Thus, it is critical to the assessment methodology to have accurate and reliable data on the major characteristics of magmatic sulfide-rich Ni-Cu±PGE deposits, particularly host lithology, tectonic setting, structure, age, ore-gangue-alteration mineralogy, geochemical and geophysical signatures, theory of deposit formation, and geoenvironmental features.

Because the purpose of this model is to facilitate the assessment for undiscovered, magmatic sulfide-rich Ni-Cu±PGE deposits in the United States, this model addresses only those sulfide-rich deposits of economic significance likely to occur in the United States based on known geology. These primarily are deposits hosted by small- to medium-sized mafic and/or ultramafic dikes and sills related to picrite and tholeiitic basalt magmatic systems generally emplaced in large igneous provinces (LIPs). The deposits in the Sudbury district are not included because they are associated with a unique meteorite impact-related melt sheet (Keays and Lightfoot, 2004; Naldrett, 2004; Ames and Farrow, 2007). There is no evidence for similar sulfide deposits being associated with any other impact structure elsewhere in the world. Also not included are the deposits associated with komatiite lava flows, dikes, and sills (Lesher and Keays, 2002). Although these deposits are an important source for nickel, particularly in Australia, Canada, and Zimbabwe, komatiites are rare in the United States and have not proven to be prospective for significant nickel sulfide mineralization.

Although this report does not focus on the magmatic Ni-Cu sulfide deposits at Sudbury or those related to komatiites, those sulfide deposits have been studied extensively and share many similarities with the deposits related to picrite and tholeiitic basalt dike-sill complexes. Therefore, reference to the Sudbury and komatiite-related deposits is made where appropriate.

2. Deposit Type and Associated Deposits

Name and Synonyms

The deposits described in this model are referred to here as magmatic sulfide-rich Ni-Cu±PGE deposits related to mafic and/or ultramafic dike-sill complexes. The name emphasizes the relation of these Ni-Cu sulfide-rich deposits to mafic and ultramafic rocks derived from picrite and tholeiitic basalt magmas and to mostly small- to medium-sized dikes and sills as opposed to the generally much larger layered mafic-ultramafic intrusive complexes that typically host sulfide-poor PGE-enriched deposits (for example, the Stillwater Complex, Montana). A variety of other names have been applied to these deposits in the literature that generally emphasize aspects of mineralization style, tectonic setting, and/or lithology of the host rocks. Names include tholeiitic basal segregation type, gabbroid-associated layered intrusive type, mafic-ultramafic intrusion-hosted type, flood-basalt-related type, and feeder/conduit-type deposits (Barnes and Lightfoot, 2005; Eckstrand and Hulbert, 2007). In addition, deposits have been named after giant deposits of that respective type, such as Noril'sk-type and Voisey's Bay-type deposits (Page, 1986c; Schulz and others, 1998).

Brief Deposit Description

These magmatic sulfide deposits are significant producers of Ni and Cu resources, primarily from deposits in Russia (Noril'sk-Talnakh, Pechenga), Canada (Voisey's Bay), and China (Jinchuan). In addition, the Noril'sk-Talnakh deposits are the world's largest producer of palladium. These sulfide deposits form when mantle-derived, sulfur-undersaturated picrite or tholeiitic basalt magma becomes sulfide-saturated, commonly following interaction with continental crustal rocks. Sulfur saturation results in formation of an immiscible sulfide liquid. The sulfide liquid tends to segregate into physical depressions or other areas in the lower parts of dike- and/or sill-like intrusions because of changes in the magma flow dynamics. Economic deposits appear to be associated almost

exclusively with dynamic magmatic systems that experience repeated surges of magma. Such dynamic systems appear to promote the interaction of sulfide liquid with a sufficiently large amount of silicate magma to concentrate chalcophile elements to economic levels.

The tectonic setting of these magmatic sulfide deposits principally is flood-basalt-dominated LIPs, generally attributed to the upwelling and melting of a buoyant mantle plume beneath crustal lithosphere (Condie, 2001). The sulfide deposits and their host intrusions range in age from Archean to at least Middle Jurassic. They generally are found close to deeply penetrating faults that allow for the efficient transport of sulfur-undersaturated magma from the mantle to relatively shallow crustal depths. Sulfur-bearing crustal rocks such as black shales, evaporates, or paragneisses are proximal to many deposits and a potential source of sulfur. Deposits are hosted by a wide range of typically olivine-bearing mantle-derived rocks related to ferropicrite (Pechenga), tholeiitic picrite (Noril'sk-Talnakh), and high-aluminum basalt (Voisey's Bay). No known economic deposits are associated with mid-ocean ridge basalts (MORB), ophiolites, or alkaline rocks.

The principal sulfide minerals in most sulfide-rich Ni-Cu±PGE deposits consist of intergrown pyrrhotite, pentlandite, and chalcopyrite. Cobalt (Co) is found in pentlandite, and PGE generally appear as small grains of PGE-bearing sulfides, arsenides, antimonides, bismithides, and tellurides. Deposits also locally contain 1 to 15 percent magnetite (Barnes and Lightfoot, 2005). The largest concentrations of sulfide minerals tend to occur either at the base of the host intrusion or in the immediate footwall. The sulfides generally are present as disseminated, matrix or net, and massive sulfide, based on a combination of the sulfide content and silicate texture of the rock. In most cases the massive and matrix ore is zoned, with Cu-rich zones relatively enriched in gold (Au), palladium (Pd), and platinum (Pt). Those zones, as footwall dikes and veins, either overlie or are separated from Cu-poor zones relatively enriched in osmium (Os), iridium (Ir), ruthenium (Ru), and rhodium (Rh). The compositional zonation is attributed to fractionation of monosulfide solid solution (MSS) from a sulfide liquid (Naldrett, 2004).

Associated Deposit Types

Magmatic sulfide-rich Ni-Cu±PGE deposits can occur with numerous other magmatic ore deposits. These include low-sulfide, contact-type and reef-type PGE deposits, chromite deposits, and Fe-Ti-V deposits. In addition, secondary processes can affect the sulfide deposits, producing asbestos, soapstone, Ni-laterite, and native-copper deposits.

Primary and Byproduct Commodities

In sulfide-rich Ni-Cu±PGE deposits, Ni constitutes the main economic commodity, with grades typically about 0.5 to 3 percent. The range of Ni grades and tonnages for some known deposits are compared with other types of Ni deposits in figure 2–1. Copper may be either a coproduct or byproduct, and Co, PGE, and Au typically are byproducts. The atypical enrichment of PGE in the Noril'sk-Talnakh deposits results in PGE as a significant coproduct. Other commodities recovered, in some deposits, include silver (Ag), sulfur (S), selenium (Se), and tellurium (Te). In addition, sulfide minerals may contain anomalous arsenic (As), bismuth (Bi), mercury (Hg), lead (Pb), antimony (Sb), and zinc (Zn), which can contribute to environmental contamination.

Example Deposits

There are relatively few sulfide-rich Ni-Cu±PGE deposits related to mafic and/or ultramafic dike-sill complexes currently recognized around the world. Selected representatives are presented in table 2–1, along with some of their general characteristics. The Eagle deposit in northern Michigan, discovered in 2002 and currently under development by Kennecott Minerals Company, is the only economic deposit of this type currently known in the United States.

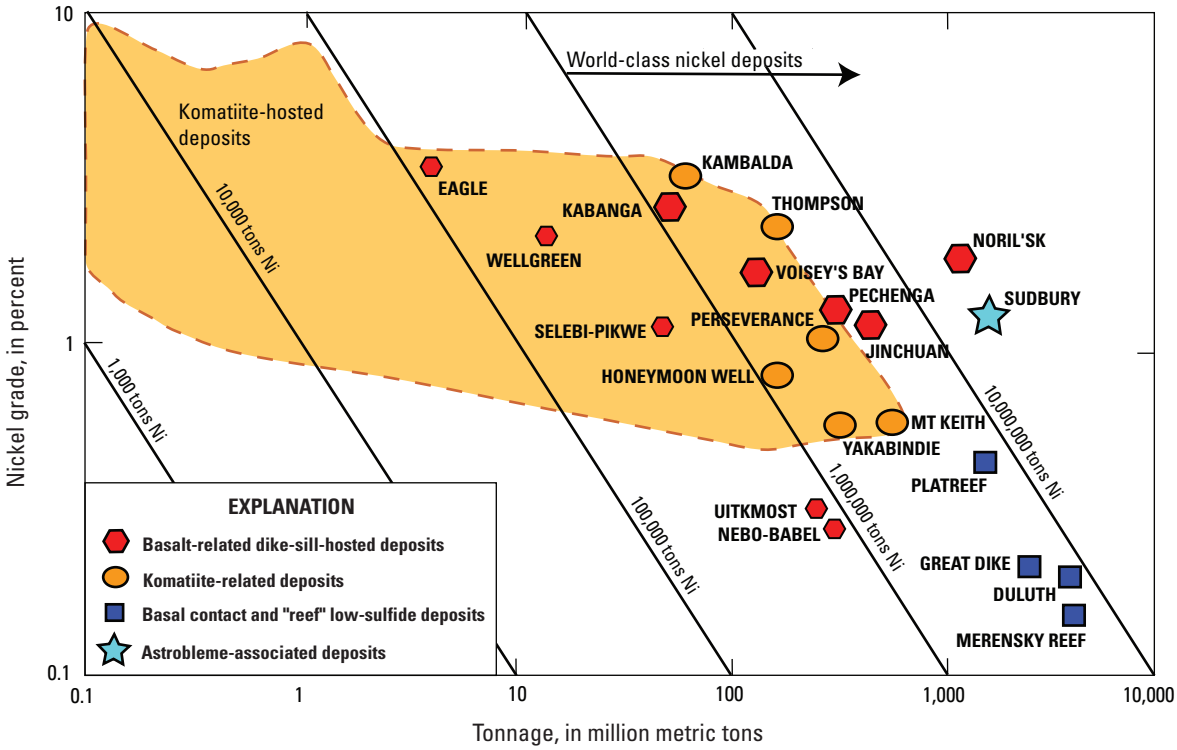

Figure 2–1. Nickel grade versus total ore tonnage for some nickel sulfide and PGE deposits of the world. Diagonal lines indicate the contained nickel metal amount in tons. World-class deposits (greater than 1 million metric tons [Mt] Ni metal) are shown by large symbols. Field in orange shows range for komatiite-hosted Ni sulfide deposits; world-class deposits are labeled.

Table 2–1. Examples of Ni-Cu±PGE deposits hosted by mafic and/or ultramafic dike-sill complexes.

[Ma, million years; Mt, million metric tons; t, metric ton; wt, weight; %, percent]

Deposit	Location	Discovered	Age (Ma)	Size (Mt)	Ni (wt. %)	Cu (wt. %)	Contained Ni (t)	Reference
Noril'sk (N) Talnakh (T)	Siberian Platform, Russia	~1926 (N) 1960 (T)	251±0.3	1309.3	1.77	3.57	23,174,610	Naldrett, 2004
Jinchuan	Sino-Korean Craton, China	1958	831.8±0.6	515.0	1.06	0.67	5,459,000	Zhang and others, 2010 Chai and Naldrett, 1992
Pechenga	Baltic Shield, Kola Peninsula, Russia	1912	1977±55	339.0	1.18	0.4	4,000,200	Barnes and others, 2001 Hanski and others, 1990
Voisey's Bay	Torngat orogen, Labrador, Canada	1993	1333±1	136.7	1.59	0.85	2,173,530	Naldrett, 2004 Amelin and others, 1999
Kabanga	Kibaran Orogenic Belt, Tanzania	1975	1275	58.2	2.62	0.33	1,524,000	Maier and others, 2010 Duchesne and others, 2004
Wellgreen	Quill Creek ultramafic complex, Alaska	1952	232	14.3	2.23	1.39	1,199,000	Schmidt and Rogers, 2007
Nebo-Babel	Giles complex, Musgrave province, Australia	2000	1078±3	330	0.3	0.3	990,000	Hoatson and others, 2006 Seat and others, 2007 and 2009
Uitkomst	Bushveld complex, South Africa	1975	2054	271.7	0.34	0.135	913,000	Maier and others, 2004
Insizwa	Mount Ayliff complex, South Africa	1865	183	0.47	0.3	0.25		Maier and others, 2002
Eagle	Baraga basin, Michigan, United States	2002	1107.2±5.7	3.67	3.57	2.9	131,019	Ding and others, 2010

3. Historical Evolution of Descriptive and Genetic Knowledge and Concepts

The history of understanding of magmatic Ni-Cu±PGE sulfide deposits has been reviewed most recently by Papunen (1991) and Naldrett (2005) and is briefly summarized here. Unlike other commodities such as iron and copper, which have long been known and extracted, the element Ni was only first identified in 1751 by the Swedish chemist Cronstedt, who separated the new metal from cobalt ores from the Los mine in Sweden (Howard-White, 1963). The earliest mining of Ni did not begin until 1848, shortly after a new Fe-Ni sulfide mineral, pentlandite, was discovered at the old Espendalen copper mine in Norway (Boyd and Nixon, 1985). Nickel production from the Espendalen deposit was soon followed by the discovery and mining of several other sulfide deposits in southern Norway, and by 1876, Norwegian production peaked at 360 metric tons (t) per year (Howard-White, 1963). Norway's position as the world's leading nickel producer was superseded in the 1880s by production of nickel from laterite deposits in New Caledonia. With discovery of the giant Sudbury Ni-Cu sulfide deposits in1883, however, Canada soon became the world's leading nickel producer, dominating the market through much of the twentieth century. Today, Russia has overtaken Canada as the world's leading nickel producer (Kuck, 2010).

Concepts of the origin of magmatic Ni-Cu±PGE sulfide deposits have been influenced strongly by studies of the Sudbury deposits (fig. 3–1). These concepts fall mostly into two opposing interpretations, one emphasizing a magmatic origin and the other a hydrothermal origin. As early as 1891, Bell (1891a) proposed that the Sudbury ores were the result of the separation and settling of a dense sulfide liquid during differentiation of the magma that gave rise to the Sudbury Igneous Complex (SIC). This conclusion was supported by Barlow (1906), who recognized (1) two principal units in the SIC, a lower noritic layer and an overlying granophyric layer; and (2) the occurrence of the ore bodies in embayments along the lower contact of the norite. Coleman (1905, 1913) subsequently showed that SIC extended around the whole of the recognized Sudbury basin (Bell, 1891b) and argued that the SIC had been emplaced as a sill along the contact between overlying breccias and metasedimentary units and older basement rocks. Further, he argued that the restriction of the sulfide deposits to the outer (that is, lower) contact of the SIC, the intimate mixture of sulfide and norite in all proportions, the lack of hydrothermal alteration, and the occurrence of the largest concentrations of sulfides in embayments along the footwall contact strongly supported the gravitationally induced settling of sulfide liquid from the SIC magma.

The magmatic interpretation was challenged by others studying the Sudbury ores. For example, Dickson (1903) suggested that the ores had been deposited by hot aqueous fluids. A hydrothermal origin also was supported by Knight (1917), based on his observation of the almost universal occurrence of the ores in breccias and of the partial replacement of breccia fragments by sulfides. A subsequent extensive microscopic study of the Sudbury ores by Wandke and Hoffman (1924) also led them to conclude that the deposits were hydrothermal in origin.

As noted by Naldrett (2005), arguments about the magmatic versus hydrothermal origin of the Sudbury ores persisted through most of the first half of the twentieth century, with those mapping and studying the SIC favoring a magmatic origin and those most familiar with the mines favoring a hydrothermal origin. However, with the publication in 1962 of J.E. Hawley's comprehensive study of the Sudbury ores (Hawley, 1962), a strong case was made for the magmatic origin of the sulfide ores with only relatively minor superimposed secondary features that include crystallization of secondary minerals, localized alteration, late hydrothermal mineralization, and local remobilization of ores by both granitic and basaltic intrusions. Since Hawley's work, the magmatic origin of the Sudbury Ni-Cu sulfide deposits has been generally accepted, although a hydrothermal origin for some footwall Cu- and PGE-enriched deposits is still debated (Naldrett, 2004, 2005).

General acceptance of a magmatic origin for Ni-Cu±PGE sulfide ores at Sudbury led to the model that magmatic sulfide ore bodies form along the base of large, layered mafic intrusions owing to gravitational settling of a dense sulfide liquid segregated from the parental magmas upon emplacement. This, in turn, led to exploration for magmatic sulfide deposits along the basal contacts of many large, layered mafic-ultramafic intrusions, which included the Bushveld (South Africa), Duluth (United States), Great Dike (Zimbabwe), Kiglapait (Canada), Muskox (Canada), Skaergaard (Greenland), and Stillwater (United States) intrusions. Although low-grade, mostly disseminated Ni-Cu±PGE sulfide mineralization was discovered along the basal contacts of several of these intrusions (for example, Bushveld, Duluth, Great Dike, Muskox, Stillwater), no economic Ni-Cu±PGE sulfide deposits were discovered.

The apparent lack of success in the discovery of major Ni-Cu±PGE sulfide deposits using the Sudbury model is now generally attributed to the ore-forming processes at Sudbury having been in a large part unique. This uniqueness derives from the now widely accepted interpretation that the Sudbury structure is an astrobleme, as first proposed by Dietz (1964). Therefore, the Sudbury model is not applicable to other layered intrusions formed by normal terrestrial igneous processes. In addition, recent geochemical and isotope studies (Walker and others, 1991; Mungall and others, 2004), as well as thermal modeling (Grieve, 1994), strongly suggest that the entire SIC is the product of an impact-generated melt sheet and that the sulfide ores were derived from in situ melting of pre-existing sulfides in crustal target rocks. Thus, the sulfide deposits likely formed by gravitational settling of a dense immiscible sulfide liquid that segregated from the parental impact melt. There is no evidence of a mantle-derived magma component in the SIC or sulfide deposits (Walker and others, 1991).

Although large, layered mafic-ultramafic intrusions have not proven prospective for economic sulfide-rich Ni-Cu±PGE deposits, important economic deposits of variable sizes have

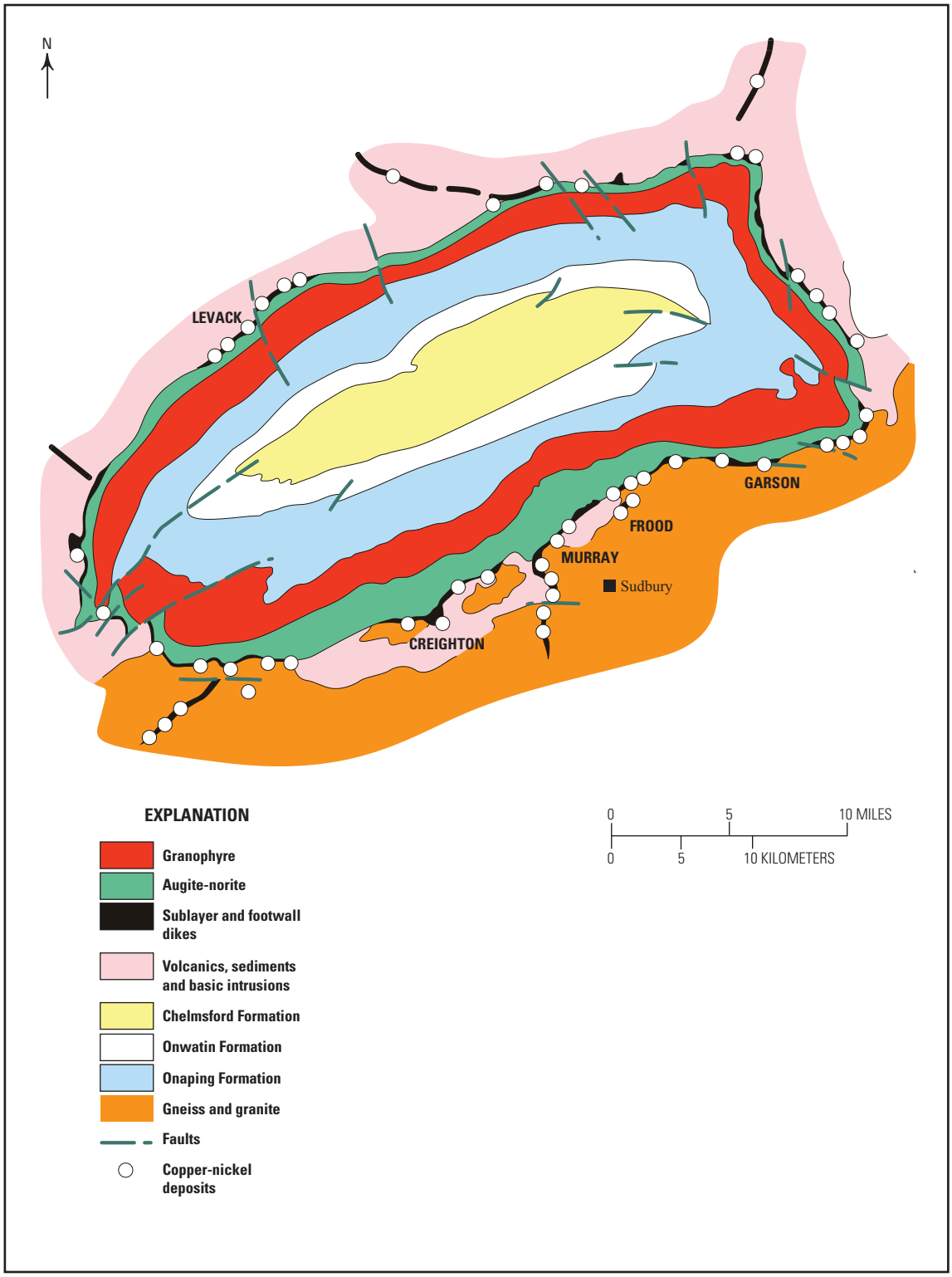

Figure 3–1. Simplified geologic map of the Sudbury, Canada, structure showing the location of major Cu-Ni sulfide deposits. Figure modified from Souch and others (1969).

been found in smaller intrusions, including those in Pechenga (Kola Peninsula, Russia) in 1921, Noril'sk (Siberia, Russia) in 1926, Jinchuan (Gansu Province, China) in 1958, Talnakh (Siberia, Russia) in 1960, Kabanga (Tanzania) in 1976, Uitkomst (South Africa) in the early 1990s, Voisey's Bay (Labrador, Canada) in 1993, and Eagle (Michigan, United States) in 2002. In addition, important Ni sulfide deposits were identified in the Eastern Goldfields region of the Yilgarn Archean craton, Western Australia (Woodall and Travis, 1969) in 1966, in association with sequences of komatiite lavas. These deposits occur mostly at or near the base of the ultramafic sequences, generally within trough-like structures along the contact with underlying metabasalts. Studies of the Ni-Cu±PGE sulfide deposits associated with the smaller mafic-ultramafic intrusions and komatiites since the mid-1960s, along with experimental studies of sulfide and sulfide-silicate systems and improvements in analytical methods, have led to important advances in the understanding of the genesis of these types of sulfide deposits (see Naldrett, 2005). In particular, studies of the Noril'sk-Talnakh and Voisey's Bay deposits in the 1990s led to the recognition of the importance of sulfur-understaturated mafic-ultramafic magmas, crustal contamination, and dynamic magmatic systems in the formation of economic sulfide-rich Ni-Cu±PGE deposits (Naldrett and others, 1995; Naldrett, 1999; Li and others, 2001). As a result, the current model for the formation of these deposits emphasizes magma-conduit systems as the most promising targets because conduits provide an ideal environment for crustal contamination and segregation of any immiscible sulfide liquid entrained in ascending mafic-ultramafic magmas (Maier and others, 2001). Changes in flow dynamics along conduit systems can lead to the deposition of sulfide as massive or highly concentrated bodies of sulfide ore (fig. 3–2). In addition, the sulfide bodies may react with new surges of magma moving along the same conduit, resulting in an increase of the Ni, Cu, and PGE tenor of the ore.

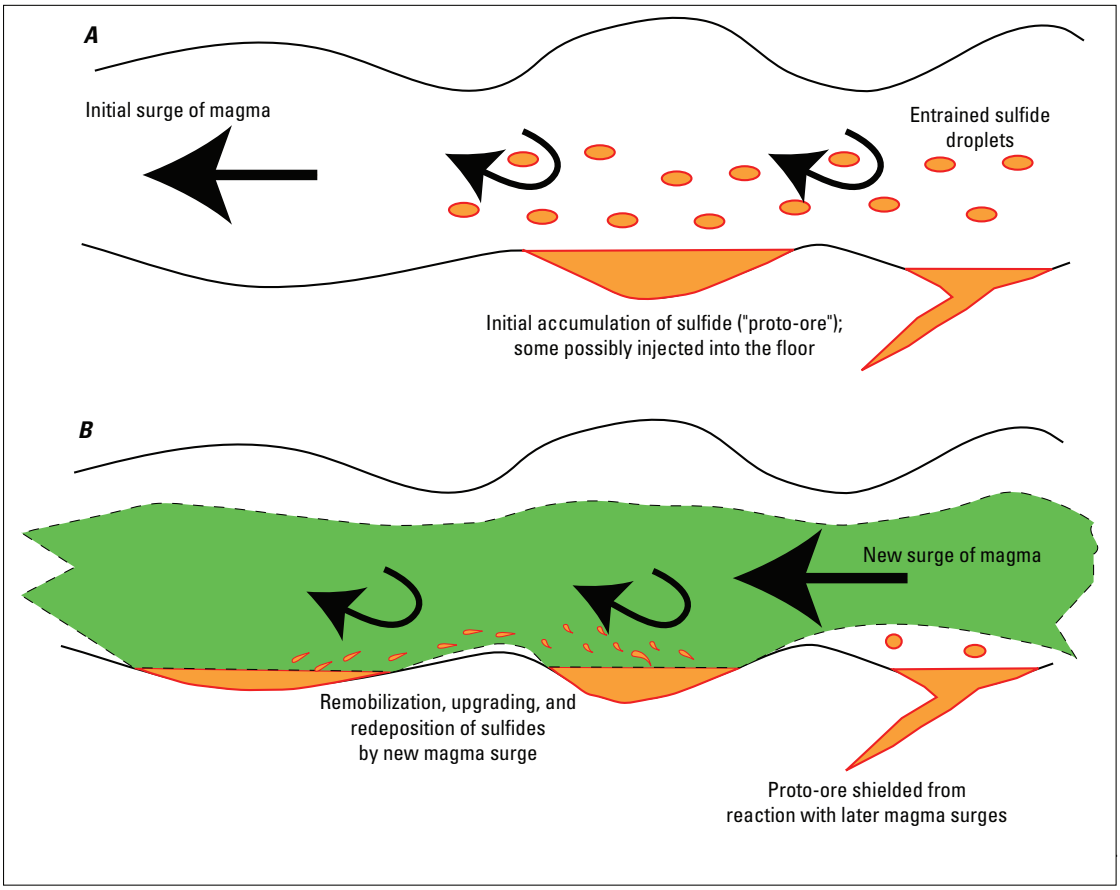

Figure 3–2. Schematic diagram illustrating the continued flow of magma through an idealized magma conduit. *A*, An initial surge of sulfur-saturated magma carries entrained sulfide droplets, which may be deposited along the footwall in widened parts of the conduit to form "proto-ore." In places, sulfide melt may be injected into the footwall. *B*, Continued surges of undepleted magma may stir up previously deposited sulfide melt, upgrading the sulfide in Ni, Cu, and PGE content and reprecipitating it downstream in the conduit. Proto-ores injected into the footwall may remain shielded from later magma surges and from upgrading in metal content. Figure modified from Maier and others (2001).

4. Regional Environment

Geotectonic Environment

The bulk of the world's large magmatic sulfide-rich Ni-Cu±PGE deposits appear to be located near the margins of cratonic blocks, where large volumes of dominantly tholeiitic mafic and lesser ultramafic magma have been emplaced in the crust and erupted on the surface by processes not associated with "normal" spreading ridge or subduction environments (fig. 4–1; Begg and others, 2010). These large igneous provinces (LIPs) are defined (Bryan and Ernst, 2008, p. 177) as:

"magmatic provinces with areal extents greater than 0.1 million km^2, igneous volumes greater than 0.1 million km^3, and maximum lifespans of approximately 50 My that have intraplate tectonic settings or geochemical affinities and are characterized by igneous pulse(s) of short duration (approximately 1–5 My), during which a large proportion (greater than 75 percent) of the total igneous volume has been emplaced."

Examples include continental flood basalts (Deccan, Karoo, Siberian Traps, Columbia River) and volcanic rifted margins (North Atlantic Igneous Province), as well as their plumbing system components (dikes, sills and layered intrusions) (Coffin and Eldholm, 1994). The LIPs in oceanic settings are represented by oceanic plateaus (Ontong-Java) and ocean-basin flood basalts (the Caribbean Flood Basalts) (Coffin and Eldholm, 1994). In addition, giant dike (and sill) swarms (McKenzie dike swarm) and some large layered intrusions (Bushveld) are interpreted as eroded remnants of LIPs (Ernst, 2007). Although LIPs mainly are mafic igneous provinces with generally subordinate ultramafic components, felsic and intermediate igneous rocks produced by fractional crystallization or partial melting of crustal rocks commonly are present and can be locally abundant in continental LIPs. A few continental LIPs are comprised mainly of felsic volcanic rocks, including the Sierra Madre Occidental in Mexico, the Chon Aike province in southern Argentina, and the Gawler province in Australia (Bryan, 2007).

The LIPs can have areal extents greater than one million km^2 and volumes greater than one million km^3 (Courtillot and Renne, 2003). The largest continental LIP, the Siberian Traps in Russia, which hosts the Noril'sk-Talnakh deposits, is estimated to have a size of four million km^3 (Ivanov, 2007). However, because the amount of intrusive and underplated rock is difficult to estimate but probably equals or exceeds the volcanic component, size estimates for LIPs are minimum values. Emplacement of such large volumes of mafic magma generally is attributed to the rise and impingement of hot mantle plumes on continental and oceanic lithospheric plates (Condie, 2001; Pirajno, 2007).

Plume-related magmatism and LIPs extend from at least 2.7 Ga to the present (Ernst, 2007). Mesozoic-Cenozoic continental LIPs are best preserved, with extensive flood basalt sections as much as several kilometers thick that consist of large tabular lava flow units typically without significant interlayered sedimentary rocks. In contrast, older Precambrian to Paleozoic LIPs commonly have no or only limited remnants of preserved flood basalts, but the plumbing system is exposed as giant dike swarms, sill complexes, and large layered

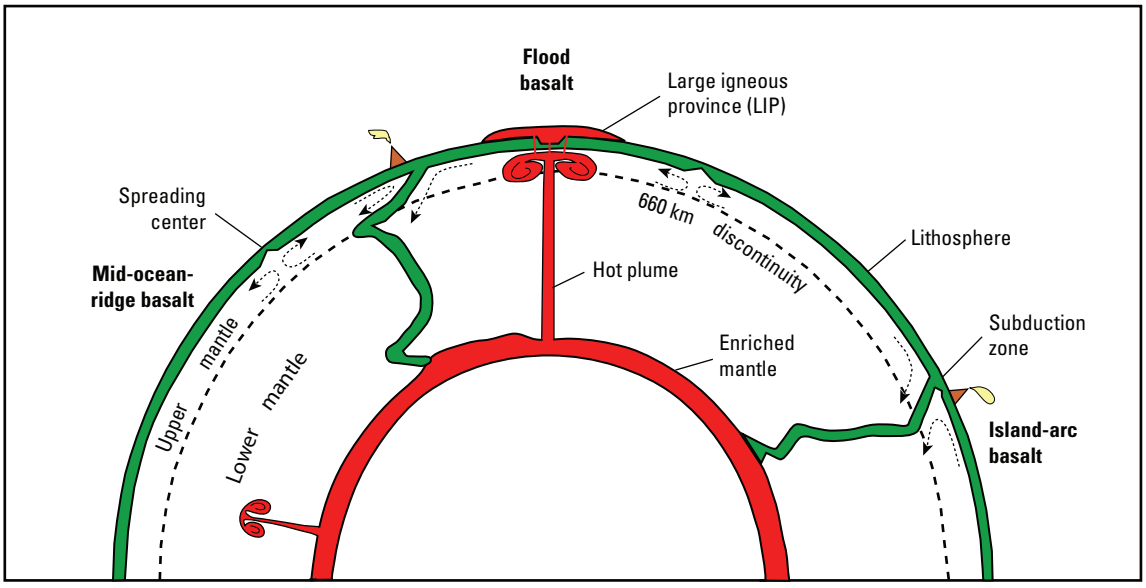

Figure 4–1. Schematic section through Earth's core and mantle showing the relations among hot plumes, spreading centers, and subduction zones. Large igneous provinces (LIPs) are characterized by large volumes of flood basalts and form above hot plumes that rise from a compositionally enriched thermal boundary layer above the core. Mid-ocean ridge basalts (MORBs) erupt at spreading centers, and island-arc basalts occur along subduction zones. Figure modified from Campbell (2001).

intrusions. Recognition of LIPs in the Archean is uncertain because most volcanic rocks and associated intrusions occur in deformed and fault-segmented greenstone belts (de Wit and Ashwal, 1997) and generally cannot be traced over LIP-scale extents. Some greenstone belts, however, consist of tholeiite and komatiite volcanic rock sequences that may be remnants of Archean LIPs originally formed as oceanic plateaus or on continental platforms (Ernst, 2007).

Continental LIPs characteristically are associated with the breakup or attempted breakup of continents (Condie, 2001; Ernst, 2007; Begg and others, 2010). As a result, pre-Mesozoic LIPs may be intensely fragmented by continental breakup, with parts of a single LIP being dispersed on different crustal blocks. This fragmentation and dispersal, as well as erosion removing some or all of the flood basalt cover, can result in magmatic units too small in size and volume to qualify as a LIP. Therefore, it is important to determine if particular dike swarms, sill complexes, layered intrusions and/or flood basalt remnants are components of a fragmented LIP. Establishing such a relation, however, can be difficult, particularly for older Paleozoic and Precambrian terranes for which plate reconstructions are less robust and constrained. A combination of dike trends, geochemistry, age measurements, and paleomagnetic determinations can be used to help reconstruct LIP fragments (Ernst and Buchan, 2001; Ernst, 2007; Bryan and Ernst, 2008).

Temporal (Secular) Relations

Economic magmatic sulfide-rich Ni-Cu±PGE deposits in LIP settings range in age from Archean to Middle Jurassic and are almost exclusively associated with (replenished) dynamic magmatic systems, including periodically replenished subvolcanic feeder sills, feeder dikes, and volcanic vents (Lesher, 2004). Less dynamic (unreplenished) systems such as sheeted sills and larger layered intrusions normally are barren of sulfide-rich Ni-Cu±PGE mineralization unless they are a lateral component in a dynamic magma system. The apparent restriction of economic sulfide-rich Ni-Cu±PGE deposits to Jurassic and older magmatic systems probably is a reflection of the more deeply eroded nature of older LIPs, thereby exposing more of the plumbing system below extensive and barren flood basalt sections. Currently, there are too few known deposits to determine if there is any significant secular variation in their occurrence (Naldrett, 2010). Studies of LIPs through time suggest, however, that there are few significant gaps in the post-2.6-Ga record, with an emplacement rate of about one LIP every 20 million years (Ernst, 2007). It does appear that more voluminous and/or more focused magmatic events produced larger and/or more abundant ore deposits than less voluminous and/or less focused magmatic events (Lesher, 2004).

Duration of Magmatic-Hydrothermal System and/or Mineralizing Processes

Few studies have been undertaken to determine the duration of magmatic systems that formed individual sulfide-rich Ni-Cu±PGE deposits. However, from studies of mafic magma systems, and thermal modeling of emplacement and cooling of intrusions, it appears that magma residence in mafic systems is approximately a few thousand years at most and generally only years to hundreds of years (Reid, 2003). For example, steady-state modeling of the most active conduit system beneath the summit of Kilauea Volcano in Hawaii suggests a basaltic magma residence time of 30 to 40 years during the late twentieth century (Pietruszka and Garcia, 1999). Geophysical estimates of magma residence time beneath Kilauea, based on volumes of magma reservoirs, range from about one hundred years to several thousand years (Reid, 2003). The largest estimate likely reflects the entire interconnected melt volume beneath Kilauea whereas the shorter duration likely represents only the liquid part of the reservoir that contributes directly to lava output.

Relations to Structures

Extension, rifting, and development or reactivation of deeply penetrating faults typically accompany development of LIPs and play an important role in providing zones of weakness and dilation along which magma may ascend into the crust (Pirajno, 2007; Begg and others, 2010). These magma-focusing structures facilitate development of dynamic subvolcanic feeder systems that typically host sulfide-rich Ni-Cu±PGE deposits (Arndt, 2005). At Noril'sk, many of the ore deposits are aligned along the major NNE-trending Noril'sk-Kharaelakh fault, which may have controlled the emplacement of the ore-forming magmas. In addition, the main ore deposits within the Noril'sk region are confined to volcanic-plutonic depressions or troughs that range from 50 to 150 km long and from 40 to 90 km wide (Diakov and others, 2002). These depressions contain thick Paleozoic sedimentary deposits, including evaporites and coal-bearing formations that host a number of mineralized intrusions, overlain by 2- to 4-km-thick sequences of barren Siberian flood basalts. Although Ni-Cu sulfide deposits commonly are spatially associated with rifted continental margins (Begg and others, 2010), the deposits may not be related directly to the rifting event that formed the margin. Rather, they may form later during deflection of a mantle plume by thick continental lithospheric root, causing lateral spreading and rise of the plume under the thinned lithosphere present along continental margins.

Relations to Igneous Rocks

The formation of sulfide-rich Ni-Cu±PGE deposits is a direct result of evolution of mantle-derived mafic and ultramafic magmas emplaced in dynamic, flow-through, replenished magmatic systems (Naldrett and others, 1995; Maier and others, 2001; Barnes and Lightfoot, 2005). Relatively high degrees of partial melting of the mantle result in parental magmas enriched in Ni and PGE (Keays, 1995). These parental magmas form a variety of olivine-bearing mantle-derived rocks related to ferropicrite (Pechenga, Russia; Eagle, United States), tholeiitic picrite (Noril'sk-Talnakh, Russia), and high-Al basalt (Voisey's Bay, Canada). Although the metal contents of the primary magmas can influence ore compositions, factors such as temperature, viscosity, volatile content, and mode of emplacement are the more important controls on ore genesis (Arndt and others, 2005). Because the parent mafic and ultramafic magmas typically are sulfur-undersaturated on their ascent from the mantle (Keays, 1995), ore formation generally involves the incorporation of sulfur from sulfur-rich crustal rocks.

Sulfide deposits generally are hosted by dike- or sill-like intrusions emplaced in the upper crust as feeders to other intrusions and/or surface lava flows. The intrusions generally are small- to medium-sized differentiated mafic and/or ultramafic dikes, sills, chonoliths (tens to a few hundreds of meters in thickness, about 100 to 2,000 meters wide, and hundreds of meters to several kilometers in length), and plug-like intrusions (generally <10 km in diameter), and range from oblate circular through sheet-shaped to rod-shaped (Lesher, 2004). The intrusions consist of a variety of igneous lithologies depending on magma composition, depth of emplacement, and the rate of cooling. Those lithologies range from fine-grained basalt and diabase to medium- and coarse-grained cumulate rocks, gabbro, pegmatite, and breccia. The largest sulfide deposits typically are concentrated along the base of the intrusions in locations where changes in footwall geometry affected magma flow dynamics (Barnes and Lightfoot, 2005).

Relations to Sedimentary Rocks

Country rocks, including basement metamorphic rocks and upper crustal sedimentary rocks, play two important roles in the formation of these deposits. First, crustal structure helps control the formation of magma chambers, defining sites where ascending magmas can be trapped at density discontinuities in the crust (Arndt, 2005). When ascending magma reaches horizontally bedded sedimentary strata, magma can spread out along bedding planes, and horizontal intrusions or sills typically form. If magma intrudes along successively higher bedding planes, a series of upward-stepping sills will form complexes of stacked, saucer-shaped intrusions (Chevallier and Woodford, 1999). Second, a common trigger for sulfur saturation and segregation of an immiscible sulfide liquid is interaction between the sulfur-undersaturated magma and crustal rocks, which may be sulfur-bearing. This interaction can change the temperature and composition of the magma by incorporation of country rock, which may decrease the sulfur solubility of the magma, and/or add sulfur to the magma; either process potentially can result in sulfur saturation in the magma. Horizontal flow through upper crustal dike-sill complexes can augment the period of interaction between magma and wall-rocks, thereby increasing the extent of contamination (Arndt, 2005). Although sulfide- and/or sulfate-bearing sedimentary rocks commonly are present in the country rocks near intrusions, the rocks that the magma(s) interacted with during ascent through the crust probably are more important for achieving sulfur saturation than are the country rocks at the final level of emplacement (Hoatson and others, 2006).

Relations to Metamorphic Rocks

Although metamorphism does not contribute directly to the formation of magmatic sulfide-rich Ni-Cu±PGE deposits, metamorphism can manifest with deposits in several ways. First, metamorphism of the country rocks due to emplacement of intrusions can result in the development of skarns and contact aureoles, such as at Noril'sk and Uitkomst. Also, post-emplacement cataclastic metamorphism may remobilize, and possibly disperse, sulfide ores, as in the development of matrix-brecciated sulfides at Pechenga (Naldrett, 2004) or the remobilization of sulfides along shear zones as at the Kabanga deposit (Maier and others, 2010). In addition, metamorphism can result in significant upgrading of the tenor of disseminated sulfide minerals if olivine is destroyed, thereby releasing Ni that will be taken up by sulfides. Also, sulfides may be recrystallized, resulting in coarser sulfide textures that can make the mineralization more amenable to mineral processing. Because massive sulfides are incompetent and concentrate stresses during deformation, massive sulfide may be mobilized and displaced away from host intrusions and concentrated into pressure shadows in deformed terranes.

5. Physical Description of Deposits

Magmatic sulfide-rich Ni-Cu±PGE deposits typically occur in clusters, and many deposits contain multiple mineralized zones. Sulfide ores occur within host intrusions and country rocks in a variety of forms (table 5–1), depending on the timing of sulfide segregation relative to the emplacement and crystallization history of the host rock and the degree of subsequent magmatic, hydrothermal, and/or tectonic mobilization (Lesher, 2004).

Size and Shape of Deposits

The size and shape of deposits and ore zones depend on the form and orientation of the host unit, generally an intrusive body and adjacent footwall rocks, on any ore-localizing feature (for example, footwall embayments), and on the nature and distribution of the sulfides (table 5–1). Host intrusions typically range from tens to a few hundreds of meters in thickness, about 100 to 2,000 meters wide, and hundreds of meters to several kilometers in length, to plug-like intrusions generally <10 km in diameter. As a result, deposits and ore zones form a continuum of shapes and sizes from large oblate spherical masses hundreds of meters across (Voisey's Bay Ovoid deposit) to meter- to tens of meters-sized pods, rods, and stringers (Noril'sk). Massive sulfide (greater than about 66 percent sulfide minerals) and matrix or net-textured (about 33 to 66 percent sulfide minerals) ores tend to form dikes and flat-lying sheets, as well as lenses at the bottom of intrusions, which, in some cases, also protrude downward into the footwall rocks (fig. 5–1). At Noril'sk, massive ores extend for several kilometers along the long axis of the host intrusion, with thicknesses of as much as 50 m and widths of as much as 1 km (fig. 5–2; Diakov and others, 2002). Massive ores typically occur in physical depressions or where changes in the geometry or topography of the footwall occur. The thickness of the massive ores often correlates with the thickness of the intrusion, generally pinching out where the intrusion thickness decreases (fig. 5–3; Diakov and others, 2002). Massive ores can show distinct sulfide mineral zonation, ranging from pyrrhotite-dominated, chalcopyrite-pentlandite assemblages in the outermost and lower parts, through progressively more Cu-rich zones, to mainly Cu-rich sulfides, commonly enriched

Table 5–1. Form, distribution, textures, and timing of segregation of Ni-Cu±PGE sulfide mineralization (after Lesher, 2004).

Type	Form/distribution	Texture	Timing
I	Stratiform or stratabound, at or near the base of host unit	Massive, net-textured, disseminated	Early magmatic segregation
II	Stratabound to podiform, internal to host unit	a. Massive, net-textured, or heavy disseminated b. Blebby disseminated c. Fine disseminated	Early magmatic segregation Early or intermediate magmatic segregation Late magmatic segregation
III	Stratiform or stratabound in country rocks adjacent to Type I ores	a. Mineralized metasedimentary rocks b. Interbreccia, interpillow, veins in footwall rocks	Early magmatic and/or metamorphic diffusion Early magmatic percolation
IV	Veins in country rocks associated with Type I ores	Massive or semi-massive veins, often with only very narrow alteration selvages	a. Magmatic-hydrothermal b. Metamorphic-hydrothermal
V	Massive to semi-massive within shears and fault zones mainly associated with Type I ores	Normally foliated, normally inclusion-bearing	Tectonically mobilized

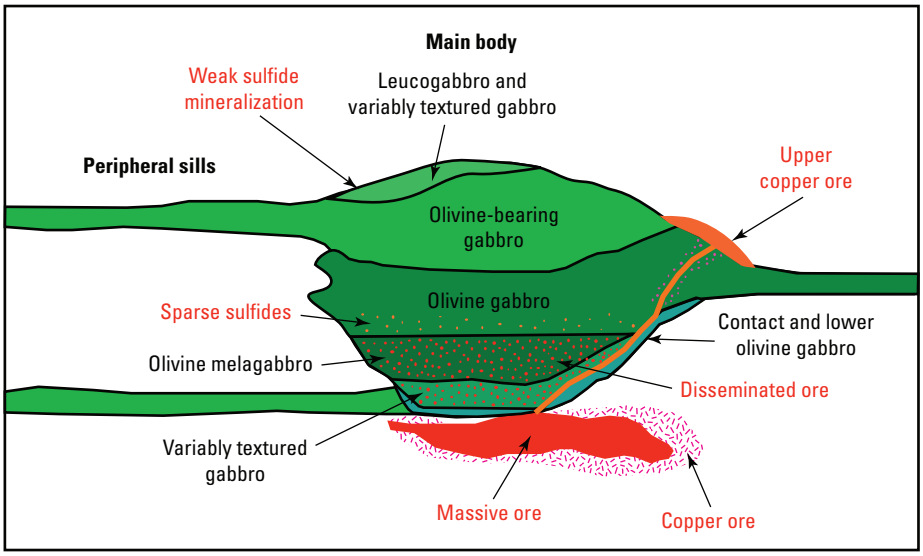

Figure 5–1. Schematic cross section of a typical Noril'sk (Russia) ore-bearing intrusion showing internal structure, lithologies, and major ore types. Figure modified after Naldrett (2004).

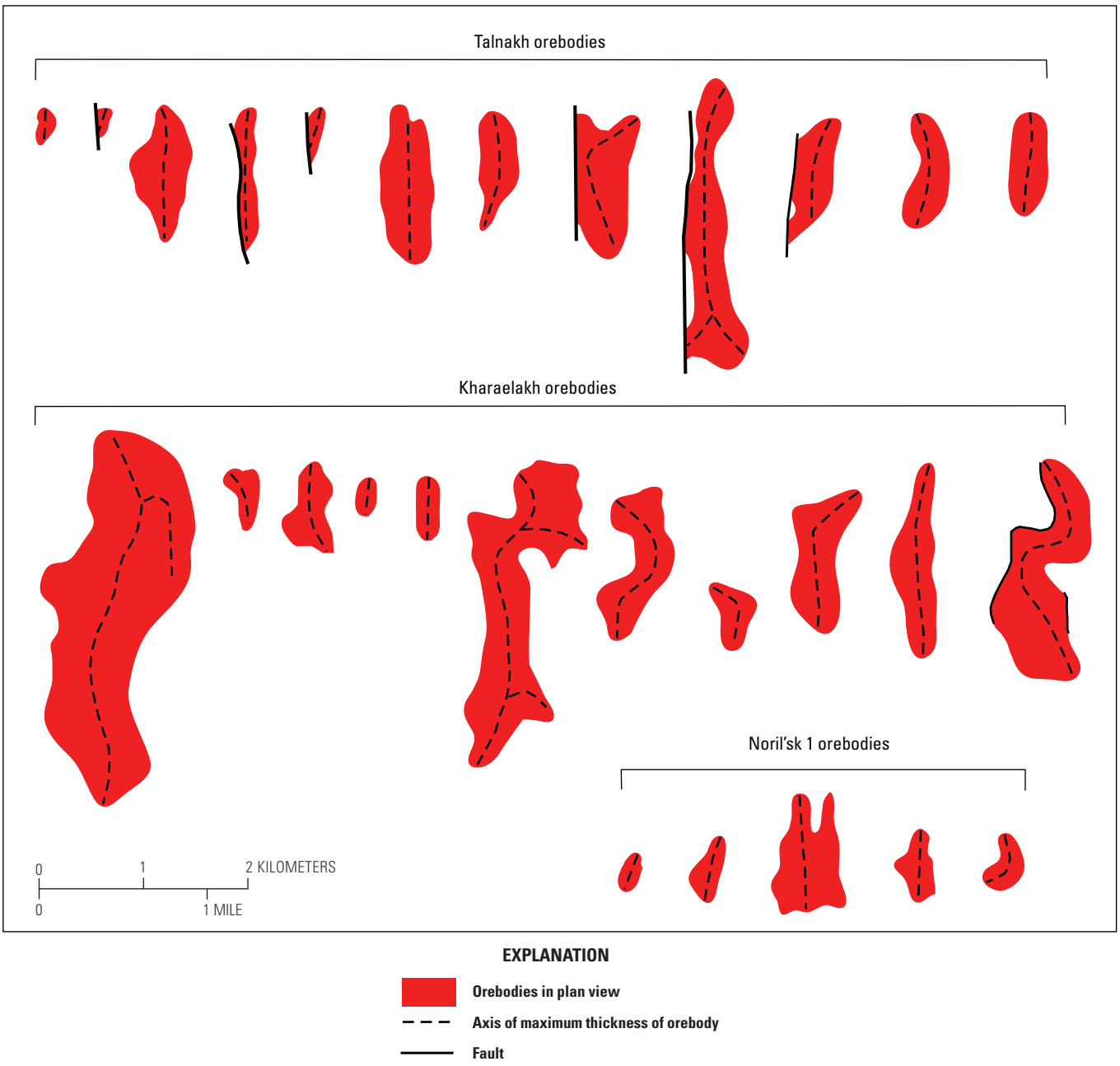

Figure 5–2. Typical shapes of ore bodies at Noril'sk, Russia. Figure modified from Diakov and others (2002).

in PGE in the middle or upper parts. That zonation of sulfides is attributed to in situ fractionation of the original sulfide liquid (Naldrett, 2004).

In contrast to massive ores, breccia ores generally form semi-conformable, sheet-like zones along both the lower and upper contacts of the intrusions and may enclose massive ore (Voisey's Bay). The breccias comprise fragments of both the intrusion and wallrocks in a matrix mainly of massive sulfide. Sulfide stringers and disseminations may accompany the breccias.

Disseminated sulfides (about 1 to 33 percent sulfides) form lenticular to tabular layers generally within the middle and lower parts of intrusions (fig. 5–1). In most cases, they occur as irregular 1-mm- to 1-cm-diameter patches interstitial to silicate and oxide minerals. However, at some localities, such as Noril'sk-Talnakh and Pechenga, disseminated sulfides can occur as 1- to 10-cm-sized spheres or globules of chalcopyrite, pentlandite, and pyrrhotite (dispersed through the host rock) and can be zoned in the manner of the massive ores, with a pyrrhotite-rich base and chalcopyrite-rich top. In the Talnakh intrusion, the thickness of the disseminated ore zone tends to follow the outline of the footwall of the intrusion. However, whereas massive ore pinches out along strike, disseminated ore is nearly continuous along the strike axis of the intrusion (fig. 5–3; Diakov and others, 2002).

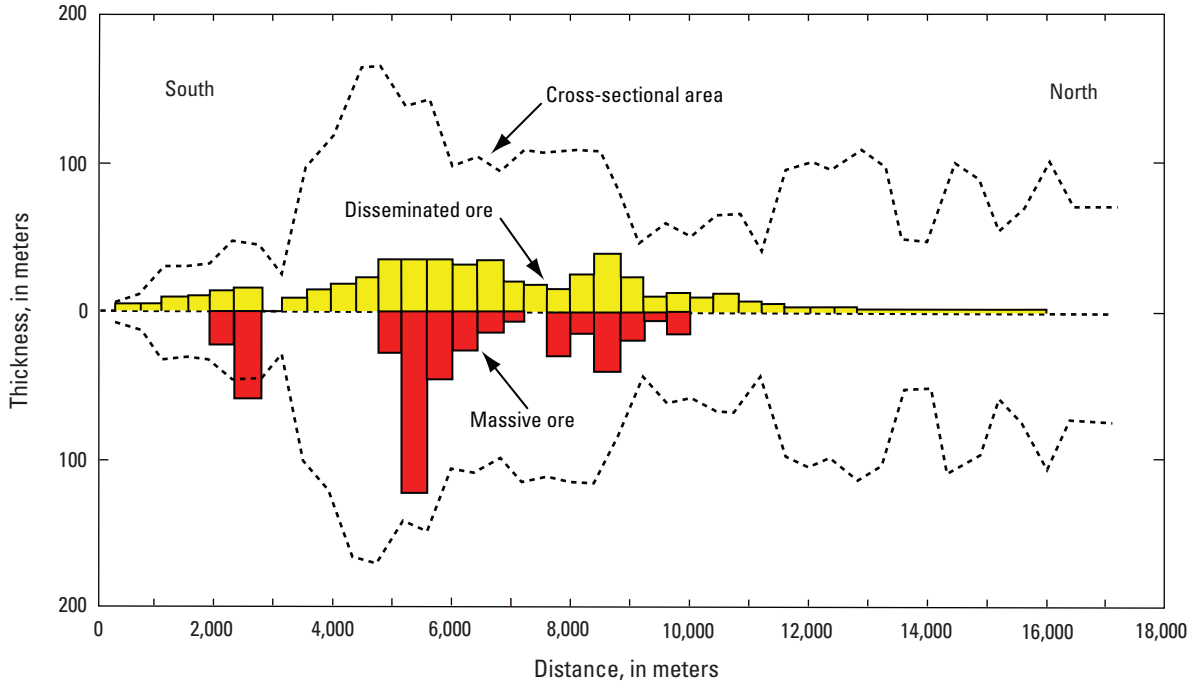

Figure 5–3. Graph showing the variation in cross-sectional area and distribution of disseminated and massive ore along the Talnakh intrusion, Noril'sk, Russia. Figure modified from Diakov and others (2002).

Size of Mineralizing System Relative to Extent of Economically Mineralized Rock

Unlike mineral deposits formed by hydrothermal processes such as porphyry copper and volcanogenic massive sulfide deposits, which generally affect areas much larger than the resulting mineral deposit, magmatic sulfide-rich Ni-Cu±PGE deposits have a relatively small "footprint" outside the deposit. However, although the individual intrusions that typically host these deposits are generally relatively small, they are often parts of larger and complex igneous systems. For example, the Pechenga greenstone belt is part of a larger, discontinuously developed Paleoproterozoic magmatic province that stretches over a distance of 1,000 km in the Kola Peninsula region of Russia. At Pechenga, there are at least 226 differentiated mafic-ultramafic intrusions present within graphitic pyrite-bearing sedimentary rocks underlying the volcanic rock sequence. Of those intrusions, 25 contain Ni-Cu±PGE sulfide ores, 68 contain Ni-Cu±PGE sulfide occurrences, and 113 are viewed as "barren" (Barnes and Lightfoot, 2005). Similarly, at Noril'sk there are a large number of intrusive complexes occupying various positions within the stratigraphic sequence of sedimentary rocks and lavas; however, only a very few of the intrusions host Ni-Cu±PGE sulfide ores (Diakov and others, 2002). Most intrusions are elongated and irregular in shape in plan view, U-shaped in cross section, and extend from a few kilometers to few tens of kilometers in length. Within the mineralized intrusions, massive sulfides generally occur within swells near pinch-outs; swells are typically spaced from 500 to 2,000 m apart and average 1,000 to 1,500 m in length (Diakov and others, 2002).

Many of the intrusive magmatic systems occur at subvolcanic levels in the crust, and contact alteration and metamorphism of the host rock commonly occur adjacent to both mineralized and unmineralized intrusions. It was noted early during exploration in the Noril'sk area, however, that unmineralized intrusions generally are surrounded by relatively thin, low-temperature hornfels aureoles, whereas ore-bearing intrusions have higher temperature hornfels aureoles 1.5 to 2.5 times as thick as the intrusion itself (fig. 5–4; Diakov and others, 2002). In addition, the aureoles above the intrusions are normally four to five times as thick as the zone below and are thicker at the terminations of intrusions (30 to 400 m) relative to their rearward counterpart. The presence of these large aureoles created by high heat flow adjacent to ore-bearing intrusions is taken as evidence that the intrusions were open conduits for magma ascending towards the surface (Naldrett and Li, 2009).

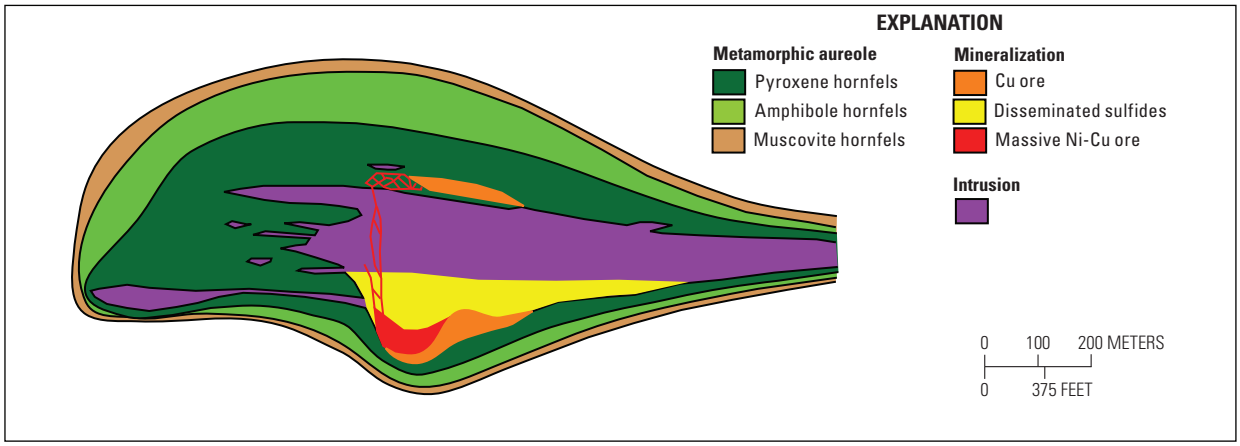

Figure 5–4. Schematic diagram showing the extent of contact metamorphism and metasomatism surrounding typical ore-bearing Noril'sk-type (Russia) intrusions. Figure modified from Naldrett and Li (2009).

Host Rocks

Magmatic sulfide-rich Ni-Cu±PGE deposits are hosted by a variety of mafic and/or ultramafic, variably textured, commonly layered intrusive rocks, as well as by adjacent sedimentary or metamorphic country rocks (Naldrett, 2004). At Noril'sk, where three main types of intrusions have been distinguished (undifferentiated, differentiated, and transitional), only the fully differentiated intrusions host sulfide ores (Kunilov, 1994). The Talnakh intrusion consists of 3 to 10 m of massive sulfide at the base of a variably textured (local term, taxitic; Zientek and others, 1994) olivine gabbro (fig. 5–1). The variably textured olivine gabbro is overlain by olivine melagabbro (local term, picritic gabbrodolerite; Zientek and others, 1994) which, with decreasing olivine content, is overlain by biotite-bearing olivine gabbro to gabbro, followed by local domains of pegmatite and leucogabbro at the upper contact (fig. 5–1). The Eagle deposit in Michigan also is associated with olivine-rich rocks that include feldspathic peridotite, melatroctolite and olivine melagabbro (Ding and others, 2010). In contrast, intrusive rocks at Voisey's Bay consist of troctolite, anorthosite, diorite, and granite; massive and matrix ores are associated with uniform- and varied-textured troctolites (Li and others, 2000).

Structural Setting(s) and Controls

As discussed above, extension, rifting, and development or reactivation of deeply penetrating faults typically accompany development of LIPs, and these structures may play an important role in focusing magma ascent and facilitate the development of dynamic subvolcanic feeder systems (Arndt, 2005). At Noril'sk, sulfide-bearing intrusions are confined to volcanic-plutonic depressions (rift basins) and aligned along major crustal-penetrating faults (Diakov and others, 2002). However, a direct connection to major faults is less evident at some other deposits, such as Voisey's Bay.

6. Geophysical Signatures

Introduction

Magmatic sulfide-rich Ni-Cu±PGE deposits, generally hosted by relatively small picrite or tholeiitic basalt dike-sill complexes, present some unique challenges to geophysical exploration. Because these types of deposits involve some combination of pyrrhotite, pentlandite, and chalcopyrite (Ford and others, 2007), they typically are associated with highly anomalous physical properties, including density, magnetization, electrical conductivity, electrical chargeability, and acoustic velocity. As a result, geophysical methods can be used effectively to detect and characterize such deposits. Unfortunately, the mafic-ultramafic host rocks, as well as the enclosing wall rocks, also can have a variety of anomalous physical properties, thereby complicating geophysical recognition of sulfide deposits. Furthermore, the geophysical signatures of the sulfide deposits, as well as of the host intrusions, may vary widely due to a variety of geometric and geologic factors. Thus, a geophysical method that works effectively in one region may not work at all in another (King, 2007). Finally, Ni-Cu±PGE sulfide deposits, as well as their host intrusions, are small, commonly only tens or hundreds of meters in width, and they present a "needle in a haystack" scenario for any regional-scale geophysical program. Overall, a successful geophysical program for these types of deposits requires a creative and highly flexible strategy.

This section provides an overview of the major geophysical signatures that generally are known to be associated with magmatic Ni-Cu±PGE sulfide deposits associated with mafic-ultramafic dike-sill complexes. This is not meant to

be a comprehensive review of all the geophysical methods that have been used on these deposits, in part because many pertinent case-histories are still unavailable because they are in proprietary company reports. In addition, this section also reviews which geophysical methods have been most effective so far, and which appear most promising for future assessments and exploration programs.

Magnetic Signature

In the magnetic method, highly precise measurements of Earth's magnetic field are used to investigate the subsurface. Once the acquired magnetic data have been corrected for temporal variations and for the geomagnetic reference field (core-derived component), the remaining anomalies reflect upper crustal geology (fig. 6–1). Most magnetic anomalies reflect variations in the quantity and physical nature of the ferromagnetic iron oxide mineral magnetite, a common accessory in many igneous and metamorphic rocks, and these anomalies typically have amplitudes ranging from a few nanoTeslas to several thousand nanoTeslas. In comparison, Earth's background geomagnetic field for much of the United States is approximately 55,000 nanoTeslas. The magnetic method is one of the most applied techniques in mineral exploration, mainly because of its sensitivity to lithologic and structural variations in igneous and metamorphic terranes that commonly host mineral deposits. In addition, the method can be readily applied using aircraft for aeromagnetic surveying, thereby allowing large areas to be covered rapidly and efficiently.

The magnetic method is particularly well-suited for reconnaissance-scale investigations for mafic-ultramafic dike-sill complexes that might host Ni-Cu±PGE sulfide deposits (Ford and others, 2007). The intrusions that host these deposits, as well as enclosing wall rocks, typically contain varying amounts of magnetite, and the magnetic method thereby is useful in recognizing intrusions and enclosing geologic frameworks where conditions for sulfide deposition may have been favorable. In addition, pyrrhotite can be strongly magnetic under certain physiochemical conditions (table 6–1), and because of its near-ubiquity in magmatic Ni-Cu±PGE deposits, magnetic surveying might, in some cases, directly detect sulfide bodies. Not surprisingly, magnetic surveying has been used extensively in the search for these deposits in Canada (Ford and others, 2007; King, 2007; Balch and others, 2010), and it has apparently also played a significant role in the discovery of the Eagle and Tamarack deposits in the United States (Ware and others, 2008; Boerboom, 2009; Ding and others, 2010). Because these deposits and their host intrusions are small in size, magnetic surveying must be conducted with very high-resolution specifications. If available, "regional" surveys with a line spacing of 200 to 400 m may be used to target more-detailed surveys that use line spacings of 100 m or less.

An example of this magnetic survey approach is illustrated for the McFaulds Lake prospects in the Hudson Bay lowlands of Canada (fig. 6–1). The regional survey, which was originally flown as part of a diamond exploration program, revealed a semicircular ring of magnetic highs that correspond to a series of mafic to ultramafic igneous rocks ringing a granodioritic pluton within the Sachigo greenstone belt of the Archean Superior Province (fig. 6–1*A*). This ring of intrusions, also known as the "Ring of Fire," has become best known, perhaps, because of the recent discovery of large chromite deposits (Mandel, 2009; Mungall, 2009; Smyk, 2010), but the exploration program here also has revealed two significant Ni-Cu±PGE sulfide deposits, the Eagle's Nest and the AT-12 (Balch and others, 2010; Mungall and others, 2010). The regional aeromagnetic survey (fig. 6–1*A*) was useful in delineating mafic to ultramafic intrusions that warranted further investigation, but it failed to resolve either of the sulfide deposits. A higher resolution total field and gradiometer survey, with 100-m line spacing and 50-m elevation, was part of a follow-up investigation. It revealed the 100- by 300-m footprint of pyrrhotite in both sulfide deposits (fig. 6–1*B* and 1*C*). In some situations ground-based magnetic methods also may be used effectively, once a favorable target has been established by either aeromagnetic data or geologic mapping (Guo and Dentith, 1997), to further delineate sulfide mineralization.

The magnetic survey method has been particularly helpful at the Noril'sk deposit, where deep burial beneath conductive sedimentary rocks can thwart electromagnetic (EM) and other geophysical applications (Diakov and others, 2002). Although the Ni-Cu±PGE deposits lack a distinctive geophysical signature, magnetic data provide clues regarding the geologic framework associated with the deposits. For example, magnetic data have been used to recognize individual flows and sills near the surface, buried intrusions, and faults that may have focused magma flow.

Unfortunately, not all Ni-Cu±PGE sulfide deposits and their host rocks provide magnetic signatures. For example, for the Voisey's Bay deposits, high-resolution aeromagnetic data from the area typically show little or no signature that can be linked to the deposits or to the host intrusions, but instead reflect the structure of the gneissic wall rocks (fig. 6–2; King, 2007). This is because pyrrhotite both in the ores and the host intrusions in this region are nonmagnetic and correspondingly provide no magnetic signature (Balch, 1999). Under such conditions, airborne EM or some other geophysical method may have to be attempted at the reconnaissance stage to identify intrusions and sulfide mineralization.

Gravity Signature

The gravity method uses very small variations (anomalies) in Earth's gravity field to investigate subsurface geology. The geologic signature, most commonly expressed as Bouguer anomaly data, is isolated by several corrections

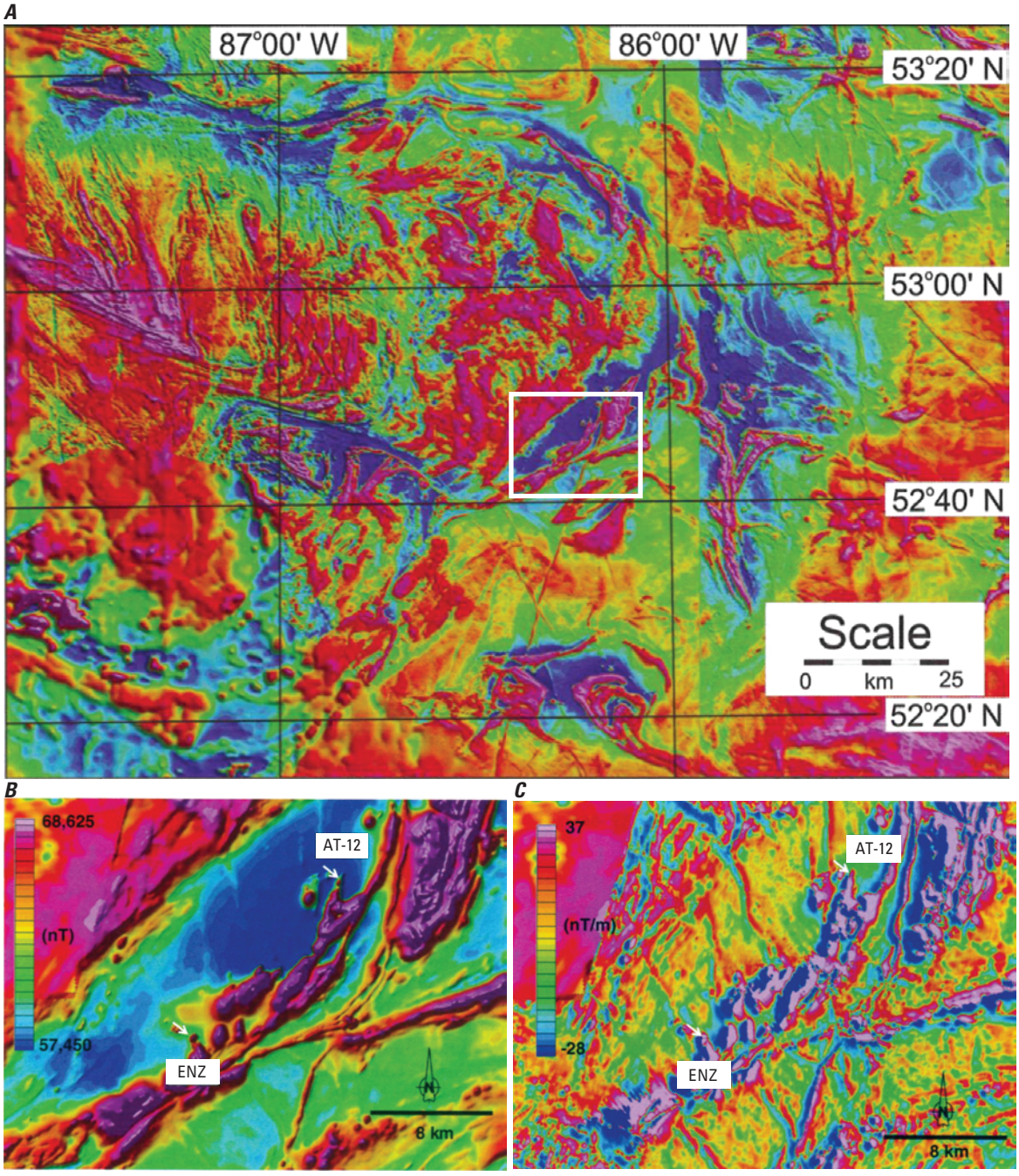

Figure 6-1. Magnetic anomaly maps of prospects in the James Bay Lowlands, Ontario, Canada. *A*, Total magnetic intensity (TMI) map from a regional-scale aeromagnetic survey in northern Ontario. Line spacing is 200 m. The 60-km-wide, semicircular ring of anomalies in the north-central part of the image roughly outlines the so-called Ring of Fire exploration area. The white box delineates the area for maps *B* and *C*. *B*, High-resolution TMI map of the McFaulds Lake area based on a fixed-wing survey with lines spaced 100 m apart and flown 50 m above terrain. Sites ENZ and AT-12 refer to the Eagle's Nest (zone) and to the AT-12 Ni-Cu±PGE sulfide deposits, respectively. *C*, Horizontal gradiometer data from same survey as map *B*. Labels ENZ and AT-12 refer to the Eagle's Nest (zone) and to the AT-12 Ni-Cu±PGE sulfide deposits, respectively. Map *A* is from Mungall and others (2010), and maps *B* and *C* are from Balch and others (2010).

Table 6–1. Copper-nickel sulfide ore mineral and host-rock magnetic susceptibilities in SI units (dimensionless proportionality) × 10^{-3}, modified from King (2007).

Rock type	Range	Average
Sulfides/oxides		
Pyrrhotite	1–6,000	1,500
Pyrrhotite (mono)		700
Pyrrhotite (hex)		2
Pentlandite		<1
Chalcopyrite		0.7
Magnetite	1,200–19,200	6,000
Host rocks		
Felsic Igneous	0–80	8
Mafic Igneous	0.5–97	25
Ultramafic Rocks (Peridotite)	90–200	150
Ultramafic Rocks (Serpentinite)	Moderately high	Moderately high

related to variations in time, latitude, elevation, and topography. Bouguer anomalies typically range from less than one milligal to several tens of milligals. In comparison, the total gravity field of the Earth is approximately 980,000 milligals. Similar to magnetic data, gravity anomaly data can be effective for investigating the geology of the igneous and metamorphic terranes where mineral deposits may occur.

Bouguer gravity anomalies ultimately reflect subsurface variations in density, which in turn are related to mineral composition and porosity. Densities of earth materials typically range from about 2.00 g/cm^3 for unconsolidated materials to about 2.95 g/cm^3 for mafic igneous rocks (table 6–2). Ni-Cu±PGE sulfide deposits can have host rock densities exceeding 3.00 g/cm^3 and ore densities exceeding 4.00 g/cm^3 (table 6–2). Thus, even relatively small mineral deposits

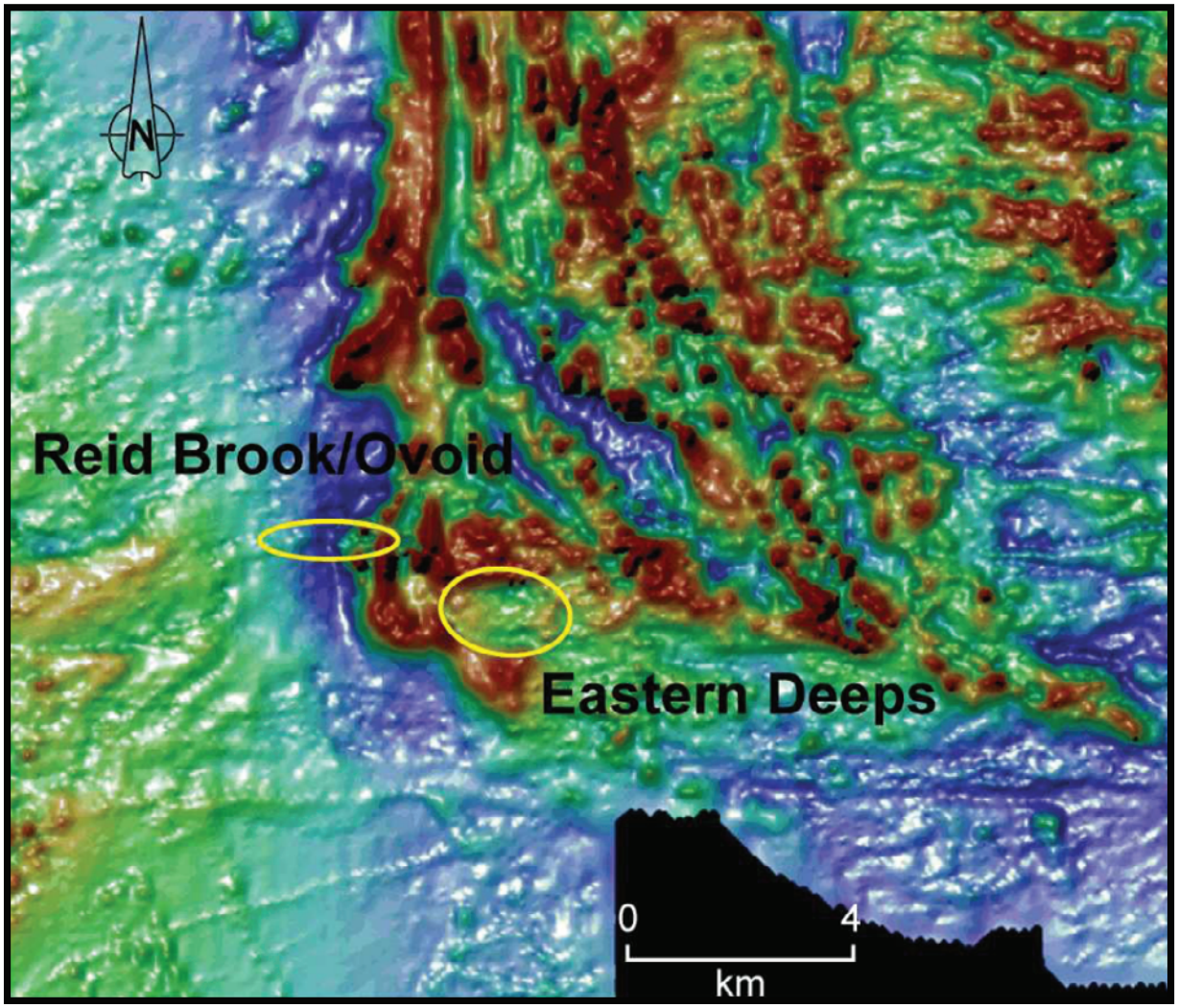

Figure 6–2. Aeromagnetic data collected over the Ovoid and Eastern Deeps deposits in the Voisey's Bay area, Canada. Figure modified from King (2007) and Balch (1999).

Table 6–2. Density values for sulfides and mafic-ultramafic host rocks from King (2007).

[Abbreviation: g/cm^3, grams per cubic centimeter]

Mineral/rock type	Range (g/cm^3)	Average (g/cm^3)
Sulfides		
Pyrrhotite	4.5–4.8	4.65
Pentlandite		4.8
Chalcopyrite	4.1–4.3	4.2
Host rocks		
Felsic igneous rocks	2.33–3.11	2.61
Mafic igneous rocks	2.09–3.17	2.79
Ultramafic rocks (Peridotite)	2.78–3.37	3.15

are capable of producing anomalies of as much as several milligals (Ford and others, 2007). Model studies of gravity data have been used effectively to investigate the subsurface extent of the Jinchuan deposit (Guo and Dentith, 1997) and the Ovoid deposit in the Voisey's Bay district (Ash and others, 2006; Ford and others, 2007), although such an approach requires careful separation of the deposit-related anomalies from those arising from other sources. The 4-milligal residual gravity anomaly that is associated with the Ovoid deposit at Voisey's Bay is shown in figure 6–3.

Until relatively recently, gravity surveying for mineral exploration relied on ground-based acquisition, thereby increasing the time and cost of acquiring data. Consequently the use of gravity methods for Ni-Cu±PGE sulfide exploration mainly has been restricted either to detailed investigations of specific targets (see above) or to regional-scale investigation of geology and crustal structure using coarsely sampled, regional data sets (Rempel, 1994; Diakov and others, 2002). Ongoing advances in airborne gravity and gravity gradiometry, however, are likely to allow greater usage of high-resolution gravity data in the reconnaissance for favorable intrusions, such as is currently implemented with aeromagnetic surveying (King, 2007). Balch and others (2010) reported that the relatively small 0.25-milligal signature associated with the Eagle's Nest deposit in the Hudson's Bay lowlands was near the resolution limits of the currently implemented Bell gradiometer system.

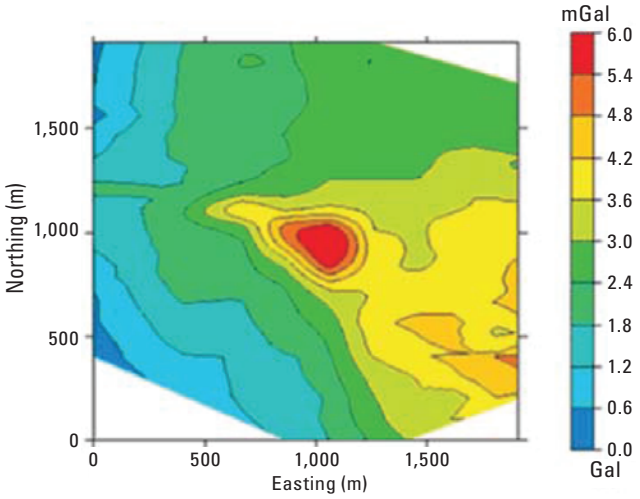

Figure 6–3. Detailed Bouguer anomaly map of the Ovoid deposit at Voisey's Bay, Canada. Image from *www.geo.pubc.ca/ubcgif/* and modified from Ford and others (2007).

Electrical Signature

Most electrical geophysical methods involve measurement of electrical potential at the surface, typically by using a pair of electrodes, to investigate geology at depth. Electrical methods are based on electrical resistivity, induced polarization, or spontaneous potential. Electrical resistivity and induced polarization methods use an artificial current that is introduced via a separate electrode pair, whereas spontaneous potential methods rely on small, passive currents that already exist in the subsurface. In all three approaches, standard electrode arrays are used, and by systematically varying the position and spacing of electrodes, the variation of electrical properties at depth, and by inference geology, can be investigated. Because all three methods rely on electrodes, ground-based deployment—with the related costs—is necessary. Consequently, use of electrical methods in exploring for Ni-Cu±PGE sulfide deposits typically is focused on specific targets or target areas that have been recognized by earlier geological, geophysical, or geochemical studies.

In electrical resistivity (ER) methods, the subsurface structure is interpreted in terms of resistivity. Resistivity, which is the inverse of conductivity, is an intrinsic property of a material that expresses the degree to which it resists electrical current, and in electrical exploration it is expressed in ohm-meters (ohm-m). Resistivity for most earth materials is a function of the quantity and quality of water that is present interstitially, and it generally ranges from a few tens of ohm-meters for clays and shales to ≥1,000 ohm-meters for fresh crystalline rocks (Sharma, 1997). Sulfide minerals have extremely low resistivities (much less than 1 ohm-meters), but their tendency to occur within discrete, three-dimensional volumes makes them difficult to image properly with standard resistivity methods, which are best suited for imaging broad, layer-like features with relatively high resistivities (King, 2007). The ER methods still could be used to investigate thickness and composition of overburden, which may have implications for other geophysical applications (Ford and others, 2007). Resistivity surveying over the Jinchuan deposit showed detectable resistivity responses over some ore bodies, although this effect can be obscured seriously by conductive alluvium (Guo and Dentith, 1997).

Induced polarization (IP) methods use the same electrode configurations as ER methods, and they are commonly conducted together (Sharma, 1997). The IP effect is a charge

buildup in the subsurface that dissipates over a short time after the current has been shut off. The effect is caused by interfacial interactions between electrolytic groundwater and highly conductive grains of sulfide or clay particles. The IP effect typically is expressed as chargeability, which is based on the decay of residual potential once the current has been shut off (time-domain IP) or as percent frequency effect (PFE), which is based on apparent resisitivity observed at two discrete current frequencies (frequency-domain IP). Because the IP effect is proportional to interactive area, disseminated sulfide deposits are more likely to produce a pronounced IP effect than massive sulfide deposits, although disseminated haloes that commonly surround massive deposits can produce a significant IP response. IP/ER surveying has been applied with some success to the Ovoid deposit at Voisey's Bay (Balch, 1999) and to ore bodies at the Jinchuan deposit (Guo and Dentith, 1997), although application in the latter case was limited in some areas by conductive overburden. Unfortunately, IP methods typically cannot discriminate between barren disseminated sulfides, perhaps with just pyrite or pyrrhotite, from those sulfides enriched in Ni-Cu or PGE (Balch, 2005).

Spontaneous potential (SP) methods are based on passive monitoring of ambient currents in the shallow subsurface. The SP currents can be caused by changes in potentials related to movement of ion-bearing groundwater (streaming or electrokinetic potential), differences in ionic concentration within groundwater (diffusion potential), or by a variety of electrochemical reactions in the vicinity of a conductive body (mineral or electrode potential). Most SP anomalies are several tens to hundreds of millivolts, although anomalies as large as 1,000 millivolts can occur. The SP surveying is among the oldest and simplest electrical methods in exploration geophysics, but its shallow depth of penetration precludes its use in most current mineral exploration programs, and the SP method's primary use today is for engineering and environmental investigations (Sharma, 1997). Guo and Dentith (1997) reported a large SP anomaly over an ore body at the Jinchuan deposit, with secondary anomalies apparently reflecting weathered ultramafic rocks and carbon-bearing marble in the wall rock.

Electromagnetic (EM) Signature

Electromagnetic (EM) methods are used extensively for sulfide exploration (Ford and others, 2007). This preference is mainly because EM methods are particularly sensitive to the high conductivities of massive sulfide bodies and because most methods do not require the use of electrodes, readily accommodating airborne applications. Typically, conductivities of sulfides range between 10^3 and10^6 Siemens/meter, which is usually one order of magnitude above that of the enclosing host rocks (King, 2007). Most EM surveys utilize artificially induced currents produced by fluctuating magnetic fields from a transmitter coil or antenna, but some economic applications utilize naturally induced currents including audio-frequency magnetotelluric (AFMAG) methods. Regardless of their source, magnetic field fluctuations induce currents in subsurface conductors, and those currents produce secondary magnetic field fluctuations that can be picked up by a receiver coil or antenna. The EM methods span a wide spectrum of frequencies, extending from the subhertz range for magnetotelluric investigations, up to the megahertz range for geo-radar applications; most EM methods used in sulfide exploration, however, operate with frequencies between 1 and 1,000 hertz.

Exploration by EM is divided into two approaches: frequency domain, where the EM response is observed at varying frequencies, or time domain, where the decay of induced currents is observed following a pulsed EM signal. Most exploration EM methods are used to investigate targets within 300 m of the surface, although the Titan 24 System developed by Quantec Geoscience combines AFMAG methods with resistivity and IP surveying to investigate targets as deep as 1,500 m (Ford and others, 2007). Similarly, ZTEM is a telluric-based airborne method that is capable of detecting conductivity variations well beyond the practical limits of current exploration (Balch and others, 2010). Initially, EM methods were used as simple anomaly detectors that were focused on locating massive sulfide occurrences, but modern methods can allow conductivity estimates of target bodies, as well as resistivity (inverse of conductivity) estimates, of wall rock and overburden (King, 2007; Ford and others, 2007). A recent improvement on time-domain methods has been the implementation of the so-called B-field, which is the integration of the decaying magnetic signal observed at the receiver. This derived parameter greatly enhances conductance resolution (Balch and others, 2010).

Sulfide minerals associated with sulfide-rich Ni-Cu±PGE deposits are highly conductive, and massive to semi-massive occurrences present highly favorable EM targets (King, 2007). The EM methods have been particularly helpful with the Voisey's Bay deposits and a variety of frequency- and time-domain methods have been successfully applied there (Balch, 1999; King, 2007; Ford and others, 2007). The results of AFMAG and helicopter-borne electromagnetic surveys of some of the Voisey's Bay deposits are shown in figure 6–4. In spite of these successes, pitfalls in the application to EM methods include the interference of conductive graphite layers in the wall rock, as well as the masking effect of conductive overburden. With regard to the latter limitation, conductive sedimentary rocks in the Noril'sk region of Russia have largely negated the use of airborne and ground-based EM methods, although borehole based applications have met with some success (Diakov and others, 2002).

Balch and others (2010) have recently reported on the highly effective application of helicopter-borne, time domain EM methods (HTEM) on the Eagle's Nest and AT-12 Ni-Cu±PGE deposits in the McFaulds Lake area of Ontario. Early exploration in the McFaulds Lake area relied on the more traditional approach of a fixed-wing (airplane), time

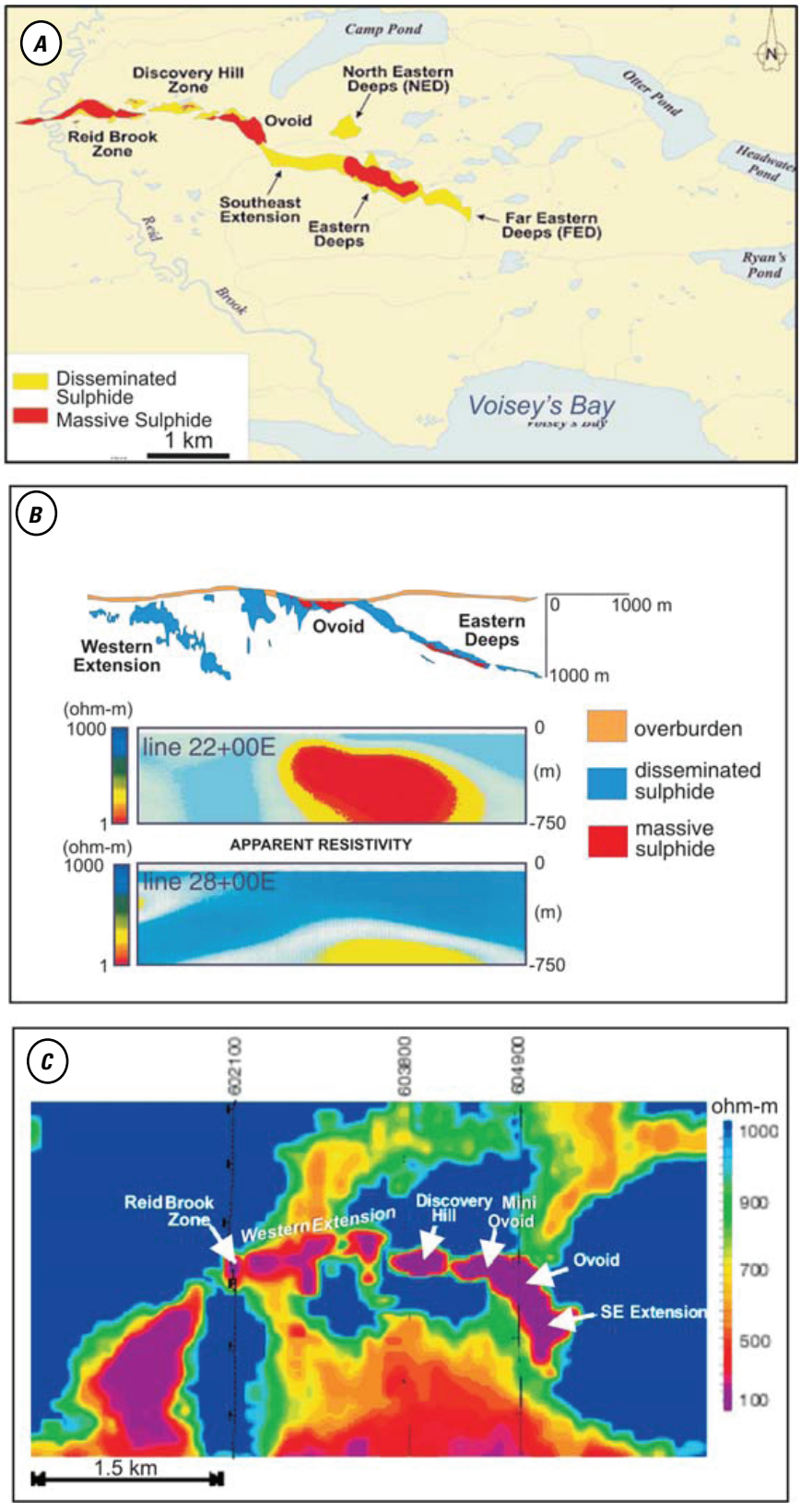

Figure 6–4. *A*, Location and extent of Voisey's Bay, Canada, sulfide deposits. *B*, Apparent resistivities calculated from an audio-frequency magnetotelluric (AFMAG) survey over the Eastern Deeps, Voisey's Bay, massive sulfide body (after Balch, 1999). *C*, Low apparent resistivity associated with the Voisey's Bay sulfide deposits, as calculated from a helicopter-borne electromagnetic (EM) survey. Image from Ford and others (2007).

domain EM system (Geo-TEM), followed by ground-based methods that typically consisted of horizontal Loop EM (HLEM) and magnetic surveying. The HTEM methods, however, were undergoing major improvements during the time of the McFaulds Lake exploration, and significant advances were made with regard to horizontal resolution, depth of penetration, and resolution of conductivities. The exploration in the McFaulds Lake area consequently evolved into in-field interpretation of line EM data, with almost immediate recommendations regarding further acquisition, such as infill lines on interesting targets. This technology, in turn, led to a drilling program that was largely directed by HTEM data, with essential elimination of the expensive ground-based programs, and to a situation where prioritization of targets was more of a problem than detection of targets. On the basis of their McFaulds Lake experience, Balch and others (2010) predict that currently existing HTEM technology will revolutionize the exploration for magmatic Ni-Cu±PGE sulfide deposits.

Seismic Signature

The geologic settings associated with most magmatic sulfide deposits have historically not been considered to be favorable for most seismic methods. The igneous and metamorphic terranes that host such deposits were generally perceived to have structures that were too complex and impedance contrasts that were too low to be properly imaged by seismic methods. Consequently, most seismic studies in such settings were generally restricted to deep-crustal refraction and reflection studies that had little direct significance to mineral deposits. One possible exception is the deep seismic imaging reported for the Noril'sk region by Rempel (1994). In this study, explosion and earthquake sources were used to image crustal layering and apparent offsets in the Moho. Some of these offsets were attributed to deep crustal-penetrating faults that, according to Rempel (1994), might have served as conduits for ore-forming magmas.

Recent seismic-reflection-profiling studies, such as those coordinated by the Canadian Lithoprobe Project (Clowes, 2010), have greatly dispelled some of the old prejudices regarding seismic applications for mineral deposits in igneous and metamorphic terranes. Recent investigations have revealed that sulfide minerals and their host rocks can have large contrasts in acoustic impedance (fig. 6–5), and that many massive sulfide occurrences should be associated with detectable reflection or diffraction signatures, provided that the seismic data are properly acquired and processed (Salisbury and Snyder, 2007). Two-dimensional seismic reflection data (data acquired along a profile) from the Sudbury basin effectively imaged several geologic horizons of the basin, including the base of the norite where many of the primary sulfide ore bodies occur (Milkereit and others, 1992, 1994, 1996). The asymmetry of the Sudbury basin, as well as the offset of the basal sequence along numerous faults, was also evident from these data (fig. 6–6). Three-dimensional seismic data (data acquired over an areal grid) from the Sudbury basin (fig. 6–7) reveal structural details regarding the footwall of the norite (green) and show a prominent diffraction pattern caused by a massive sulfide deposit (Salisbury and Snyder, 2007). The seismic technology developed for the Sudbury basin should be readily applicable to mafic-ultramafic dike- and sill-hosted Ni-Cu±PGE sulfide deposits.

Although not focused on mineral deposits, two recent three-dimensional seismic investigations of Cretaceous–Paleocene intrusive sill complexes in the Faroe-Shetland Basin of the northeastern Atlantic Ocean have findings that may be significant to sulfide assessments and exploration. Hansen and others (2004) describe individual sills that occur as trough- or saucer-like bodies, 2 to 8 km in diameter and with a relief of several hundred meters. The seismic data reveal that the sills are interconnected by a variety of junctions that yield important clues on the emplacement history of the sill complex (fig. 6–8). Three–dimensional seismic imaging of a sill by Trude and others (2004) revealed a complex of ridges along the top of one sill that appear to indicate magma flow. These ridges, with wavelengths of 220 to 350 meters and amplitudes of 25 to 50 m, were likely created by viscous drag near the top of the sill and appear to radiate from distinct feeder zones (fig. 6–9). Sill geometry, as well as magma flow, is important to the development of dike- and sill-hosted Ni-Cu±PGE sulfide deposits, particularly near feeder zones. The seismic studies in the Faroe-Shetland Basin indicate that three-dimensional seismic imaging may be a powerful tool for recognizing intrusion geometry and identifying magma feeder systems.

Another seismic method that may assist in exploration for dike- and sill-hosted Ni-Cu±PGE sulfide deposits is vertical seismic profiling (VSP). The VSP methods are particularly useful for imaging steeply dipping structures (>60°) not properly imaged by two- or three-dimensional reflection profiling (Salisbury and Snyder, 2007). For example, VSP could be used to image a vertical feeder beneath a sill. In this method, a receiver (seismometer) is lowered to the bottom of a drill hole and then raised in stages as shots are fired at the surface (fig. 6–10). If the positions of the shots and the drill hole geometry are precisely known, then velocities can be calculated from the shot receiver distances and the geometry of steep reflectors can be imaged through processing. Cross-hole seismic methods are essentially a variation of VSP where one has an array of holes. By systematically interchanging source and receiver positions at various positions in the holes (fig. 6–11), the three-dimensional velocity structure between holes can be imaged (King, 2007). Such a procedure can be used to detect hidden sulfide deposits that might lie between test holes.

In spite of their great potential, seismic reflection surveys are very expensive, and their selection must be weighed very seriously. Salisbury and Snyder (2007) estimated that two dimensional surveying would cost about $6,000/line km, whereas three dimensional surveying would cost about

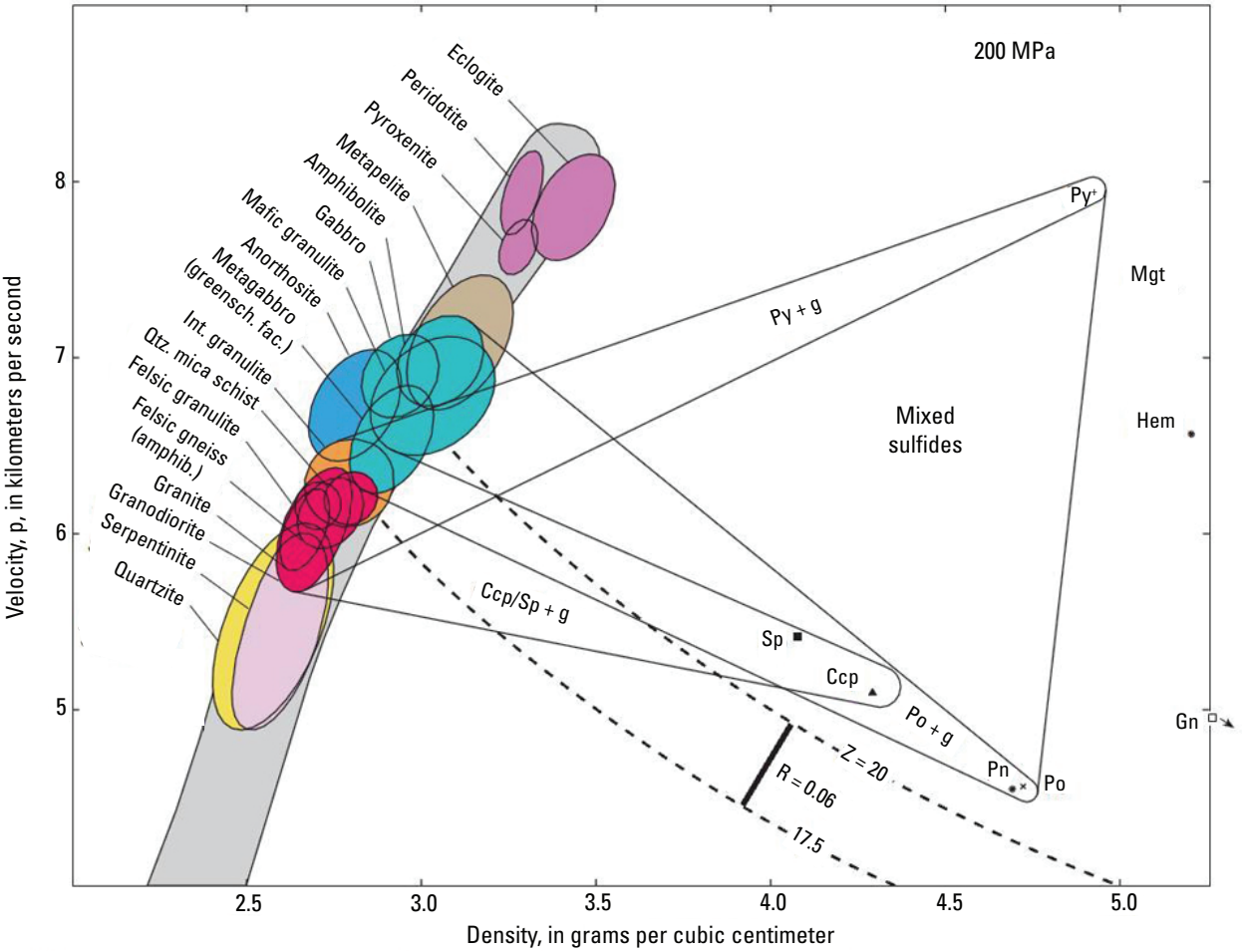

Figure 6–5. Velocity values of various rock types plotted against their density with lines of constant acoustic impedance (Z) overlain within field and Nafe-Drake curve (gray) for common rocks at a standard confining pressure of 200 MPa (from Salisbury and others, 2003). Also shown are values for pyrite (Py), pentlandite (Pn), pyrrhotite (Po), chalcopyrite (Ccp), sphalerite (Sp), hematite (Hem), magnetite (Mgt), gangue (g), and fields for host rock–ore mixtures. A reflection coefficient (R) of 0.06 is sufficient to give a strong reflection. Galena (Gn, off scale) has a velocity of 3.7 km/s and a density of 7.5 g/cm^3.

$60,000/km^2 on land. Assuming a suitable drill hole already exists, VSP surveying to a depth of 500 m would cost about $30,000. These costs are large for many mineral exploration budgets, and they assure that if seismic methods are used, they will most likely be attempted at a very advanced stage of a prospect exploration. For example, two-dimensional data might be best used in the final stages of reconnaissance, three-dimensional data might be best used during discovery and delineation, and VSP might be best used in delineation only. As pointed out by Salisbury and Snyder (2007), "it is important to match the method to the intent of the survey and the type of deposit sought." If the expense can be justified, then no other geophysical method can offer the depth of penetration and degree of resolution provided by seismic reflection methods.

Spectral Characteristics

Spectral absorption features associated with mafic and ultramafic rocks in the Visible-Near Infrared to Short Wave Infrared (0.5–2.5 micrometers; VNIR–SWIR) range typically are subdued by the low reflectance characteristics of mafic and ultramafic minerals, including magnetite, biotite, and hornblende that have Fe^{2+} spectral absorption features in the 0.5- to 1.65-micrometer region (fig. 6–12*A*; Rowan and others, 2005). Olivine, an exception among ultramafic VNIR–SWIR low-reflectance minerals, has a broad spectral absorption feature centered at 1.05 micrometers (fig. 6–12*A*). Additional SWIR Fe(Mg)OH spectral absorption features in phlogopite, hornblende, and biotite are centered at 2.31 to 2.33 micrometers (fig. 6–12*B*).

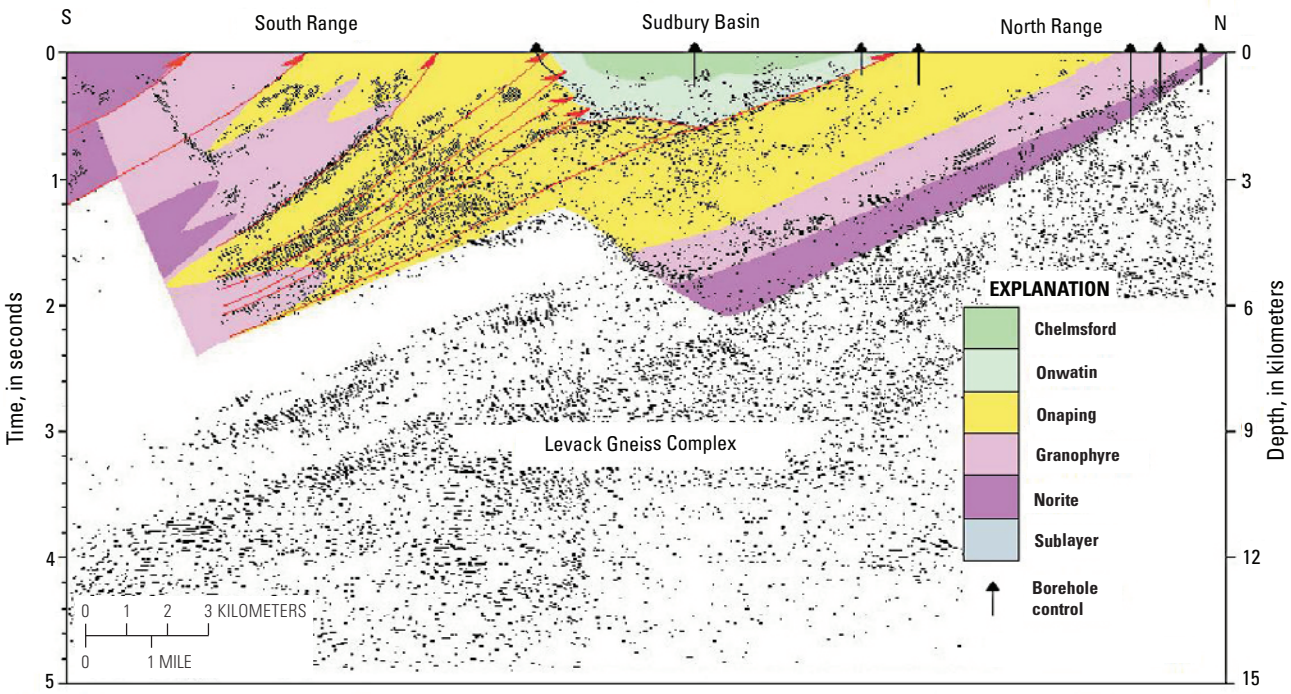

Figure 6–6. Two-dimensional reflection section across the Sudbury Basin, Ontario, Canada, showing reflectors associated with deep structure and lithologic contacts. Data from Milkereit and others (1992); image modified from Salisbury and others (2007).

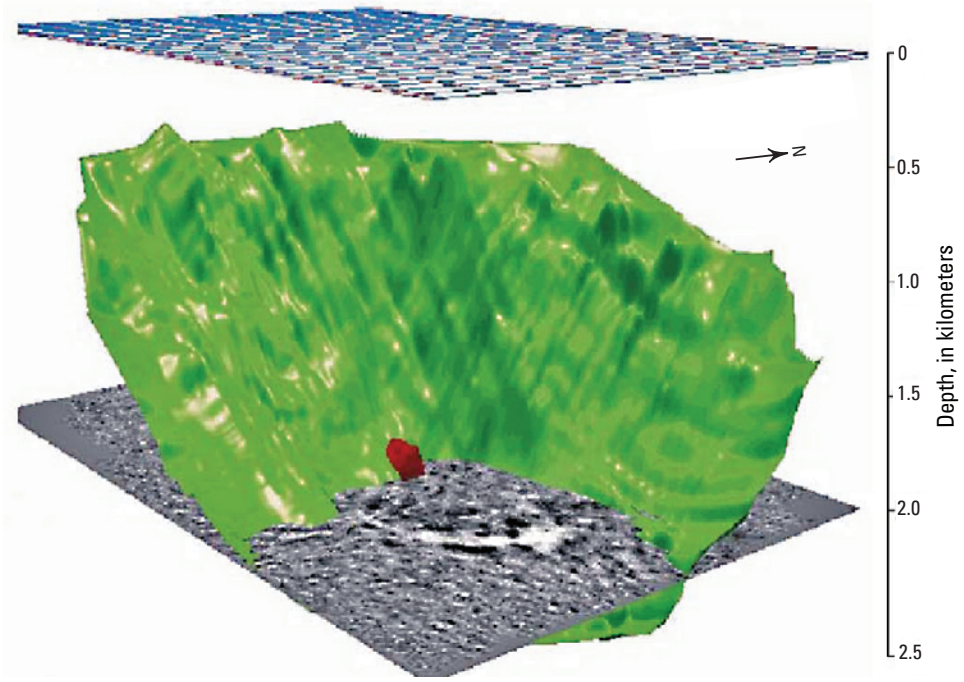

Figure 6–7. Three-dimensional seismic image of the Sudbury area, Ontario, Canada, showing surface grid (horizontal plane), horizon slice (green) corresponding to the footwall complex, and time slice corresponding approximately to 2,000-m depth. Red spot represents known position of the Trillabelle sulfide deposit. Note diffraction in time slice corresponding to sulfide deposit. Data from Milkereit and others (1997); image modified from Salisbury and others (2007).

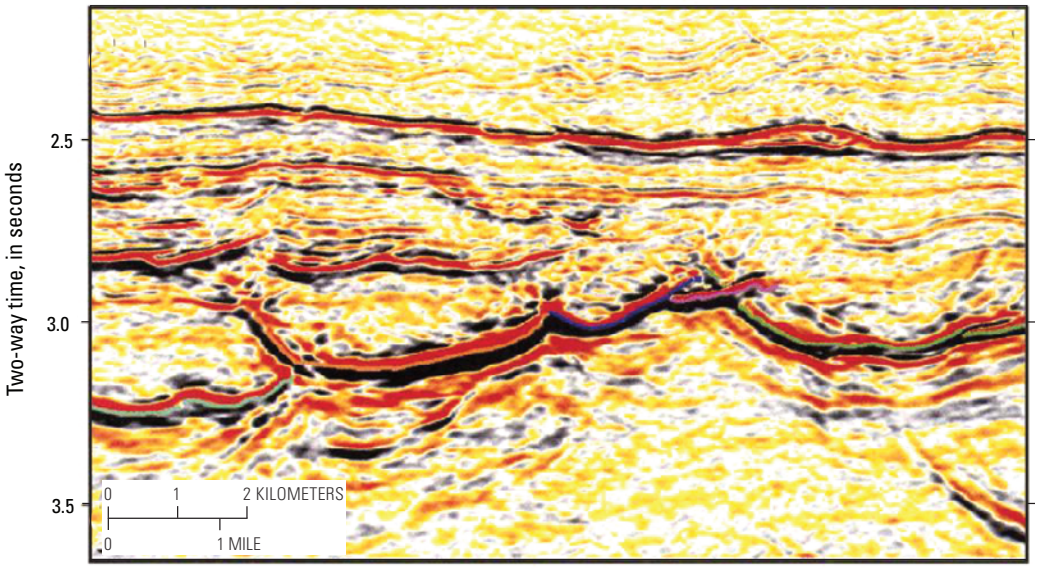

Figure 6–8. Vertical slice of a three-dimensional seismic reflection survey of the Faroe-Shetland basin, northeastern Atlantic Ocean margin. Individual sills are delineated by strong, concave-upwards reflections along and below 3 seconds. Note apparent interconnections between individual sills. Figure modified from Hansen and others (2004).

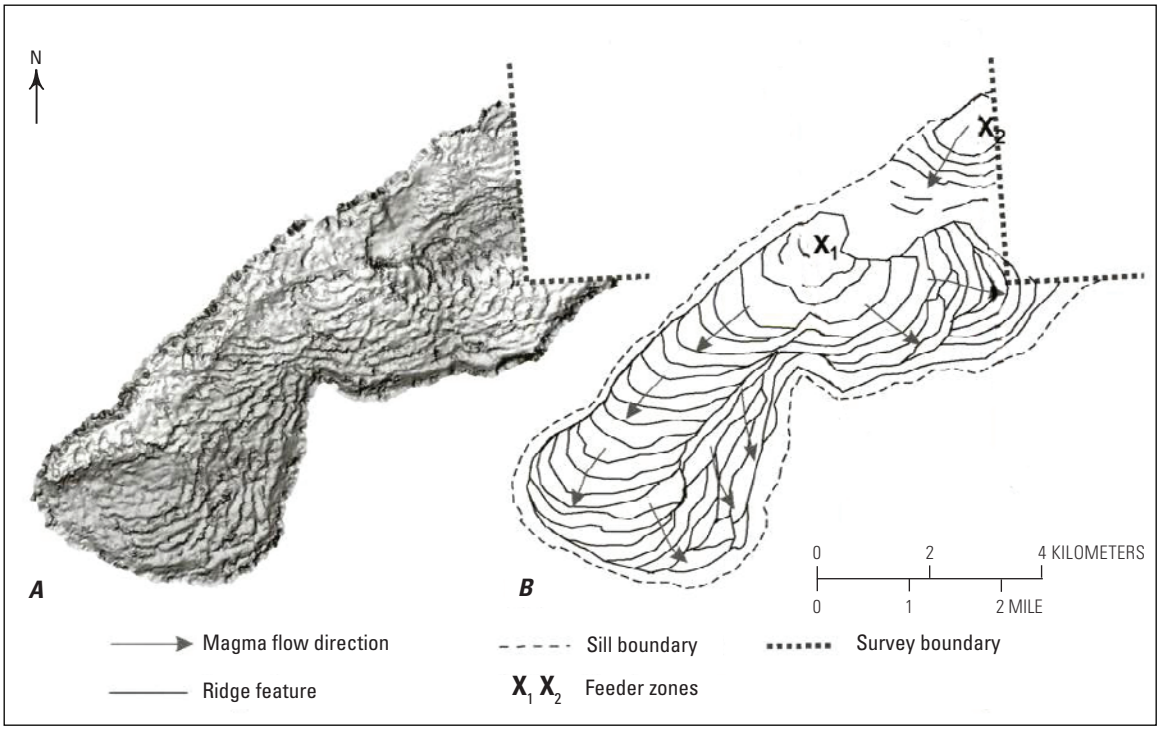

Figure 6–9. *A*, Horizon slice image of the top surface of a ridged sill in the Faroe-Shetland Basin, northeastern Atlantic Ocean margin. Schlumberger GeoViz software with false illumination from southeast. *B*, Simplified interpretation of the ridge features with proposed magma flow directions and magma feeder zones. Figure modified from Trude and others (2004).

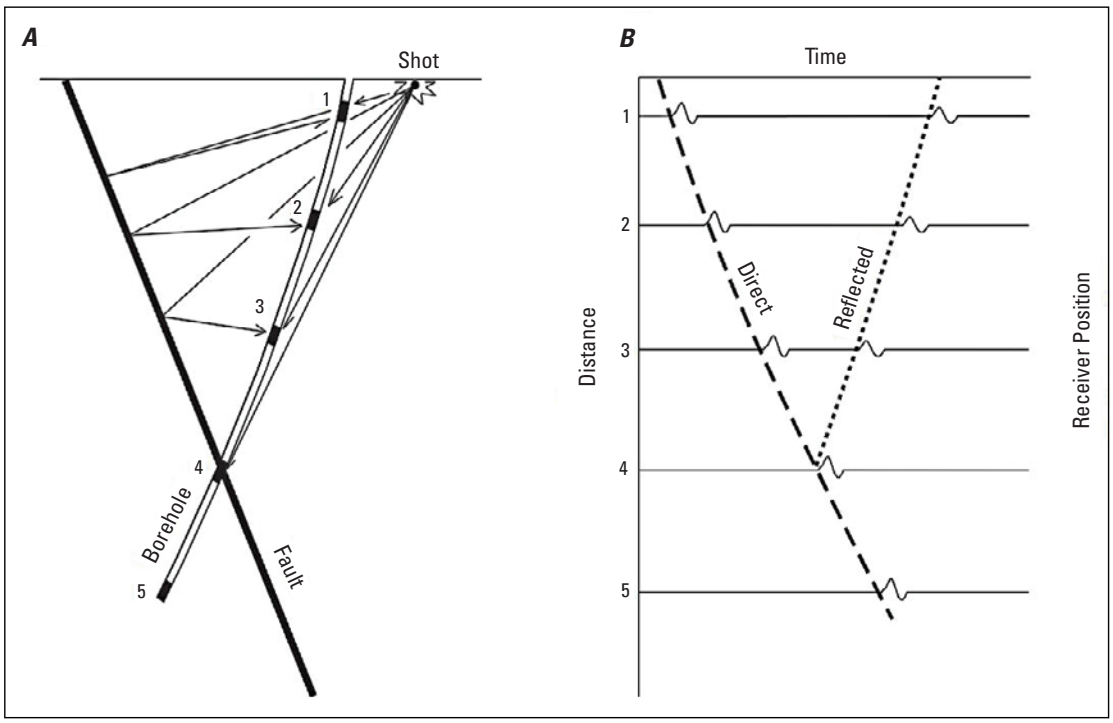

Figure 6–10. *A*, Fundamental layout for a vertical seismic profiling (VSP) survey. *B*, Distance-versus-time plot showing transit times for direct and reflected arrivals from a steeply dipping reflector. Figure modified from Salisbury and others (2007).

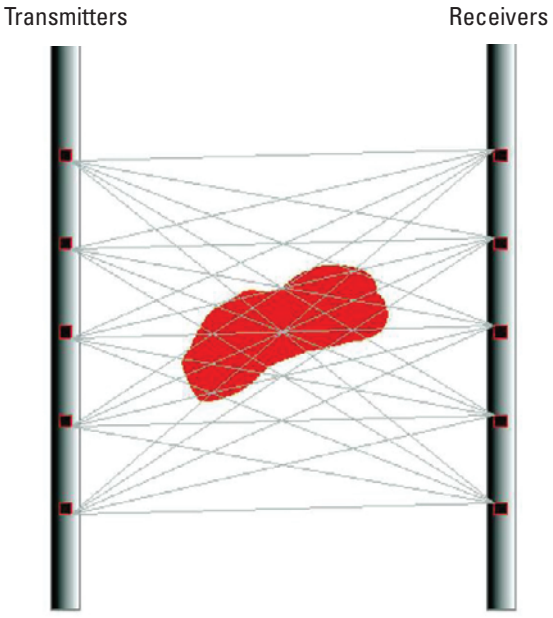

Figure 6–11. Schematic illustration of cross-hole seismic methods (red marks rock body). Modified from King (2007).

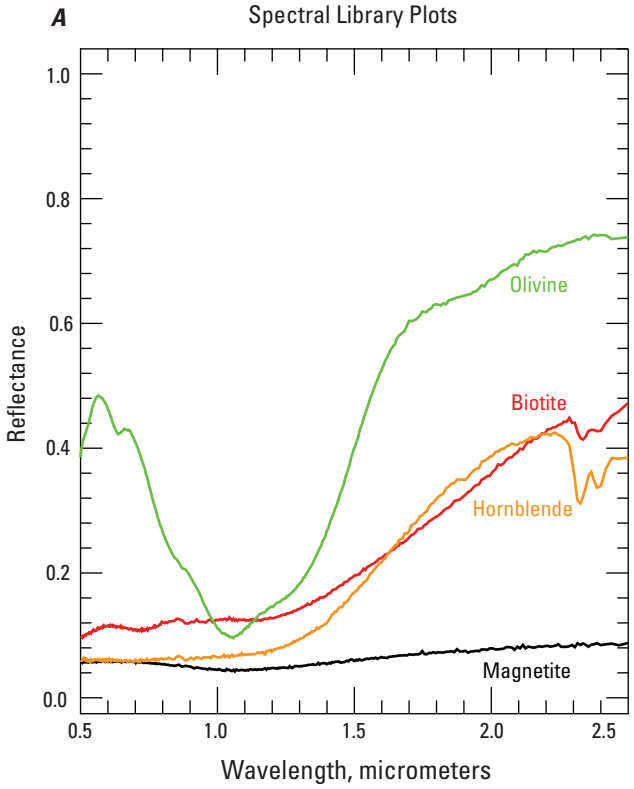

Figure 6–12. *A*, Visible-near infrared to short-wave infrared (VNIR–SWIR) reflectance sample library spectra of olivine, biotite, hornblende, and magnetite. Biotite, magnetite, and hornblende have low spectral reflectance when compared to olivine.

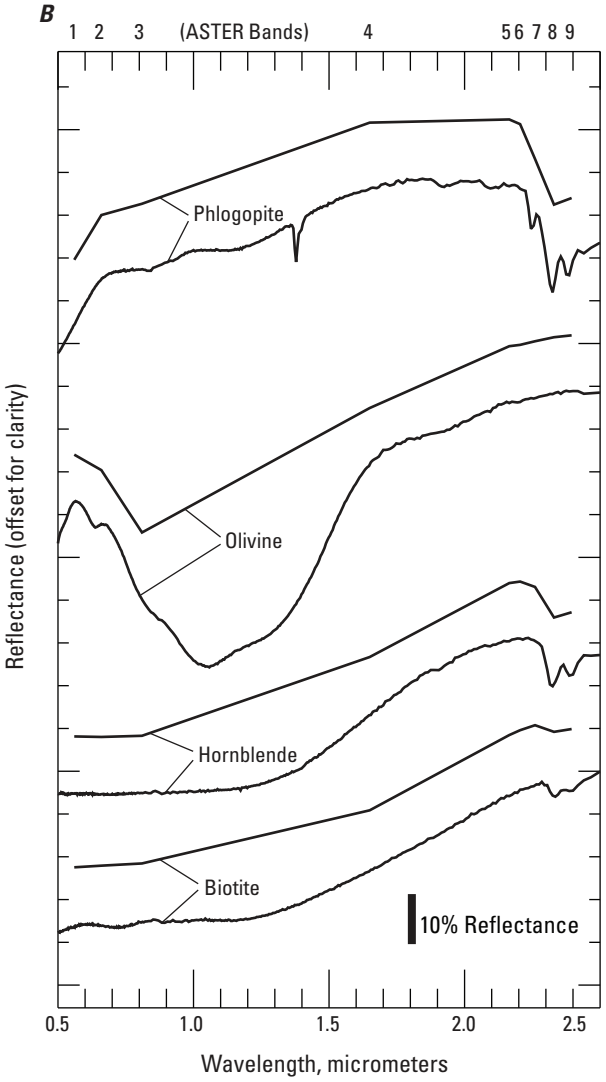

Figure 6–12. *B*, VNIR–SWIR reflectance sample library spectral pairs of biotite, hornblende, olivine, and phlogopite (lower spectrum) and the same mineral spectra resampled to Advanced Spaceborne Thermal Emission and Reflection Radiometer (ASTER) bandpasses (upper spectrum). The sample spectra biotite, hornblende, and phlogopite have 2.33- to 2.31-micrometer spectral absorption features illustrated in the ASTER spectra. Olivine has a 1.05-micrometer absorption feature expressed as low band-3 reflectance in the resampled ASTER spectrum. Spectra are offset for clarity of spectral shapes. The ASTER-band center positions are illustrated at top of graph.

Mafic and ultramafic host rocks for many deposits may be metamorphosed to greenschist facies. Serpentinization of mafic and ultramafic rocks forms serpentine, actinolite, epidote, and chlorite, which have prominent Fe(Mg)OH 2.31- to 2.33-micrometer absorption features (fig. 6–13). These minerals also have broad Fe^{2+} spectral absorption features in the 1.65- to 0.5-micrometer region (fig. 6–13). The feldspathic peridotite and altered gabbro metamorphosed to greenschist facies at the Eagle deposit exhibit low VNIR–SWIR reflectance and contain weak 2.31- to 2.33-micrometer spectral absorption features (fig. 6–14). Fifteen- and 30-m Advanced Spaceborne Thermal Emission and Reflection Radiometer (ASTER) VNIR–SWIR data also have been used to map the 2.31- to 2.33-micrometer spectral absorption features and low reflectance of mafic and ultramafic rocks in Mordor, Australia (Rowan and others, 2005).

Minerals associated with mafic and ultramafic rocks tend to have diagnostic spectral absorption features in the Thermal Infrared (TIR) 8.0- to 12.0-micrometer region (fig. 6–15). Fundamental vibrations of the Si-O bond in silicate minerals cause diagnostic emissive spectral absorption features from 9.75 to 11 micrometers in mafic and ultramafic minerals, such as olivine (10.2 micrometers), phlogopite (9.75 micrometers), hornblende (10.05 micrometers), diopside (10.25 and 10.8 micrometers), augite (10.25 and 10.9 micrometers), and biotite (9.8 micrometers) (fig. 6–15). Serpentinized mafic and ultramafic rocks also exhibit TIR spectral absorption features in the 9.75- to 11-micrometer region (fig. 6–15). Thus, mafic and ultramafic rocks, such as feldspathic peridotite and altered gabbro from the Eagle deposit and syenite, pyroxenite, and shonkinite rocks from Mordor in Australia, typically exhibit high emissivity in the 8- to 9-micrometer region and low emissivity in the 9- to 12-micrometer region (fig. 6–16; Rowan and others, 2005). Mafic and ultramafic rocks at Mordor also have been mapped successfully using ASTER TIR data (90-m resolution; Rowan and others, 2005). The ASTER 90-m resolution TIR data lack a spectral band positioned at 10 micrometers but still have sufficient spectral resolution to resolve diagnostic spectral absorption features of mafic-ultramafic mineral groups and rocks (figs. 6–15 and 6–16; Rowan and others, 2005).

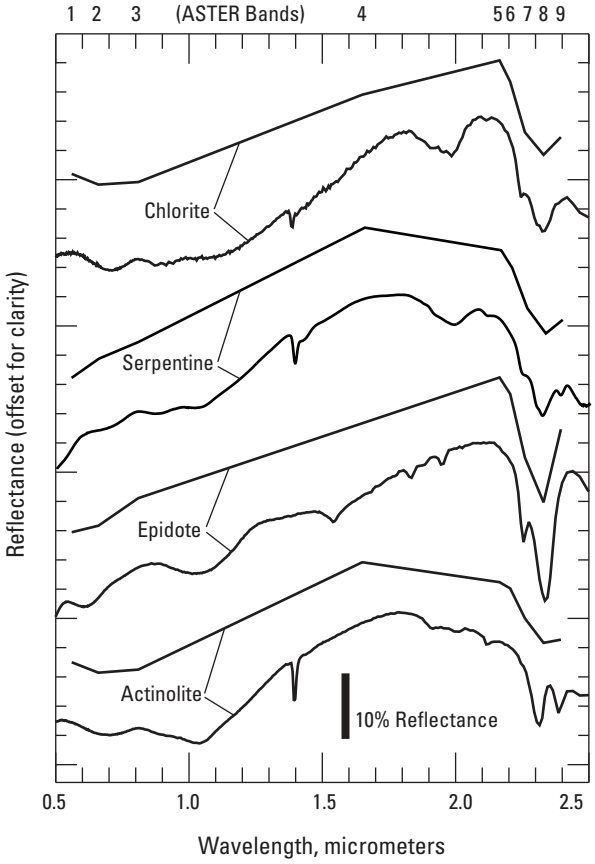

Figure 6–13. Visible-near infrared to short-wave infrared (VNIR–SWIR) reflectance sample library spectral pairs of actinolite, epidote, serpentine, and chlorite (lower spectrum) and the same mineral spectra resampled to Advanced Spaceborne Thermal Emission and Reflection Radiometer (ASTER) bandpasses (upper spectrum). The sample spectra have 2.33- to 2.31-micrometer spectral absorption features illustrated in the ASTER spectra. The spectra also exhibit broad Fe^{2+} absorption in the 0.5- to 1.65-micrometer region. Spectra are offset for clarity of spectral shapes. The ASTER-band center positions are illustrated at top of graph.

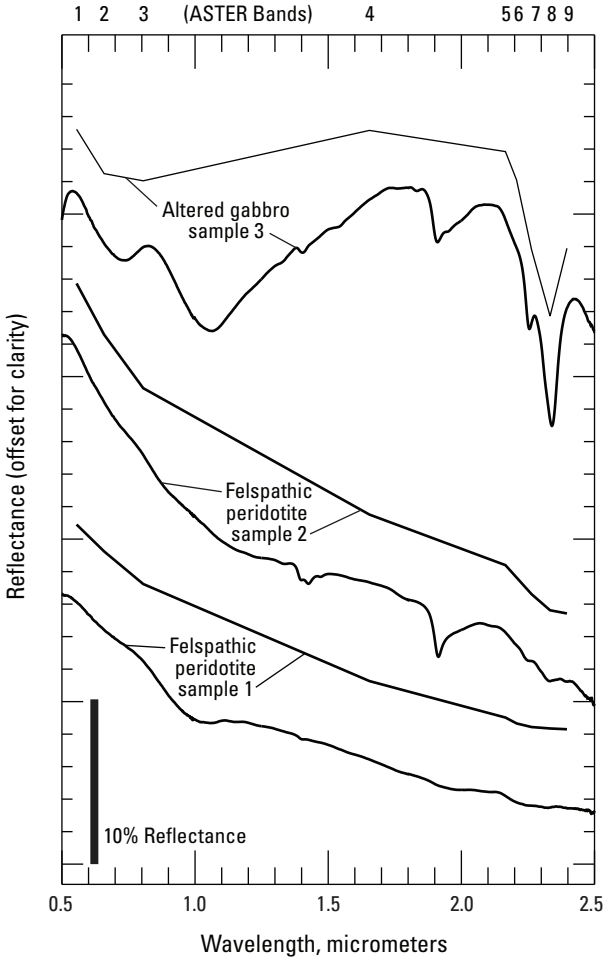

Figure 6–14. Thermal infrared (TIR) emissivity sample spectral pairs of mafic and ultramafic rocks and the rock spectra resampled to Advanced Spaceborne Thermal Emission and Reflection Radiometer (ASTER) bandpasses (upper spectrum). The sample spectra exhibit high emissivity in the 8- to 9-micrometer region. Spectra are offset for clarity of spectral shapes. The ASTER band center positions are illustrated at top of graph.

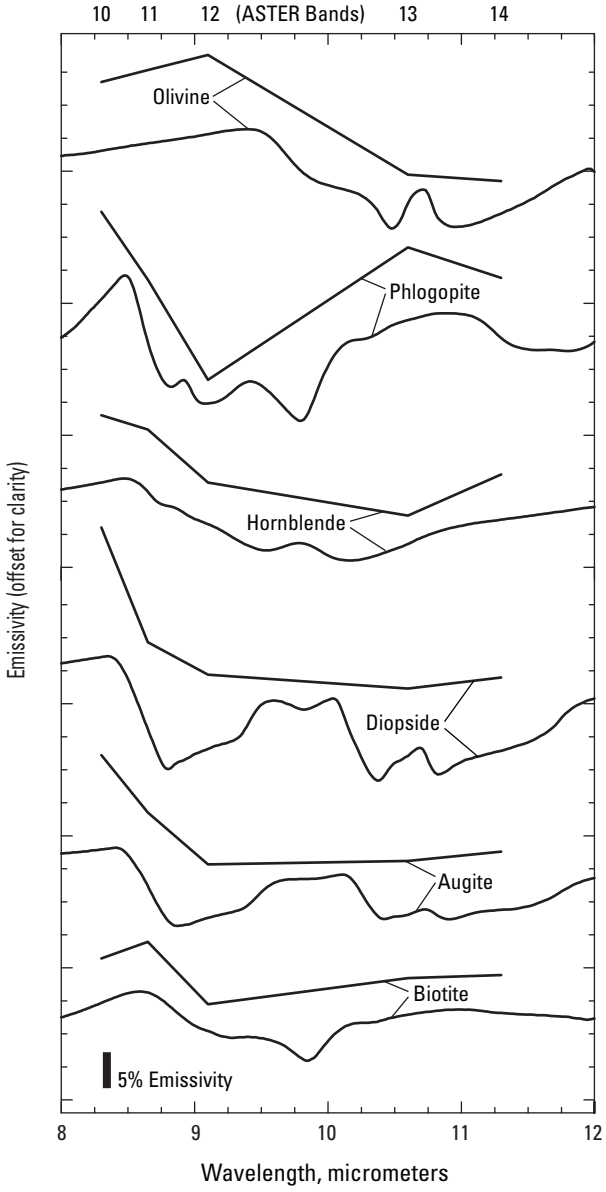

Figure 6–15. Thermal infrared (TIR) emissivity sample library spectral pairs of biotite, augite, serpentine, diopside, hornblende, phlogopite, and olivine (lower spectrum) and the same mineral spectra resampled to Advanced Spaceborne Thermal Emission and Reflection Radiometer (ASTER) bandpasses (upper spectrum). Sample spectra primarily have spectral absorption features in the 9- to 12-micrometer region illustrated in the ASTER spectra. Spectra are offset for clarity of spectral shapes. The ASTER band center positions are illustrated at top of graph.

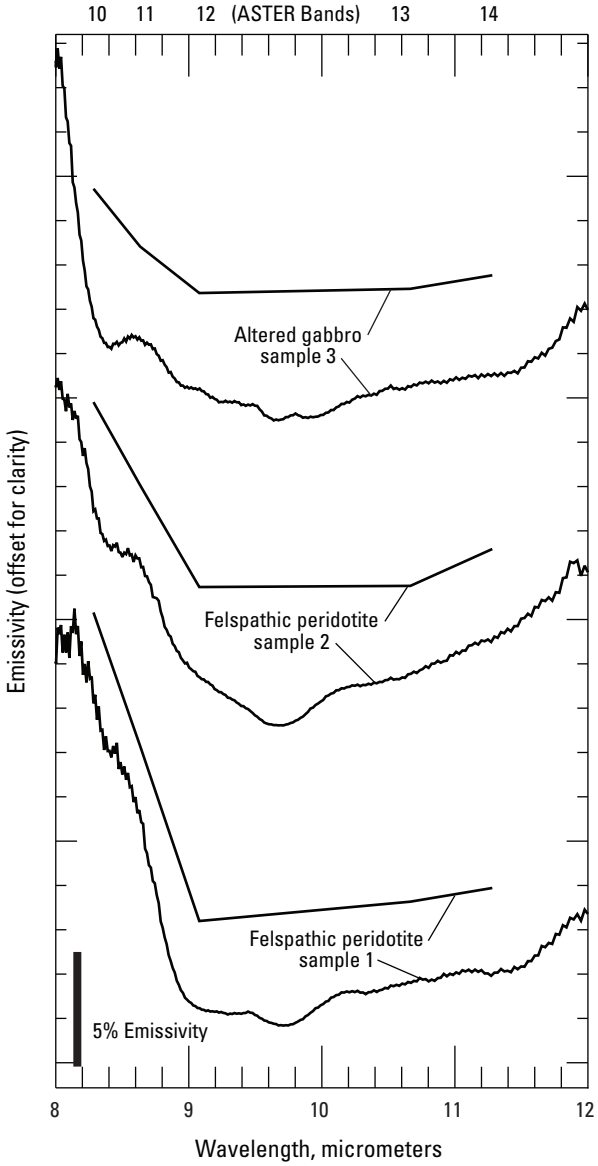

Figure 6–16. Thermal infrared (TIR) emissivity sample spectral pairs of mafic and ultramafic rocks and the rock spectra resampled to Advanced Spaceborne Thermal Emission and Reflection Radiometer (ASTER) bandpasses (upper spectrum). The sample spectra exhibit high emissivity in the 8–9 micrometer region. Spectra are offset for clarity of spectral shapes. ASTER band center positions illustrated on top of graph.

7. Hypogene and Supergene Ore Characteristics

Hypogene Ore Characteristics

Mineralogy and Mineral Assemblages

The hypogene ore minerals for magmatic Ni-Cu±PGE sulfide deposits are low-temperature assemblages of high-temperature sulfide liquids that have undergone fractionation, physical redistribution and separation, recrystallization with cooling, possible reheating and remelting by recurring igneous injections, and potential remobilization by both magmatic and nonmagmatic hydrothermal fluids. The dominant sulfide minerals in magmatic Ni-Cu±PGE deposits mainly are variants of Fe-, Cu-, and Ni-bearing sulfides, which typically are pyrrhotite, pentlandite, chalcopyrite, and, less consistently, cubanite and troilite (table 7–1).

The mineral assemblage of an individual ore body is dependent on many factors, including the composition of the silicate magma and contaminants, temperature of formation, chalcophile element concentrations, sulfur and oxygen fugacities, and the cooling history of the original immiscible high-temperature sulfide liquid. Within a district, different ore bodies may have different mineral assemblages depending on varying combinations of the factors listed above. For example, in the Ovoid deposit of the Voisey's Bay district, a high metal/sulfur ratio of the high-temperature sulfide liquid resulted in formation of abundant cubanite, rather than chalcopyrite, and troilite, rather than pyrrhotite. In contrast, at the Eastern Deeps deposit, cubanite is rare and troilite is absent, implying that the sulfide liquid had a much lower metal/sulfur ratio (Naldrett and others, 2000). Similar variations in primary sulfide mineralogy are observed among the different deposits at Noril'sk (Naldrett, 2004).

The occurrence of platinum group minerals (PGMs) in magmatic Ni-Cu±PGE deposits is of critical economic interest as PGE, typically present only in trace amounts, may ultimately make a Ni-Cu±PGE deposit economically viable. Noril'sk stands out among other major magmatic Ni-Cu±PGE sulfide deposits because of exceptionally high concentrations of PGE, possibly due to upgrading by influxes of new magma interacting with pre-existing sulfides (Naldrett, 2004). However, there are differences in PGE contents among Noril'sk deposits. Sulfides from the Talnakh area are one order of magnitude richer in PGE than sulfides from the Oktyabr'sky area (Barnes and others, 1997). At Noril'sk the majority of PGMs occur as coexisting minerals in disseminated ore, rather than in massive ore (Distler, 1994). The list of PGMs described for Noril'sk is given in table 7–2.

Table 7–1. Major and minor minerals, with chemical formula, typically found in magmatic Ni-Cu±PGE sulfide deposits.

Major minerals	Formula
Monoclinic pyrrhotite	Fe_9S_{10}
Hexagonal pyrrhotite	$Fe_{11}S_{12}$
Troilite	FeS
Chalcopyrite	$CuFeS_2$
Talnakhite	$Cu_9(Fe,Ni)_8S_{16}$
Mooihoekite	$Cu_9Fe_9S_{16}$
Putoranite	$Cu_9(Fe,Ni)_9S_{16}$
Pentlandite	$(Fe,Ni)_9S_8$
Cubanite	Fe_2CuS_3
Magnetite	Fe_3O_4
Minor/secondary minerals	**Formula**
Bornite	Cu_5FeS_4
Bravoite	$(Fe,Ni)S_2$
Digenite	Cu_9S_5
Cassiterite	SnO_2
Chalcocite	Cu_2S
Covellite	CuS
Galena	PbS
Gersdorffite	NiAsS
Haycockite	$Cu_4Fe_5S_8$
Ilmenite	$FeTiO_3$
Linnaeite	Co_3S_4
Mackinawite	$(Fe,Ni)S_{0.9}$
Marcasite	FeS_2
Maucherite	$Ni_{11}As_8$
Melonite	$NiTe_2$
Millerite	NiS
Native bismuth	Bi
Native copper	Cu
Native gold	Au
Native platinum	Pt
Native silver	Ag
Niccolite	NiAs
Parkerite	$Ni_2Bi_2S_2$
Pyrite	FeS_2
Sphalerite	ZnS
Tsumonite	AgTe
Violarite	Ni_3S_4

Table 7–2. Platinum-group element (PGE) minerals reported for Ni-Cu-sulfide deposits from Noril'sk, Russia (Distler, 1994).

PGE minerals	Formula
Atokite	Pd_2Sn
Braggite	(Pt,Pd,Ni)S
Cabriite	Pd_2SnCu
Cooperite	PtS
Froodite	$PdBi_2$
Geversite	$PtSb_2$
Hessite	Ag_2Te
Hollingworthite	(Rh,Pt,Ru,Ir)AsS
Insizwaite	PtB_2
Isoferroplatinum	Pt_3Fe
Isomertieite	$Pd_{11}Sb_2As_2$
Kharayelakhnite	$(Cu,Pt,Fe,Pb,Ni)_9S_8$
Kotulskite	PdTe
Laurite	RuS_2
Majakite	PdNiAs
Maslovite	PtBiTe
Menshikovite	$Pd_3Ni_2As_3$
Merenskyite	$Pd(Te,Bi)_2$
Mertieite II	$(Pd,Pt)_8(Sb,As)_3$
Michenerite	PdBiTe
Moncheite	PtT_2
Niggliite	PtSn
Palarstanide	$Pd_5(As,Sn)_2$
Palladoarsenide	Pd_2As
Paolovite	Pd_2Sn
Plumbopalladinite	Pd_3Pb_2
Polarite	Pd(Bi,Pb)
Rustenburgite	Pt_3Sn
Sobolevskite	PdBi
Sopcheite	$Ag_4Pd_3Te_4$
Sperrylite	$PtAs_2$
Stannopalladinite	$(Pd,Pt)_5Sn_2Cu$
Stibiopalladinite	Pd_5Sb_2
Stillwaterite	Pd_8As_3
Sudburyite	PdSb
Taimyrite	$(Pd,Pt)_9Sn_4Cu_3$
Telargpalite	$(Pd,Ag)_3T$
Tetraferroplatinum	PtFe
Tulameenite	Pt_2FeCu
Urvantsevite	$Pd(Bi,Pb)_2$
Vincentite	Pd(As,Te)
Vysotskite	(Pd,Ni)S
Zvyagintsevite	Pd_3Pb

Paragenesis

Paragenesis is the sequence of mineral deposition in an ore body. Determining the paragenesis of magmatic Ni-Cu±PGE sulfide deposits is complicated by the recrystallization of early formed sulfides and the potential for separation of solids and liquids during cooling and fractionation of the sulfide liquid. The concentrations of metals and sulfur in a silicate magma and the timing of the development of an immiscible sulfide liquid from its silicate host influence the partitioning of chalcophile elements into the immiscible sulfide liquid. At high temperatures, Ni, Cu, Co, Ag, Au, and PGE strongly partition into a sulfide liquid from silicate magma. Copper and Ni have relatively high sulfide/silicate liquid partition coefficients ($D = 10^2$ to 10^3; Peach and others, 1990; Peach and Mathez, 1993), whereas PGE have extremely high partition coefficients ($D = 10^3$ to 10^4; Peach and others, 1990; Fleet and others, 1999). The ultimate concentrations of Ni, Cu, and PGE in a sulfide liquid are controlled not only by their relative partition coefficients, but also by the R-factor, the relative mass ratio between silicate liquid and sulfide liquid (Campbell and Naldrett, 1979).

Immiscible sulfide liquids fractionate as they cool, and the fractionation path has a direct influence on sulfide mineralogy and metal contents. A schematic of an idealized fractionation path for a cooling sulfide liquid that has segregated from its host silicate magma is presented in figure 7–1. Chalcophile elements concentrate into a high-temperature, homogeneous sulfide liquid (fig. 7–1*A*). With initial cooling, an Fe-rich monosulfide solid solution (MSS) crystallizes (Naldrett and others, 1967; Kullerud and others, 1969) (fig. 7–1*B*). Iron, Os, Ir, Ru, and Rh partition into MSS, whereas Cu, Co, Au, Ag, Pd, and Pt remain in the co-existing sulfide liquid (Barnes and others, 1997; Mungall and others, 2005). Any Bi, Te, As, and Sb present in the silicate magma will accumulate in the Cu-rich liquid (Howell and McDonald, 2010). The partitioning of Ni between MSS and the Cu-rich sulfide liquid is complex and dependent on temperature, as well as sulfur and oxygen fugacities (Mungall and others, 2005). Nickel is moderately incompatible with MSS at temperatures >1,150 °C, whereas at temperatures <1,100 °C, Ni becomes moderately compatible with MSS (Barnes and Lightfoot, 2005; Barnes and others, 2006). Experiments by Mungall and others (2005) found that though the partition coefficient between Ni and MSS was variable, Ni ultimately was incompatible with MSS at all experimental conditions, although less incompatible than Cu. Cobalt can behave similarly to Ni, with a slight preference for the Cu-rich liquid at high temperatures and a slight preference for Fe-rich sulfides at low temperatures (Fleet and others, 1993, Barnes and others, 1997). With continued cooling, the Cu-rich sulfide liquid crystallizes to intermediate solid solution (ISS) (fig. 7–1*C*). Palladium, Pt, and Au do not partition into ISS, but rather concentrate into a residual sulfide liquid. At temperatures below 600 °C, MSS undergoes subsolidus conversion to pyrrhotite and pentlandite (Naldrett and others, 1967), and ISS

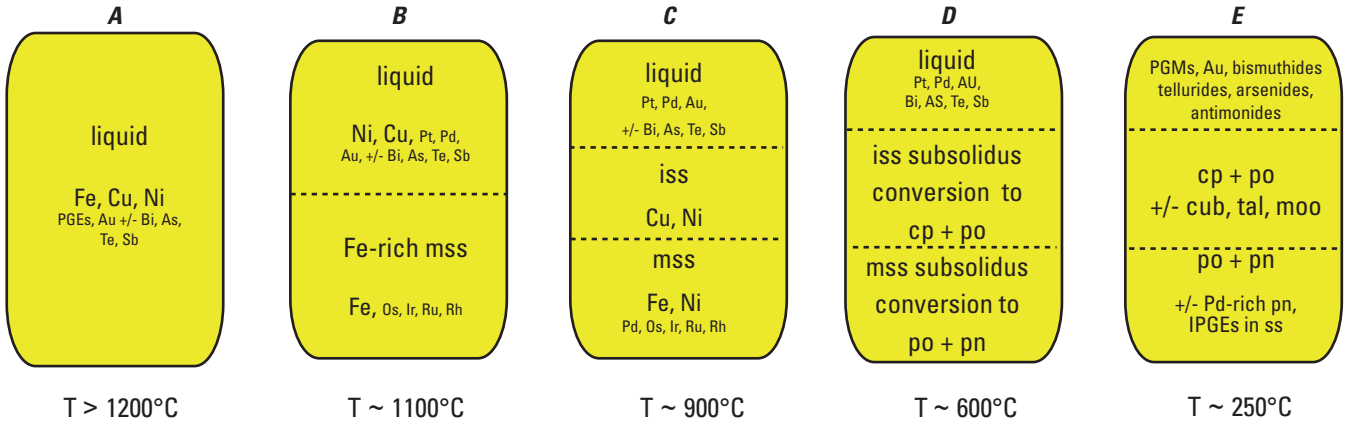

Figure 7–1. Idealized fractionation path of an immiscible high-temperature sulfide liquid: *A*, chalcophile elements strongly partition in a high-temperature, immiscible sulfide liquid; *B*, as the sulfide liquid cools, Fe-rich monosulfide solid solution (MSS) crystallizes; *C*, with continued cooling to about 900 °C, the Cu-rich liquid crystallizes to intermediate solid solution (ISS); *D*, below 600 °C, ISS begins to exsolve to chalcopyrite (cp) and pyrrhotite (po), and MSS begins to exsolve to pyrrhotite and pentlandite (pn); *E*, below 250 °C, Cu-rich minerals include chalcopyrite, cubanite (cub), talnakhite (tal) and moohoekite (moo). The size of an element's name in the illustration represents its relative abundance. Figure modified after Prichard and others (2004), Barnes and others (2006), and Howell and McDonald (2010).

converts to pyrrhotite and chalcopyrite, with lesser cubanite, mooihoekite, and talnakhite (Cabri, 1973; Craig and Scott, 1974; Naldrett, 1989) (fig. 7–1*D*).

The behavior of PGE in the fractionation of a sulfide liquid can be dependent on the presence or absence of semimetals such as Bi, Te, Sn, and As. Because of strong bonding with these semimetals, Pd and Pt concentrated in residual liquids with Bi, Te, Sn, and As will form late-stage PGM bismuthide, telluride, antimonide, and arsenide minerals (Hemley and others, 2007). In the Noril'sk deposits, Genkin and Evstigneeva (1986) suggested that Pt, Pd, Sn, Te, Pb, As, Sb, and Bi were concentrated in a Cu-rich liquid that accumulated in pockets along the upper contacts of the ore bodies or filled veins crosscutting the massive base-metal sulfides. In the absence of these semimetals, Pt and Pd will enter the lattice of high-temperature sulfides and subsequently exsolve as lamellae in pentlandite (Barnes and others, 2006). In sulfide droplets from the Medveszky Creek mine at Noril'sk, which mainly preserves a closed sulfide fractionation sequence, Barnes and others (2006) concluded that Pd was mostly concentrated into pentlandite; Os, Ir, Re, and Rh were concentrated into both pyrrhotite and pentlandite that exsolved from MSS; and Au and Pt were retained in the final fractionated liquid to form discrete grains among ISS minerals.

The sulfide liquid fractionation path in figure 7–1 represents the ideal path that may not reflect the nonideal physical world. Analyses of MSS cumulates often have much higher concentrations of incompatible elements than would be expected by sulfide liquid fractionation (Mungall and others, 2005). Mungall and others (2005) suggested that deviations from an ideal sulfide fractionation path may best be explained by adopting a model of equilibrium crystallization for sulfide melt. Mungall (2007) has constructed an empirical thermodynamic model for magmatic sulfide crystallization supporting the conclusion that Ni is incompatible for all sulfide magma compositions until very high Ni contents and very low temperatures are reached. Mungall (2007) recommends that all sulfides in a magmatic system be considered as cumulates rather than products derived from residual liquids. Thus, it is likely that the pattern of element distribution between a sulfide liquid and silicate magma falls along a continuum between fractional crystallization and equilibrium crystallization of the sulfide liquids, constrained by always unique physical parameters and events.

A complication in parsing element partitioning behavior among sulfide species based on observations of sulfide minerals in silicate rocks is the fact that the mineral paragenesis and suggested element distributions (fig. 7–1) may be radically modified by later events. During final cooling, many elements may diffuse into different sulfide phases, which complicate the simple zoning patterns (fig. 7–1*E*). For example, at Voisey's Bay, high-temperature hexagonal pyrrhotite recrystallized into monoclinic pyrrhotite, and troilite exsolved from sulfur-poor hexagonal pyrrhotite (Naldrett and others, 2000).

In a dynamic magmatic environment, there is potential for modification and redistribution of fractionating sulfide liquids and crystallized sulfides. At the Eastern Deeps deposit in Voisey's Bay, massive sulfide is rich in Os, Ir, Ru, and Rh, but depleted in Pt, Pd, Au, and Cu. This indicates that during fractionation, the bulk of the Cu-rich sulfide liquid was displaced from crystallizing MSS (Naldrett and others, 2000). At the Noril'sk–1 deposit, massive Ni-rich ore and related Cu-rich ore were mined, but an upper Cu-rich ore, typically found at other deposits in the district, was missing, although PGE-rich low-sulfide mineralization was well-developed (Naldrett, 2004).

Early formed sulfides collected in some type of conduit or other trap may be modified by interaction with new, hot silicate magma (fig. 3–2*B*). New magma pulses may partly disaggregate and remelt previously formed sulfides or upgrade metal tenor through interaction of early formed sulfide with later batches of metal-bearing silicate magma (Kerr and Leitch, 2005). Li and others (2009) suggested that an influx of new, fertile magma interacting with sulfide was responsible for upgrading of sulfide tenor, particularly for PGE, in the Talnakh deposit, Noril'sk. In the Jinchuan deposit, disseminated sulfides that did not form a continuous network, particularly sulfides trapped near the margins of the ore bodies, have lower Ni contents and form an envelope surrounding higher grade ore. This suggests that metal contents of early formed sulfides in the central parts of ore bodies were upgraded by interaction with influxes of fresh magma (Chai and Naldrett, 1992). Kerr and Leitch (2005) also suggested that dissolution of early formed sulfides could proceed to completion, with sufficient new magma input; in other words, all sulfide liquid could be dissolved and metals reincorporated into the silicate magma. They pointed out that this scenario has important implications for mineral assessment because metal-distribution patterns in such a situation would not be informative of mineralization potential.

Because a late-stage Cu-rich liquid does not crystallize until its temperature is <850 °C, but an enclosing silicate matrix becomes mostly solid by 1,000 °C, there can be a stark contrast in the behavior of a sulfide liquid and its brittle silicate matrix under deformation stress. Barnes and others (1997) proposed that on-going magma movement in an intrusive system has the potential to create fractures and to open spaces in both host rocks and country rocks such that late-stage Cu-rich sulfide liquids may be injected into interstitial and fracture spaces, effectively removing late liquids from proximity to crystallized MSS. The migration of residual Cu-rich liquids may be enhanced because, with increasing Cu and decreasing sulfur contents, those residual liquids develop strong wetting abilities against silicates (Naldrett, 1969). The capacity for redistribution of late-stage Cu-rich sulfides is an explanation for the commonly reported occurrence of fractures and breccias filled with Cu-rich sulfides at many deposits, including "Upper Copper Ore" at the Kharaelakh intrusion at Noril'sk (Naldrett and others, 1994). At Pechenga, it was suggested that chalcopyrite-rich veins formed when a Cu-rich residual liquid was squeezed into surrounding sediments (Brügman and others, 2000). Also, at the Eagle deposit in Michigan, Cu-rich veins with variable mineralogy cut the surrounding metasedimentary country rocks (Ding and others, 2010).

Zoning Patterns

The fractionation path in figure 7–1 implies a closed system and is in part modeled on the mineralogy and chemistry of confined sulfur droplets that typically have a pyrrhotite bottom and a chalcopyrite top, as described for Noril'sk (Barnes and others, 2006), Waterfall Gorge at Insizwa, South Africa (Lightfoot and others, 1984), and the Crystal Lake intrusion in Ontario, Canada (Cogulu, 1993). In general, the mineralogy and distribution of elements and minerals within crystallized sulfide globules mimics the mineralogy of larger deposits. For example, the Ovoid deposit at Voisey's Bay has a large basal zone of massive sulfide that was interpreted to have crystallized from the base upward, with a fractionated, residual liquid enriched in Cu, Au, Pd, and Pt concentrated near the top (Naldrett and others, 2000). Chai and Naldrett (1992) described similar mineralogical zoning for the Jinchuan deposit. In the western ore bodies at Jinchuan, Ni, Cu, and PGE contents increase from the margins to the center of the bodies.

Two types of mineral zoning, complex and simple, are recognized in massive ores in the Talnakh area of Noril'sk. Simple zoning mimics the fractionation sequence described above for a sulfide liquid, with gradual changes in the ore-mineral assemblage due to changes in the proportions of pyrrhotite and chalcopyrite (Torgashin, 1994). At Talnakh, ores change from pyrrhotite to pyrrhotite+chalcopyrite to chalcopyrite+pyrrhotite to chalcopyrite, with pentlandite present with all assemblages (Torgashin, 1994). Massive ores that occur in intrusive rocks display complex zoning, with a roughly spherical pattern of varying mineralogy that defines zones based on Cu content, as shown by the Oktyabr'sky massive sulfide body (fig. 7–2). Pentlandite occurs throughout the ore body. Ores with the lowest Cu content surround ores with increasing Cu contents, with maximum Cu content in the center of the massive sulfide body (fig. 7–2; Distler, 1994; Torgashin, 1994). Platinum-group element concentrations at Oktyabr'sky have a similar zoning pattern. Lower-position and marginal ores mainly are Fe-Os-Ir-Ru-Rh-rich pyrrhotite ores, whereas the central overlying ores are Cu-Pd-Pt-Au-rich chalcopyrite and mooihoekite (Distler, 1994; Barnes and Lightfoot, 2005; Gorbachev, 2006). Platinum and Pd in the central area are found as PGMs, rather than in solid solution (Distler, 1994).

This zoning pattern generally is attributed to fractionation of an immiscible sulfide liquid (Torgashin, 1994; Zientek and others, 1994; Gorbechev, 2006). The sulfide ores are composed of pyrrhotite and pentlandite, typically containing several weight percent Ni and <3 weight percent Cu, and represent a primary magmatic cumulate of MSS with minimal trapped intercumulus sulfide liquid. The sulfide rocks, composed of pyrrhotite, pentlandite, and chalcopyrite, but typically containing <3 weight percent Ni and as much as 35 weight percent Cu, represent fractionated sulfide liquids removed from the MSS cumulates.

In deposits that have undergone post-depositional metamorphism and deformation, however, such as Pechenga (Distler and others, 1990) or Baimazhai in China (Zhang and others, 2006), the distribution pattern for sulfide minerals and metals may be significantly different from patterns expected for mainly unmetamorphosed magmatic deposits. Zhang and others (2006) suggested that the occurrence of

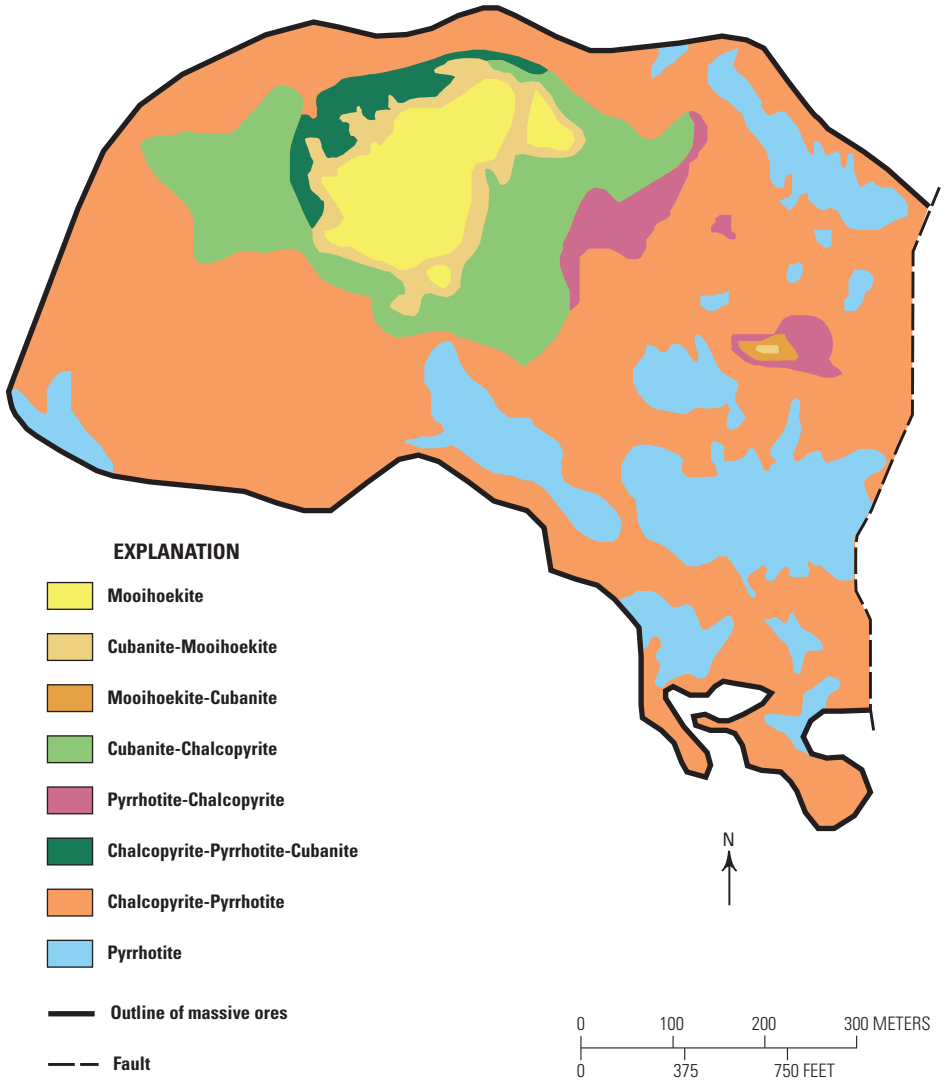

Figure 7–2. Plan map of mineral-assemblage zonation in massive sulfide ores in the Oktyabr'sky mine area, Kharayelakh intrusion, Noril'sk region, Russia. Figure modified after Torgashin (1994).

"alteration-modified" sulfides, enriched in Cu, Au, and Pd, with hydrous silicates, is the result of the pervasive hydrothermal alteration of the sulfide body at the Baimazhai deposit.

Textures and Structures

For the most part, sulfides in magmatic deposits worldwide may be divided into disseminated sulfides, matrix- or net-textured sulfides, and massive sulfide, based on the relative percentages of sulfides and silicates and the rock texture. Sulfide mineralization also can occur with tectonic and magmatic breccias and in veins cutting earlier ore or country rock. Where sulfides are not connected to one another, the texture is considered to be disseminated. Disseminated sulfides occupy from 1 to about 33 percent of a rock and typically fill interstitial space between silicate minerals. Disseminated sulfides commonly are 1-mm to 10-mm irregular sulfide patches interstitial to silicate and oxide minerals. At some deposits, such as Medvezky Creek, Noril'sk, Russia, (Barnes and others, 2006), disseminated sulfides also occur as small (1 to 10 cm) sulfide droplets crystallized into rounded forms of globular sulfide that may have a chalcopyrite (Cu-rich) top and a pyrrhotite (Fe-rich) bottom, mimicking liquid sulfide fractionation.

Net-textured or matrix-textured sulfides are interconnected to form a matrix with silicate minerals and occupy about 33 to 66 percent of the space. A variant of net texture is "leopard texture," a term used to describe sulfide with black

spots of augite and olivine oikocrysts in a yellow sulfide matrix common at the Eastern Deeps deposit at Voisey's Bay, Labrador (Evans-Lamswood and others, 2000).

When sulfide exceeds 66 percent of the rock volume, it is considered semi-massive to massive. Massive sulfides typically can be divided further into contact sulfides, which occur along or near the lower contact between mafic rocks and country rocks, or vein sulfides, which occur in offshoots from the main massive sulfide body (Barnes and others, 1997).

At Voisey's Bay, mineralization occurs as semi-massive to massive sulfide, leopard-textured sulfides, magmatic breccias with medium- to coarse-grained blotchy sulfides, and locally disseminated sulfides (Evans-Lamswood and others, 2000; Naldrett and others, 2000). In a conduit-style deposit such as Voisey's Bay, magma dynamics and conduit geometry, rather than simple gravitational settling, controlled ore textures (Evans-Lamswood and others, 2000). Sulfides entrained in magma moving through a conduit are concentrated preferentially in traps where physical irregularities in dike morphology, such as swelling and pinching or splaying, favor precipitation, capture, and preservation of sulfides due to resultant changes in magma velocity and viscosity (Evans-Lamswood and others, 2000). The Reid Brook mineralized zone is a near-vertical, thickened part of the Voisey's Bay feeder conduit with mineralized leopard-texture sulfides enclosed by mineralized breccias and transected by steep massive sulfide veins. The Ovoid deposit is a flat-lying concave-shaped lens of massive sulfide enclosed in mineralized leopard-textured troctolite and breccias in a widened part of the feeder conduit. The Eastern Deeps, located where the feeder conduit widened into a larger magma chamber, exhibits a massive sulfide lens enclosed in a complex mineralized sheath of leopard-textured troctolite and breccia (Evans-Lamswood and others, 2000). These ore types represent sulfide-enriched traps in the feeder conduit: where the through-going flow of magma physically changed, and suspended droplets of immiscible sulfide liquid settled gravitationally out of the moving magma, thus producing sulfide accumulations that crystallized to form massive Ni-Cu±PGE sulfide.

At the Baimazhai magmatic Ni-Cu±PGE deposit, China, massive sulfide forms an inner core surrounded by orthopyroxenite, websterite, and gabbro (Wang and Zhou, 2006). Massive sulfide ores are composed mainly of pyrrhotite, with lesser pentlandite and chalcopyrite. The massive ores generally have sharp contacts with net-textured ores that fill interstitial voids in orthopyroxene cumulates (Wang and Zhou, 2006). Coarse-grained pyrrhotite commonly is associated with pentlandite that occurs as rims surrounding pyrrhotite, as oriented lamellae, or as blades along fractures and grain boundaries (Wang and Zhou, 2006). Chalcopyrite forms variably sized anhedral grains and typically occurs as aggregates in interstices between pentlandite, pyrrhotite, and magnetite grains. Wang and Zhou (2006) determined the order of crystallization for ore minerals at Baimazhai as magnetite, then pyrrhotite+pentlandite, and finally, chalcopyrite.

Massive sulfide at Uitkomst, South Africa, occurs as a series of lenticular bodies, which originally may have been a single body prior to tectonism, located in the immediate footwall of a tabular intrusion (Maier and others, 2004). In contrast, in massive ore at Jinchuan, China, pyrrhotite and pentlandite generally form a banded texture with disseminated chalcopyrite and magnetite, which Chai and Naldrett (1992) took as evidence that the massive sulfide was affected by stress and that sulfide melt flowed during crystallization. At Pechenga, Russia, ore types are classified as magmatic-textured and include disseminated sulfides in mafic-ultramafic intrusions and brecciated and veined ore in fault zones (Distler and others, 1990).

At a number of deposits, such as Jinchuan, Voisey's Bay, and Noril'sk, massive ore or ore breccias locally cut host rocks or are found within underlying country rock. Those occurrences indicate that the ores may have been injected at or near the base of intrusions as separate pulses of massive sulfide liquid or sulfide-rich breccias (Arndt and others, 2005). The movement of dense sulfide liquids invoked for this mode of occurrence suggests mobilization during structural readjustments or deformation along pre-existing structures.

Grain Sizes

Grain size varies across deposits. In massive sulfide from Voisey's Bay, pyrrhotite occurs as very coarse crystals, exceeding 10 cm in diameter in some samples. Pentlandite is characterized by coarse grains 1 to 2 cm in diameter, except at the Eastern Deeps where coarse pentlandite is rare, and pentlandite more typically forms rims surrounding pyrrhotite crystals or occurs as lamellae within pyrrhotite (Naldrett and others, 2000). Troilite, where present, occurs as fine exsolution lamellae in pyrrhotite, and cubanite occurs as discrete grains and exsolution lamellae in chalcopyrite (Naldrett and others, 2000). At Noril'sk, pyrrhotite grain size ranges from very fine (< 1 mm) to very coarse (>10 cm in so-called "pegmatoid ore"; Stekhin, 1994). That coarse pyrrhotite always contains flame pentlandite lamellae. Where present, PGEs typically form small euhedral crystals (0.005 to 0.2 mm) at the boundaries of Ni-Cu sulfides (Distler and others, 1990; Chai and Naldrett, 1992). At the Eagle deposit, Michigan, pentlandite occurs both as early formed euhedral crystals and as late-stage exsolution lamellae and flame structures in pyrrhotite (Kooistra and Chesner, 2010). Chalcopyrite is massive or occurs as exsolution lamellae in generally massive pyrrhotite (Kooistra and Chesner, 2010). Pyrrhotite at Jinchuan forms anhedral to subhedral 0.1- to 3-mm crystals; pentlandite commonly forms subhedral to euhedral 0.1- to 2-mm crystals enclosed by anhedral pyrrhotite (Chai and Naldrett, 1992). Exsolution flames of pentlandite in pyrrhotite are rare at Jinchuan, in contrast to textures at Noril'sk, where flame pentlandite is very common (Chai and Naldrett, 1992).

Supergene Ore Characteristics

Supergene processes can affect all types of mineral deposits, and supergene enrichment can provide an important upgrade in the metal tenor, especially for some iron, nickel, gold, and copper deposits. Such processes are not generally significant, however, either for development or further enrichment of mafic- and ultramafic-hosted Ni-Cu±PGE sulfide deposits. The gossans that can develop from weathering of sulfides can be important guides to mineralization. Gossans represent advanced chemical weathering in which sulfide minerals are extensively oxidized and leached of most metals, leaving behind hydrated iron oxides and, rarely, sulfates. Gossans can be very large and may be targeted remotely using various satellite and airborne multispectral and hyperspectral data because iron oxides and hydrous iron oxides possess distinctive spectral signatures in the VISNIR range (Hunt and Ashley, 1979). The gossan zone at Voisey's Bay is very large and easily can be seen from the air. It had been mapped as a "pyritic gossan" by government geologists before two prospectors looking for diamond indicators found chalcopyrite stringers in freshly broken gossan. A subsequent geochemical prospecting program in the area eventually resulted in recognition of disseminated Ni-Cu-Co mineralization on Discovery Hill, leading to the initial diamond-drill discovery holes. Following the Voisey's Bay discovery, exploration activity in northern Labrador rapidly expanded, and gossans were a significant target that focused geophysical exploration (Kerr and Smith, 1997).

8. Hypogene Gangue Characteristics

Mineralogy and Mineral Assemblages

Gangue mineralogy for magmatic Ni-Cu±PGE deposits can be divided into three categories: (1) magmatic silicates and oxides of the mineralized host mafic-ultramafic intrusion, (2) minerals in partially ingested xenoliths and hornfelsed country rock, and (3) metamorphic minerals from magmatic hydrothermal and post-deposition metamorphic events. Magmatic gangue minerals for most deposits are the minerals of the host mafic and ultramafic silicate rocks. Typical minerals primarily are olivine, orthopyroxene, clinopyroxene, plagioclase, magnetite, ilmenite, and Cr-spinel. At Pechenga, minerals in the ultramafic intrusions also include magmatic kaersutite [$NaCa_2(Mg_4Ti)Si_6Al_2O_{23}(OH)_2$] and Ti-bearing phlogopite [$KMg_3(Si_3Al)O_{10}(F,OH)_2$] (Hanski and Smolkin, 1995).

Minerals formed by reactions with country rock, either by contact metamorphism or by ingestion of xenoliths, are much more complex because of the wide range of lithologies enclosing mineralized host rocks. Xenoliths may be incorporated into magma by thermal erosion of conduit walls. At Voisey's Bay, contaminating country rock generally is orthogneiss or paragneiss. Near-total fusion of gneissic xenoliths in magma produced immiscible aluminous liquids, garnet oxidized to form hercynite and magnetite, hypersthenes and potassium feldspar reacted together to also produce hercynite, and plagioclase broke down to produce corundum (Li and Naldrett, 2000). At Noril'sk, metamorphism of sedimentary country rock, which there includes dolomite, argillite, evaporates, and terrigenous coal measures, involved prograde development of hornfels and marble and retrograde development of calc-silicates/skarn (Likhachev, 1994). Anhydrite occurs in evaporitic xenoliths, and in some intrusions may be a trace magmatic mineral (Li and others, 2009).

Evidence of reaction with country rock, particularly country rock with potentially readily available sulfur, such as in pyrite, is a favorable indicator when evaluating an intrusion as a potential deposit target (Naldrett, 2004). The extent of wallrock alteration may be an indication of the duration of the thermal pulse related to ore deposition. At Noril'sk, the hornfels facies of the hanging wall is about 250 m wide and is about 100 m wide in the footwall (Likhachev, 1984).

Gangue minerals at deposits that have undergone magmatic and post-depositional alteration typically reflect the original mineralogy. At Uitkomst, cumulate rocks were affected by widespread serpentinization of olivine, uralitization of pyroxene, and saussuritization of plagioclase (de Waal and others, 2001; Sarkar and others, 2008). In addition, there was intense talc-carbonate alteration in the lower ultramafic units enclosed by dolomitic country rock, which may have strongly influenced the alteration mineralogy (de Waal and others, 2001). At Pechenga, host peridotites variably are altered to serpentinites and talc-chlorite-carbonate-serpentine, pyroxenites are altered to chlorite-actinolite, and gabbros are strongly saussuritized (Naldrett, 2004). At Noril'sk, metamorphism of the intrusive rocks is characterized by deuteric alteration of original host mineralogy, with development of biotite, amphibole, serpentine, talc, chlorite, iddingsite, bolingite, sericite, prehnite, pumpellyite, potassium feldspar, and quartz (Likhachev, 1994). The Baimazhai Ni-Cu±PGE deposit in China was subjected to pervasive hydrothermal alteration some time after formation (Zhang and others, 2006). At Baimazhai, the host mafic and ultramafic rocks were altered to mineral assemblages containing varying proportions of tremolite, actinolite, epidote, biotite, chlorite, quartz, talc, serpentine, clinochlore, prehnite, and carbonate (Zang and others, 2006).

Paragenesis

The paragenetic sequence for gangue magmatic silicates and oxides of the mineralized host mafic to ultramafic intrusions provides important information about the potential for formation of an economic sulfide deposit. Mantle-derived mafic magmas crystallize minerals, such as olivine, pyroxene, plagioclase, and oxides, according to their solidus

temperatures, which in turn depend on the temperature, pressure, and oxygen fugacity of the magma. The following paragenetic sequence was modeled by Li and others (2001a) from the composition of the chilled margin of the Bushveld Complex and is applicable to many intrusions that host Ni-Cu±PGE deposits. At 100 bars total pressure and a QFM-1 (quartz-fayalite-magnetite) buffer, olivine crystallizes between 1,358 and 1,312 °C, followed by orthopyroxene between 1,312 and 1,301 °C, then by orthopyroxene plus spinel between 1,301 and 1,166 °C; plagioclase begins to crystallize at 1,166 °C; and clinopyroxene begins to crystallize at 1,158 °C (Li and others, 2001a).

Variations in this paragenetic sequence can have an impact on sulfur solubility and thus on the timing of sulfur saturation and development of an immiscible sulfide liquid (Li and others, 2001b). The timing of silicate crystallization can dictate sulfide texture. Early crystallizing silicates, for example, may include sulfide blebs as inclusions. In disseminated and matrix-textured sulfide ores, sulfide-silicate contacts commonly suggest that an early immiscible liquid sulfide was interstitial to silicate cumulus phases. The relative timing of olivine crystallization and sulfide segregation can have a profound influence on Ni content, with important implications for sulfide tenor. In a mantle-derived melt, Ni partitions to both olivine and sulfide liquid. If a sulfide liquid forms prior to crystallization of olivine, then Ni is depleted in the silicate magma, but there is no change in the FeO/MgO ratio of the magma. Olivine that crystallizes after sulfide separation will be depleted in Ni, with no change in its major element chemistry. In contrast, early crystallization of olivine will deplete magma in Ni and increase its FeO/MgO ratio. Thus, olivine chemistry can provide clues to a mafic body's silicate/sulfide crystallization sequence and provide an assessment/exploration tool. Li and others (2001b) also pointed out that pervasive Ni depletion by early crystallization of olivine prior to sulfide immiscibility may result in development of Ni-depleted sulfide of questionable economic value. An example of this effect may be the Katahdin pyrrhotite body, hosted within a gabbro stock in northern Maine (Miller, 1945). The huge, but very low-grade, sulfide mineralization occurs primarily as interstitial sulfide between silicate minerals and is composed almost entirely of pyrrhotite. The sulfides at Katahdin have very low Ni and Cu contents relative to typical magmatic sulfides related to mafic intrusions (Thompson and Barnes, 1984).

9. Geochemical Characteristics of Ores

Trace Elements and Element Associations

Nickel and copper found in sulfide ores in magmatic sulfide-rich Ni-Cu±PGE deposits related to mafic and/or ultramafic dike-sill complexes commonly are associated with Co (typically present at the 0.1- to 0.3-percent level) and Pt, Pd, and Au (which may be present to as much as the ppm level). Other elements present in trace concentrations may include Ag, As, Bi, S, Sb, Se, Zn, Os, Ir, Ru, Rh, and Te (Barnes and Lightfoot, 2005).

Trace element associations can be used for exploration, however, concealed Ni-Cu deposits buried more than a few meters are difficult to identify from geochemical analyses of soil, lake-sediment, till, or water samples alone. Multi-element soil or sediment sampling has been successful in identifying very shallow (<5 m) Ni-Cu mineralization. For example, the Nebo and Babel deposits in arid western Australia initially were discovered by broad surface sampling of soil and lag deposits (Baker and Waugh, 2005) in an area previously targeted through satellite and geophysical imagery. Anomalous concentrations of both Ni (about 550 ppm) and Cu (as much as 950 ppm), coupled with moderately elevated Pt (as much as 27 ppb), led to discovery of subcrop mineralization (Baker and Waugh, 2005). In the arid region around the Karatungk deposit in China, rock and soil analyses found Cu, Ni, and Co anomalies around exposed intrusions with Ni-Cu mineralization but not over concealed bodies. Anomalous concentrations of As, B, Ba, and Mo were present, however, over what proved to be mineralized Ni-Cu bodies concealed at depths >100 m (Yinggui and others, 1995). Soil sampling at the exposed Discovery Hill deposit at Voisey's Bay showed high concentrations of Pd (as much as 824 ppb) in a halo that extends several hundred meters away from the deposit (McConnell, 2003). Although soil geochemistry over buried mineralization at Voisey's Bay does not show geochemical anomalies, lake-sediment geochemical surveys in areas near known or suspected Ni-Cu mineralization do show elevated Pt (as much as 56 ppb) and Pd (as much as 42 ppb) (McConnell, 2003). In Minnesota, surface waters interacting with shallow Ni-Cu mineralization cause dissolution of sulfides, resulting in mobilization of Ni, Cu, and SO_4, which can be important pathfinders for Ni-Cu mineralization in a cool, humid climate (Miller and others, 1992). In a similar climate, the Ni-Cu mineralization associated with the Thompson Nickel Belt (komatiite-hosted magmatic Ni-Cu deposits with similar sulfide mineralogy) has been shown to be identifiable in the <0.063-mm sediment fraction separated from glacial till. Those analyses show elevated Ni (as much as 3,760 ppm), Cu (to 215 ppm), Cr (to 209 ppm), PGE (Pt, as much as 13 ppb; Pd, to 98 ppb), Au (as much as 27 ppb), as well as elevated Co, As, Cd, Sb, Bi, Se, Te and S in the ppb range (McClenaghan and others, 2011). The presence of these elements, in conjunction with a Pd/Pt ratio >3, suggests the presence of magmatic Ni-Cu mineralization (McClenaghan and others, 2011).

Metal Normalizations and Ratios

The metal contents of sulfides can be used to evaluate the origin and evolution of the magmatic system and whether there is potential for economic accumulations of

sulfides. Barnes and others (1988) and Barnes and Lightfoot (2005) showed two normalization methods for interpreting Ni-Cu±PGE data: (1) normalizing whole-rock and sulfide data to primitive mantle and (2) normalizing sulfide data to 100 percent sulfide.

By normalizing metal contents of silicate rocks to primitive mantle, it is possible to distinguish among the patterns of several mantle-derived magma types (for example, komatiites, ocean floor basalts, high-MgO basalts, and ophiolitic chromitites). Likewise, by normalizing the metal contents of sulfides to primitive mantle, it is possible to use the shape of the normalized pattern to identify those sulfides that have separated from magmas that previously experienced some sulfide segregation. When a sulfide liquid separates from a silicate liquid, the resulting fractionated silicate liquid is depleted in PGE compared to Ni and Cu because of the very strong affinity for PGE in sulfide versus silicate melts. Any subsequent crystallization of silicates or sulfides from the fractionated melt would continue to show the relative depletion of PGE (a trough-shaped plotted pattern). For example, sulfides from the Jinchuan and Noril'sk deposits show relatively smooth normalized patterns (fig. 9–1), suggesting segregation from a source that had not seen significant prior sulfide segregation. However, sulfides from Voisey's Bay show significant depletion in PGE compared to Ni and Cu (Barnes and Lightfoot, 2005), suggesting that at least some of the magma had previously undergone sulfide segregation that scavenged the PGE.

Normalization of metal values to 100 percent sulfide is used in order to compare rocks with different sulfide contents (Barnes and Lightfoot, 2005). This assumes that all chalcophile elements are hosted only by sulfides and that there is no loss or gain of sulfur due to metamorphism or alteration. This normalization can be used to highlight variations among disseminated, matrix, and massive sulfide ores. For instance, disseminated sulfides are commonly richer in Pt, Pd, and Au than average matrix and massive sulfides (fig. 9–2), whereas vein sulfides commonly are enriched in Cu, Pd, and Pt (Barnes and Lightfoot, 2005). Because Ni in mafic/ultramafic rocks containing low modal percentages of sulfide may largely be present in olivine, and rocks with low sulfide content are more vulnerable to sulfur redistribution during weathering and metamorphism, the composition of sulfides should not be recalculated for rocks containing <1 modal percent sulfides. For rocks where the bulk of the sulfides are present as pyrrhotite, pentlandite, and chalcopyrite, the concentration of an element in the sulfide may be calculated element in the sulfide may be calculated as:

$$C_{(100\%\ sulf)} = C_{wr}*100/(2.527*S + 0.3408*Cu + 0.4715*Ni), \quad (1)$$

where $C_{(100\%\ sulf)}$ represents concentration of an element in 100 percent sulfides; C_{wr} indicates concentration of the element in the whole-rock analysis; and S, Cu, and Ni indicate concentrations of the respective elements in the whole-rock data, in weight percent (Barnes and Lightfoot, 2005).

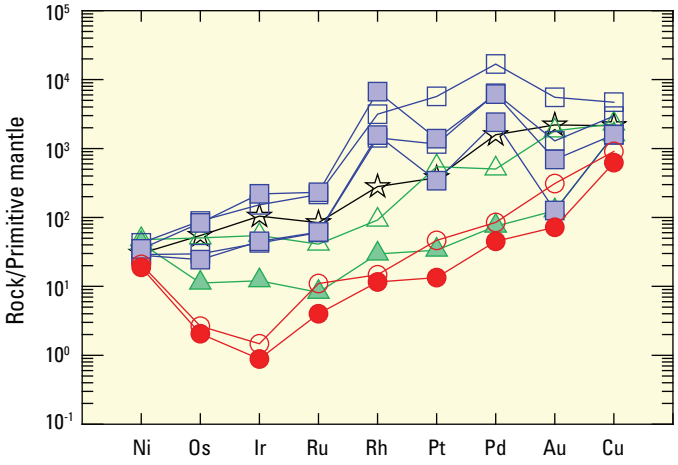

Figure 9–1. Platinum-group and related elements for magmatic sulfides from tholeiitic sill/dike Ni-Cu deposits, normalized to primitive mantle, using normalization factors reported in Barnes and Lightfoot (2005). Disseminated ores (open symbols) tend to be slightly more platinum-group-element-rich than massive ores (solid symbols). Data from Naldrett (2004). [Symbols: Voisey's Bay, Ontario, Canada, circles; Jinchuan, China, triangles; Insizwa, South Africa, star; and Noril'sk, Russia, squares]

Metal ratios provide another means to compare trace elements in sulfides without necessarily having to recalculate the data to 100 percent sulfide or to normalize the data as in figure 9–1 (Barnes and others, 1988). For example, Se/S ratios in sulfide-bearing rocks have been used to evaluate whether the rocks have sustained a loss of sulfur due to alteration or metamorphism (Maier and others, 1998) and as an approximate guide to the presence of sedimentary contaminants to the magmas (for example, Ripley, 1990). The Se/S × 10^6 ratio of the mantle is about 230 to 350 (Eckstrand and Hulbert, 1987). For sulfide-bearing rocks with high Se/S × 10^6 ratios (>1,000), metamorphism may have led to sulfur loss (Maier and Barnes, 1999). Low Se/S × 10^6 ratios (<250) suggest that sedimentary rocks may have contributed sulfur to the magma and to the resulting sulfide liquid (Ripley, 1990). However, use of Se/S ratios is complicated by other processes that may cause changes in either Se or S concentrations (for example, the R factor, alteration or metamorphism, and variations in initial concentrations of S and Se in sulfides and crustal rocks), and thus, this ratio should be used with caution (Queffurus and Barnes, 2010).

For assessment and exploration purposes, metal ratios such as Cu/Pd in both whole-rock silicate and sulfide analyses also can be used as a general guide to evaluate whether sulfides have already segregated from the melt (Barnes and others, 1993; Maier and others, 1998). When a sulfide liquid separates from a silicate melt, the Cu/Pd ratio of the sulfide liquid is much lower than the Cu/Pd ratio of the silicate melt due to the very high partition coefficient for Pd in sulfide liquid (fig. 9–2A) (Maier and others, 1998). The fractionated silicate melt will have high Cu/Pd as will any rocks that crystallize from

that previously fractionated melt. A primitive mantle magma without prior sulfide segregation should have a Cu/Pd value of about 6,500 (Barnes and others, 1988); thus, rocks with Cu/Pd <6,500 should contain Pd-rich sulfides, whereas silicate rocks with whole-rock values of Cu/Pd >6,500 are likely to have previously segregated sulfides (Maier and others, 1998). As an example, massive sulfides associated with the Uitkomst complex have low Cu/Pd ratios (about 2,700) when compared to disseminated sulfides in the overlying gabbro (Cu/Pd about 8,450; Maier and others, 1998). The low ratios in the massive sulfides suggest crystallization from a magma that had not lost PGEs through prior sulfide segregation, whereas the disseminated sulfides likely crystallized from another magma from which sulfides had previously fractionated. Practically speaking, this suggests that when rock units have very high Cu/Pd ratios, they have experienced sulfide segregation and sulfide deposits, if present, would occur in the rock units stratigraphically below the PGE-depleted units (Barnes and Lightfoot, 2005).

The Cu/Pd ratio of the sulfide phases also can be used as a graphical guide (fig. 9–2*B*) to estimate the R value (the weight ratio of silicate liquid to sulfide liquid; Barnes and others, 1993; Barnes and Lightfoot, 2005), which can be an important factor in determining the potential for economic accumulations of sulfides. Three factors control the metal content in a sulfide liquid (assuming a closed system): the concentration of the metal in the silicate liquid, the partition coefficient between the silicate and associated sulfide liquids, and the volume of silicate magma from which the sulfide scavenges the metal—the R value (Campbell and Naldrett, 1979; Barnes and Lightfoot, 2005). In basaltic systems (such as those that give rise to conduit-hosted Ni-Cu deposits), maximum enrichment of Ni occurs at R values of 1,000–3,000, whereas maximum enrichment of PGEs occurs at R >10,000 (Barnes and Lightfoot, 2005). For example, Barnes and Lightfoot (2005) evaluated the Cu/Pd ratio for the Noril'sk and Talnakh intrusions to estimate the R values required to produce the observed sulfide ores (fig. 9–2*B*). For the Noril'sk intrusions, the Cu/Pd ratios of disseminated ores suggest R values of about 10,000, whereas for the Talnakh intrusions, R values appear lower (about 1,000). Such high R values imply a very high volume of magma flow, enhancing PGE enrichment, which is indeed characteristic of the Noril'sk sulfide ores.

Other metal ratios such as Pd/Ir, Ni/Pd, Cu/Ir, Ni/Co, and PGE/Ni+Cu can be used along with Ni/Cu to examine the effects of sulfide segregation (Barnes and others, 1988; Barnes and Lightfoot, 2005). For instance, the Pd/Ir versus Ni/Cu diagram can be used to distinguish among magma suites, and within suites, to distinguish between massive and disseminated sulfides (fig. 9–3*A*). Barnes and Lightfoot (2005) used this diagram to show that for a given deposit, the disseminated sulfides (which tend to be Cu-rich) generally have higher Pd/Ir and lower Ni/Cu ratios than associated massive sulfides (which tend to be Fe-rich). The Pd/Ir ratio has also been used to distinguish magmatic from hydrothermal sulfides (Keays and others, 1982). Although there are exceptions, in general a Pd/Ir ratio >100 suggests a hydrothermal origin, whereas a Pd/Ir ratio <100 suggests a magmatic origin (Maier and others, 1998).

In a Ni/Pd versus Cu/Ir plot (fig. 9–3*B*), Barnes and Lightfoot (2005) demonstrated, using examples from Voisey's Bay, that once a sulfide liquid segregates from a silicate

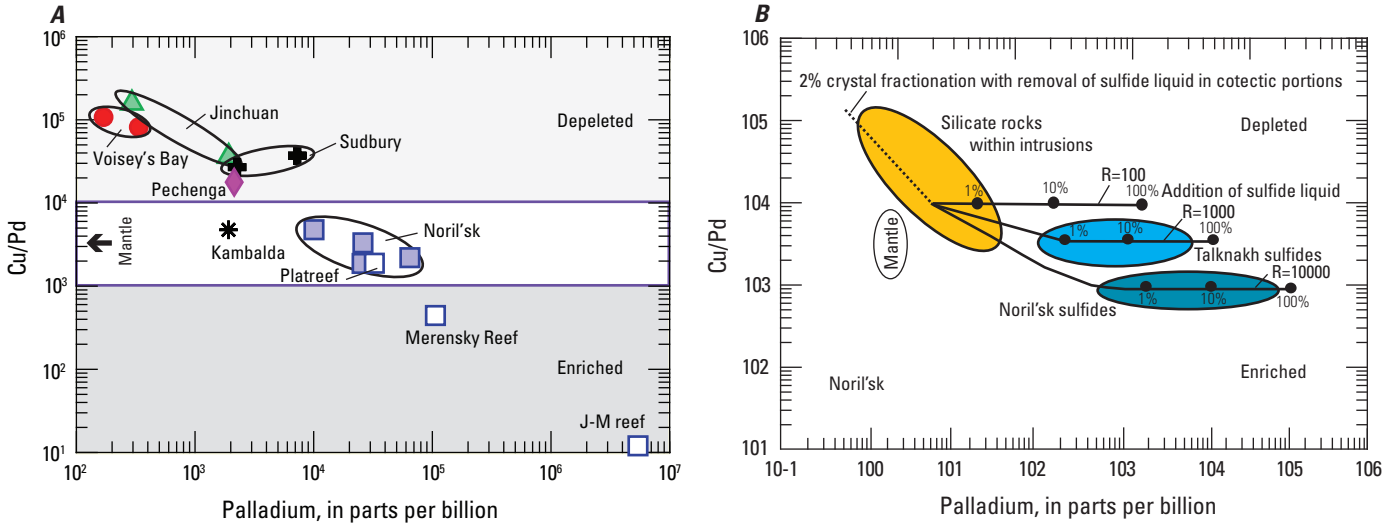

Figure 9–2. *A*, Cu/Pd versus Pd for sulfides from tholeiitic Ni-Cu deposits (solid symbols) compared with sulfides from reef deposits (open squares), komatiite (asterisk) and impact-related deposits (crosses), from Barnes and others (1993). This emphasizes that the reef deposits typically are enriched in PGE, whereas the tholeiitic sill/dike deposits are enriched in Cu (and Ni). Data from Naldrett (2004). *B*, Cu/Pd versus Pd for the Noril'sk, Russia, magmatic system. This plot from Barnes and Lightfoot (2005) shows tie lines between silicate liquid compositions represented by volcanic flows and sulfides in equilibrium with those liquids at several different R factors. The dots represent the composition of a rock that contains mixtures of 1, 10, or 100 percent sulfides. Sulfides in the Noril'sk intrusions appear to result from R values an order of magnitude larger than the apparent R values that produced sulfides in the Talnakh intrusions.

Table 9–1. Ratios of metals calculated as concentration of metal in 100 percent sulfides for magmatic Ni-Cu±PGE deposits (from Naldrett, 2004).

[Symbol: dash, data not available]

	Ni/Cu	Ni/Co	Pd/Pt	Pd/Ir	(Pt+Pd) (Ni+Cu)
Tholeiitic sill/dike deposits					
Eagle (Michigan)[a]	1.23	35.7	0.64	—	0.2
Jinchuan (China)	1.76	56.0	1.00	14.37	0.04 to 0.45
Kabanga (Tanzania)[b]	5 to 10	10 to 15	0.3 to 2.0	2 to 20	0.06 to 0.4 (+1.6)
Nebo-Babel (Australia)[c]	1.1	—	0.97	22	0.03
Noril'sk-Talnakh (Russia)	0.58	58.0	3.43	217.34	1.1 to 4.8
Pechenga (Russia)	1.86	26.0	1.33	9.7	0.05 to 0.26
Voisey's Bay (Canada)	1.87	18.0	1.29	59.98	0.05
Wellgreen (Alaska)[d]	1.6	—	0.71	3.68	0.05
Insizwa (South Africa)	0.91	—	2.40	18.12	0.73
Komatiitic Ni-Cu deposits					
Kambalda (Australia)	13.5	0.07	1.39	8.87	0.19 to 0.26
Contact and reef-type deposits					
Duluth (Minnesota)	0.33	10.50	3.35	184.17	2.9 to 4.8
J-M reef (Montana)	2.03	—	3.47	901.7	353.99
Merensky reef (South Africa)	2.6	—	0.54	14.69	17.4 (+112.6)
Platreef (South Africa)	1.27	—	1.5	88 to 166	2.1 to 4.4
Meteoritic impact-related deposits					
Sudbury (Canada)	1.11	32.00	1.26	30.65	0.06 to 1.3

[a]Unpublished data (USGS)

[b]Data from Macheyeki (2011) and Maier and Barnes (2010)

[c]Data from Godel and others (2011)

[d]Data from Schmidt and Rogers (2007)

liquid, the remaining silicate liquid (and any sulfides that subsequently segregate from this remaining silicate liquid) will be significantly depleted in PGE compared to Ni and Cu and will have very high Ni/Ir and Cu/Ir ratios. Thus, where sulfides are substantially displaced towards higher Ni/Pd and Cu/Ir and away from primary melt fields, as at Voisey's Bay, it is possible to infer that the sulfides were segregated from a magma from which an earlier episode of sulfide segregation had already occurred, leaving behind a depleted silicate liquid. This suggests that there may be PGE-rich sulfides present at depth. Where the sulfides plot within the fields of primary melts, it is possible to infer that the sulfides were segregated from a fertile mantle source, as suggested for sulfides at Noril'sk (Barnes and Lightfoot, 2005).

Stable Isotopes

Sulfur Isotopes

For many economic magmatic Ni-Cu±PGE deposits, the large quantities of sulfur required to reach sulfur saturation and development of an immiscible sulfide liquid are assimilated from external sources (Barnes and others, 1997). As a result, sulfur isotopes of the sulfide ore minerals commonly reflect the highly variable sulfur sources of the country rocks that the ultramafic to mafic magmas intrude. The wide variation in sulfur isotope values reported for a number of magmatic Ni-Cu±PGE deposits is shown in figure 9–4.

Deviations of $\delta^{34}S$ values from mantle-like values of 0±2 per mil provide the strongest evidence by which to evaluate the importance of externally derived S in mafic magmatic systems (Ripley and Li, 2003). At Voisey's Bay, $\delta^{34}S$ values for massive and brecciated sulfides range from –4.0 to +1.8 per mil (Ripley and others, 1999), but there is a distinct zonation of values. In the western area (Reid Brook deposit), $\delta^{34}S$ ranges from –4.1 to –2.3 per mil whereas in the eastern part (Eastern Deeps, Ovoid, Mini-Ovoid, and Discovery Hill deposits), $\delta^{34}S$ ranges from –2.4 to 0 per mil, with slightly more positive values (–0.5 to +1.8 per mil) found in unmineralized troctolite at Eastern Deeps (Ripley and others, 1999). These data indicate that much of the assimilated sulfur in the Reid Brook deposit was derived from the Tasiuyak Gneiss country rock, with $\delta^{34}S$ values ranging from –17 to 18.3 per mil (Ripley and others, 2002). The eastern deposits were emplaced in low-sulfur orthogneiss that has $\delta^{34}S$ values ranging from 4.6 to +3.3 per mil (Ripley and others, 1999).

In the Pechenga area, two populations of sulfur isotopes among the deposits suggest two different sources of sulfur (Abzalov and Both, 1997). Deposits in the western part of the Pechenga Complex (Kaula, Kotselvaara, and Kamikivi) have $\delta^{34}S$ values close to mantle values, ranging from –5 to +2 per mil; deposits in the larger and generally more productive intrusions in the eastern part of the complex (Kierdzhipori and Pilgujarvi) have $\delta^{34}S$ values that range from +2 to +6 per mil.

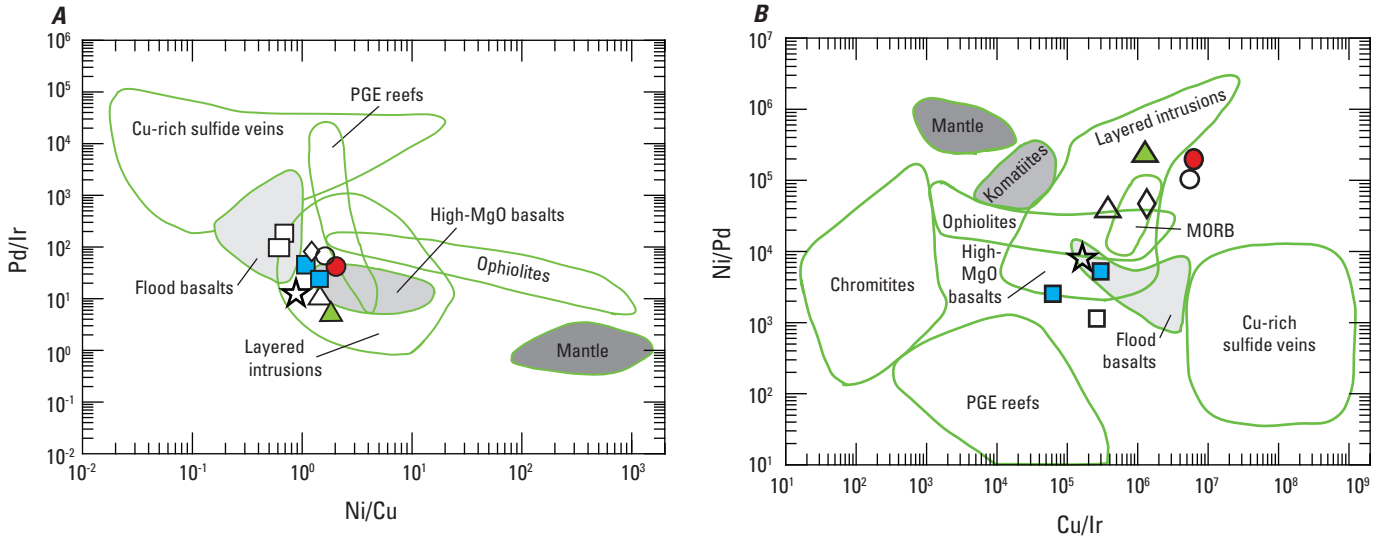

Figure 9–3. *A*, Pd/Ir versus Ni/Cu plot showing that for a given deposit, disseminated sulfides (open symbols) generally have higher Pd/Ir and lower Ni/Cu ratios than associated massive sulfides (solid symbols) (after Barnes and others, 1993; Barnes and Lightfoot, 2005). *B*, Ni/Pd versus Cu/Ir plot showing sulfides that segregated from magmas that have been contaminated by substantial amounts of crust (for example, Jinchuan, China, and Voisey's Bay, Canada), and have likely experienced an early episode of sulfide segregation, have higher Ni/Pd and Cu/Ir ratios than uncontaminated (PGE-enriched) magmas that still retain their mantle signature (for example, Noril'sk, Russia, and Insizwa, South Africa). Fields after Barnes (1990). Data from Naldrett (2004). [Symbols: Voisey's Bay, circles; Pechenga, Russia, diamond; Jinchuan, triangles; Insizwa, star; and Noril'sk, squares]

Sedimentary rocks in the region have early diagenetic pyrite, with $\delta^{34}S$ values ranging from –4.5 to +2 per mil, and later sulfides with values from +8 to +20.9 per mil. Barnes and others (2001) suggested the western deposits assimilated sulfur from unconsolidated sediments, whereas sulfur in the eastern deposits reflects the heavier sulfur of the later sulfides. At the Uitkomst Complex, sulfide-bearing units have $\delta^{34}S$ ranging from –7.1 to +2.6 per mil, whereas values for sulfide-poor units range from –0.9 to +2.6 per mil, suggesting assimilation of sulfur from a source with negative sulfur isotope values (Li and others, 2002; Sarkar and others, 2008). There is good agreement among the sulfur isotope values for sulfides, intrusions, and country rock at the Kabanga deposit, indicating relatively proximal derivation of most sulfides (Maier and others, 2010).

Several deposits have $\delta^{34}S$ values similar to the 0±2 per mil range expected for mantle-derived $\delta^{34}S$ (fig. 9–4). Primary sulfides at Jinchuan have $\delta^{34}S$ values close to mantle values (mostly about –2 to +2 per mil), but secondary pyrite in veins and stringers, and as rare replacement of pyrrhotite, has very negative values (ranging from –27 to –7 per mil), attributed to secondary oxidation of primary sulfides during a hydrothermal/metamorphic event (Ripley and others, 2005). Sulfides from the Waterfall Gorge deposit at Insizwa have $\delta^{34}S$ values close to 0 per mil, but Lightfoot and others (1984) suggest that this does not rule out a crustal source of sulfur. The Nebo-Babel deposit in Western Australia has a very small range of $\delta^{34}S$ values (0 to +0.8 per mil), which Seat and others (2009) invoke as evidence that crustal sulfur addition was not a factor in the genesis of that deposit, a potentially important observation for the generally accepted genesis for this type of magmatic Ni-Cu±PGE deposit.

Oxygen Isotopes

Partly ingested xenoliths at Voisey's Bay provide evidence that silicate rocks were incorporated into the magma during emplacement, and oxygen isotopes provide some information on the processes involved. Oxygen isotope values of minerals in xenoliths record a geochemical history that includes rapid thermal equilibration with magma and production of a refractory mineral assemblage (Ripley and others, 2000; Mariga and others, 2006). High ^{18}O partial melts were generated from quartz- and feldspar-bearing protoliths, and a part of that melt was dispersed in magma that passed through the conduit system (Mariga and others, 2006). Leucogabbronite units at the Nebo-Babel deposit locally also contain country rock orthogneisses that were partly to fully resorbed (Seat and others, 2007). Seat and others (2009) state that oxygen isotope results indicate contamination of the Nebo-Babel intrusion was from orthogneissic country rock rather than from deeper pelitic rocks.

Oxygen isotope data for ore-bearing intrusions from the Kabanga area also suggest incorporation of country rock (Maier and others, 2010). Typical $\delta^{18}O$ values for rocks derived from the mantle are about +5.5 to +6.0 per mil (Ripley, 1999). Olivine, plagioclase, and pyroxene at Kabanga have $\delta^{18}0$ values that range from +5.2 to +7.8 per mil, generally heavier than what would be expected for magmatic

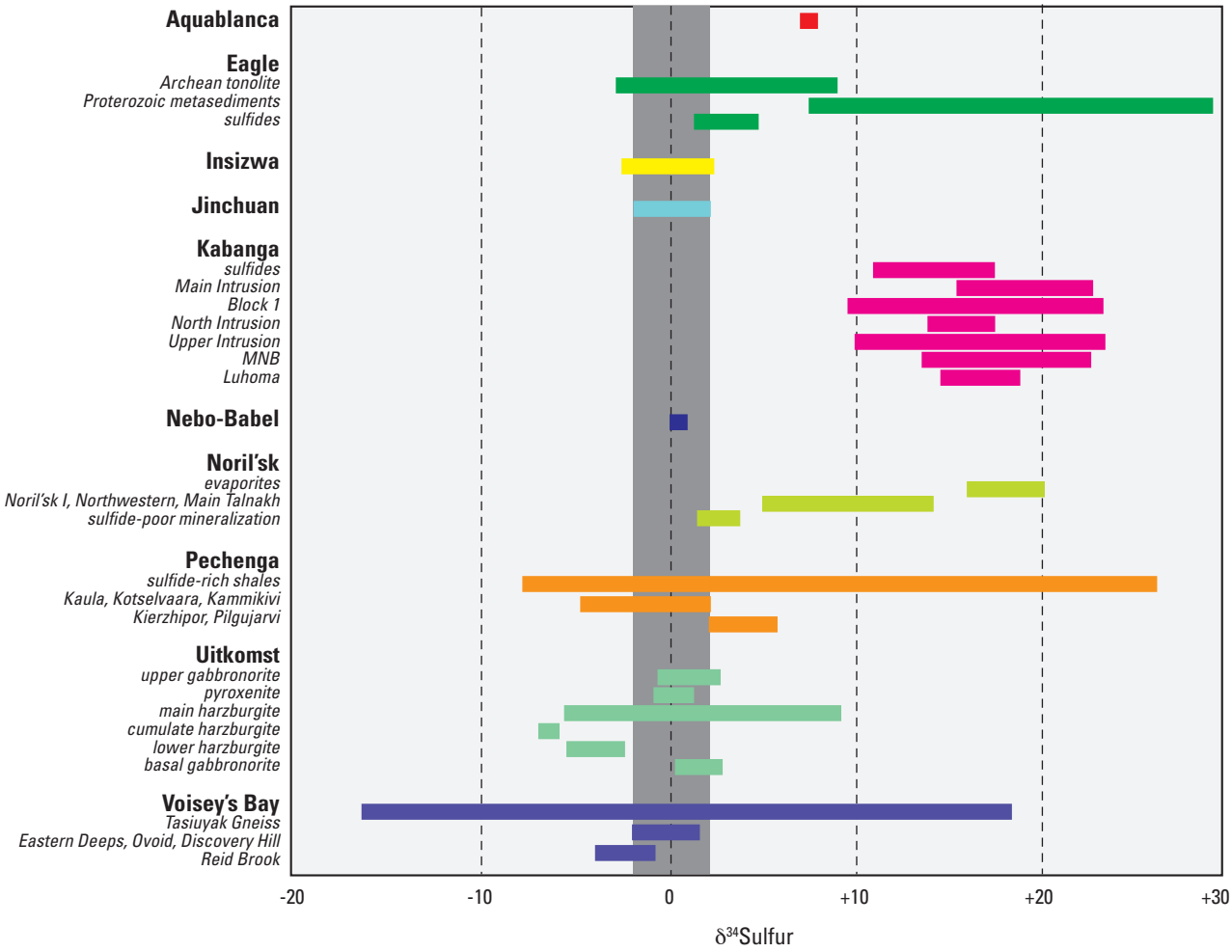

Figure 9–4. Comparison of sulfur isotope variations (delta 34 S, $\delta^{34}S$) in magmatic Ni-Cu±PGE deposits (figure modified from Maier and others, 2010). Sources for data include Eagle, United States (Ding and others, 2009); Insizwa, South Africa (Lightfoot and others, 1984); Jinchuan, China (Ripley and others, 2005); Kabanga, Tanzania (Maier and others, 2010); Nebo-Babel, Australia (Seat and others, 2009); Noril'sk, Russia (Grinenko, 1985; Ripley and others, 2003; Li and others, 2003); Pechenga, Russia (Abzalov and Both, 1997; Barnes and others, 2001); Uitkomst, South Africa (Li and others, 2002); and Voisey's Bay, Canada (Ripley and others, 1999). The gray, shaded area indicates the range of sulfur isotope values typical for mantle-derived sulfides (0 ± 2 per mil).

values. Oxygen isotope values for pelitic metasedimentary country rocks that host the intrusions at Kabanga range between +8.9 and +12.6 per mil. Differences in $\delta^{18}O$ values between harzburgites and gabbronorites suggest that parental gabbroic magma assimilated approximately 20 percent of the country rock and the parental harzburgite magma assimilated approximately 10 percent of the country rock (Maier and others, 2010). The model proposed by Maier and others (2010) suggests that fine-grained pyroxenites and gabbronorites formed by bulk assimilation of country rock by convecting picritic magmas within large staging chambers, followed by intrusion of contaminated magma into the shallow crust. Heavy $\delta^{34}S$ values for sulfides in the Kabanga area are similar to $\delta^{34}S$ values for the pelitic metasedimentary rocks, supporting wholesale incorporation of country rock. In contrast, at the Uitkomst Complex, $\delta^{18}O$ values of olivine and pyroxene from the sulfide-bearing harzburgite horizon have a very small range (from +5.2 to +5.9 per mil), which is consistent with magmatic values rather than assimilation of high ^{18}O country rock. Heavy $\delta^{34}S$ values for the same horizons suggest that sulfur was added to magmas as a hydrothermal fluid, rather than with assimilated country rock (Sarkar and others, 2008). Sulfide-poor intrusions at Uitkomst have oxygen and sulfur isotope values consistent with magmatic values (Sarkar and others, 2008).

At the Jinchuan deposit, $\delta^{18}O$ values for olivine (+3.5 to +5.9 per mil), plagioclase (+1.1 to +3.1 per mil), serpentine (+2.1 to +4.3 per mil), and amphibole (+2.4 to +4.1 per mil) are all lower than magmatic values and thus record a non-magmatic process. Ripley and others (2005) concluded that these oxygen isotope data, along with δD data, suggest extensive interaction with evolved meteoric water or seawater,

consistent with large-scale hydrothermal convection and a rift-related origin for the magmatism. Post-magmatic hydrothermal alteration is an unlikely contributor based on the water-poor nature of the metamorphic rocks and the large volume of water necessary to account for observed alteration and isotope characteristics (Ripley and others, 2005).

Radiogenic Isotopes

Radiogenic isotope systems can play an important role in identifying intrusions that have experienced sulfide segregation and those that have not. Because Re and Os behave very differently in response to geologic processes (Lambert and others, 1998, 1999a), Re and Os can be used as tracers in determining the origin of the metals in the ores and the extent of crustal contamination. However, caution is necessary when interpreting Re-Os isotope characteristics of sulfides in dynamic magmatic systems because significant variation in the R factor (that is, the mass of silicate magma that has equilibrated with a given mass of sulfide magma) can mask strongly the effects of crustal contamination when compared to those crustal effects seen in other isotopic systems (for example, S, Sm-Nd; Lambert and others, 1998). Whereas Re and Os partition strongly into metals and sulfides, the lithophile elements involved in other isotopic systems such as Sm-Nd, Rb-Sr, and U-Th-Pb partition strongly into silicate minerals. Whole-rock neodymium, strontium, and Pb isotope analyses of intrusions that host sulfides are used to evaluate the magmatic sources and possible crustal contaminants of the intrusions and, where possible, the age of magmas. Whole-rock Sr and Pb isotope analyses also may be used to evaluate the effect of hydrothermal mobilization of elements (Lightfoot and others, 1993; Arndt and others, 2003).

Rhenium-Osmium Isotopes

Early models for the Noril'sk deposits by Naldrett and others (1992, 1995) and Lightfoot and Hawkesworth (1997) postulated that magmas staged at intermediate levels in the crust, and the resulting contamination by granitoid rocks led to sulfide saturation and the segregation of massive sulfide. However, Arndt and others (2003) used the Re-Os isotopic compositions of silicate rocks to suggest another model, one in which the massive sulfides are derived from a second, less contaminated magma. At Noril'sk there are three main ore-bearing (or Noril'sk-style) intrusions: (1) Noril'sk I, (2) Talnakh, and (3) Kharaelakh, each of which hosts Ni-Cu-PGE massive sulfides. Silicate rock samples from these ore-bearing intrusions exhibit γ_{Os} (gamma osmium, relative Os deviation from the chondritic upper mantle value) ranging from +4.0 to +10.4 (Horan and others, 1995; Arndt and others, 2003), and their ores exhibit a range in γ_{Os} from +1 to +13 (Walker and others, 1994), similar to mantle compositions. These data indicate that the metals were derived from a primitive mantle magma that experienced little crustal contamination (Arndt and others, 2003). Other intrusions in the area host disseminated sulfides (Lower Talnakh-style) or are unmineralized. Rocks from those intrusions typically have γ_{Os} ranging from +10.2 to +71.0 (Arndt and others, 2003; Walker and others, 1994), which Arndt and others (2003) attributed to contamination of a primitive magma by anhydrite-rich evaporitic sediments in the upper crust (table 9–2). Thus, at Noril'sk, Arndt and others (2003) found isotopic evidence of strong crustal contamination of some magmas at intermediate crustal levels (as shown by the elevated S and Re-Os isotopic data), leading to early sulfide segregation in some units. However, the major ore bodies appear to be derived from magmas that did not reach sulfur saturation at depth and thus still retained their chalcophile elements until the magmas assimilated differing amounts of anhydrite-rich sediments at shallow crustal levels, resulting in sulfide saturation and ore deposition in the Noril'sk-I and Kharaelakh deposits (Arndt and others, 2003; Li and others, 2009). The apparent discrepancy between the Re-Os isotopic results and those of other isotopic systems (for example, S) may reflect the tendency for Re-Os isotopic signatures to mask input from crustal contamination when the system is very dynamic (R factor about 40,000) and the sulfide melt interacts with an enormous volume of mantle-derived magma (Lambert and others, 1998).

In other sulfide-rich Ni-Cu±PGE deposits such as Wellgreen (250 Ma; Marcantonio and others, 1994) and Eagle (1.1 Ga; Ding and others, 2008), the g_{Os} values of massive sulfides and their host rocks are about 0 but can be as great as +80. Because typical mantle g_{Os} values are near 0, this suggests that the primary magmas from which the ores segregated were unlikely to have had much interaction with continental lithosphere or crust. However, in order to explain the higher g_{Os} values of some ores at Wellgreen, Marcantonio and others (1994) invoked the addition of radiogenic Os from surrounding country rocks, via a hydrothermal fluid during emplacement of the intrusion, as a mechanism for altering primary isotopic values. In the case of the Eagle deposit, Ding and others (2008) suggested that the Os isotopic variation might be related to late-stage hydrothermal processes accompanying widespread serpentinization.

At the 1.33-Ga Voisey's Bay deposit, the three main areas of mineralization (Ovoid, Eastern Deeps, and Discovery Hill) all exhibit very high initial g_{Os} values (+898 to +1,127) for pyrrhotite and chalcopyrite analyzed from massive, disseminated, and matrix ores. These data suggest that a primary basaltic magma strongly interacted with adjacent gneisses (fig. 9–5; Lambert and others, 1999b, 2000). However, these variable, but commonly high initial g_{Os} values also suggest a very dynamic magma system through which large volumes of geochemically distinct magmas passed; calculated R values are relatively low, ranging from 50 to 500 (Lambert and others, 2000). Using Re-Os isotopic characteristics, Lambert and others (2000) corroborate the proposal of Li and Naldrett (1999) that the Voisey's Bay deposit represents a magmatic system that encompasses two magma chambers about one

Table 9–2. Characteristics of the five chemical components identified in the Norilsk-Talnakh intrusions, Russia, calculated using an emplacement age of 251 Ma (data from Arndt and others, 2003).

[Abbreviations: $\varepsilon_{Nd,}$ epsilon neodymium; $^{87}Sr/^{86}Sr$, strontium 87/86 ratio; γ_{Os}, gamma osmium; $\delta^{34}S$, delta sulfur 34; and $^{206}Pb/^{204}Pb$, lead 206/204 ratio]

Component	ε_{Nd}	$^{87}Sr/^{86}Sr$	γ_{Os}	$\delta^{34}S$	$^{206}Pb/^{204}Pb$
Mantle	+4	0.7045	+6	0	
Ore-bearing Noril'sk-type intrusion	0 to +2	0.7055	+6	+7 to +13	17.66 to 18.12
Noril'sk II	+0.6	0.7056	+6		18.04 to 18.08
Lower Talnakh-type intrusion	–5	0.708	+10 to +71		18.04 to 18.34
Younger intrusions	–12 to +3	0.704 to 0.707	+5 to +68	+16 to +20	
Contaminant A (evaporates)	–7	>0.710	>+75	+16 to +20	
Contaminant B (granitoids)	0	>0.709	+5	+1	

kilometer apart and connected by a feeder zone. At least two stages of crustal contamination also occurred. Some sulfides and a related troctolite yield an isochron age as young as about 1,000 Ma, suggesting that a later hydrothermal event may have at least partially reset the Re-Os isotope systematics of the deposit and some of the surrounding country rocks (Lambert and others, 1999b).

Rubidium-Strontium, Samarium-Neodymium, and Lead Isotopes

At Noril'sk, four groups of intrusions are recognized, each with their own isotopic characteristics (table 9–2) (see Arndt and others, 2003; Wooden and others, 1992). The ore-bearing intrusions (Noril'sk I, Talnakh, and Kharaelakh) have the following isotopic signatures: ε_{Nd} (epsilon neodymium, relative Nd deviation from the chondritic upper mantle value) = –0.8 to +1.4, $^{87}Sr/^{86}Sr$ = 0.707 to 0.709, and $^{206}Pb/^{204}Pb$ = 17.5 to 18.175, $^{207}Pb/^{204}Pb$ = 15.43 to 15.56, and $^{208}Pb/^{204}Pb$ = 37.16 to 37.98. Noril'sk II is mineralized but does not contain massive sulfides and has the following isotopic signatures: ε_{Nd} = +0.5 to +0.8, $^{87}Sr/^{86}Sr$ = 0.705, and $^{206}Pb/^{204}Pb$ = 18.03 to 18.06, $^{207}Pb/^{204}Pb$ = 15.4 to 15.48 and $^{208}Pb/^{204}Pb$ = 37.82 to 37.86. Unmineralized intrusions (lower Talnakh-type) show significantly more negative e_{Nd} (–4.8 to –5.4), higher $^{87}Sr/^{86}Sr$ (>0.707) and somewhat higher $^{206}Pb/^{204}Pb$ (18.04 to 18.33), and similar $^{207}Pb/^{204}Pb$ (15.47 to 15.49) and $^{208}Pb/^{204}Pb$ (37.68 to 37.95) than the ore-bearing intrusions (Arndt and others, 2003). The youngest intrusions in the area show distinctly different isotopic signatures (table 9–2). Arndt and others (2003) propose a model in which the mantle-derived magma that fed the Lower Talnakh-type intrusions interacted with continental, likely granitoid crust, causing sulfur saturation and the early segregation of sulfides. This in turn led to contaminated but depleted magmas forming some of the unmineralized Lower Talnakh-type intrusions and volcanic suites. The contamination by crustal rocks substantially altered the Nd, Sr, and Os isotopic characteristics of the resulting magma. The negative ε_{Nd} (–5) and high $^{87}Sr/^{86}Sr$ (>0.707) are consistent with crustal contamination of mantle-derived magma. In contrast to these magmas, Arndt and others (2003) suggested that different magmas fed the ore-bearing intrusions (Noril'sk, Talnakh

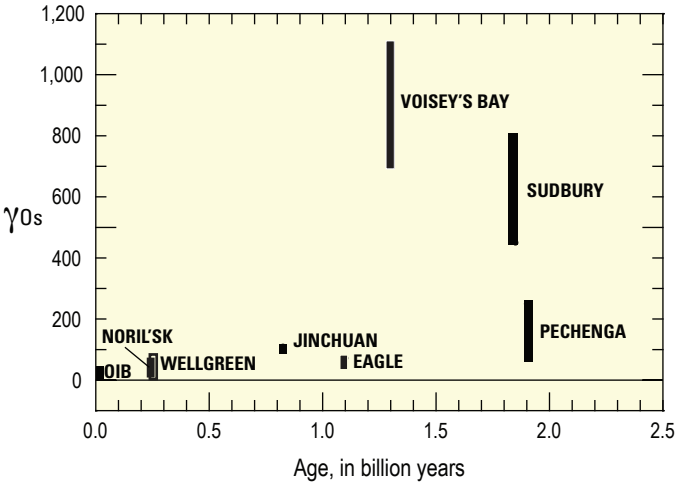

Figure 9–5. Gamma osmium (γ_{Os}) versus age in billions of years for some sulfide-rich Ni-Cu deposits. Modern ocean-island basalts (OIB) show nearly chondritic γ_{Os} (about 0). Most of the deposits show a Re-Os signature dominated by the mantle. In comparison, Sudbury, Canada (an impact-related deposit) has a high Re-Os signature dominated by crust. The deposits at Pechenga, Russia, and especially at Voisey's Bay, Canada, also show isotopic compositions dominantly derived from continental crust. Data sources include OIB (Shirey and Walker, 1998); Noril'sk, Russia (Horan and others, 1995); Wellgreen, Alaska (Marcantonio and others, 1994); Jinchuan, China (Yang and others, 2008); Eagle, Michigan (Ding and others, 2008); Voisey's Bay (Lambert and others, 1999b); Sudbury (Walker and others, 1991); and Pechenga (Walker and others, 1997). [Abbreviation: γ_{Os}, gamma osmium, relative Os deviation from the chondritic upper mantle value]

and Kharaelakh) and underwent less crustal contamination in intermediate-level magma chambers, and thereby, no sulfide segregation at mid-crust levels. The chondritic ε_{Nd} value (about 0) is consistent with the Nd isotopic signature of a primitive mantle-derived magma, but the high initial $^{87}Sr/^{86}Sr$ (>0.707) suggests that additional Sr may have been added after emplacement (Naldrett, 2004). These chalcophile-enriched magmas ultimately interacted at higher crustal levels with anhydrite, which was probably the catalyst for sulfide segregation in those magmas. The Nd and Sr isotopic systems were

significantly altered by this interaction, but the Os isotopes were not (Arndt and others, 2003). This complex history of multiple mantle-derived magmas interacting with various crustal contaminants is reflected in the isotopic compositions of the sulfides ores and the particular host rocks (table 9–2) (for example, Wooden and others, 1993).

Amelin and others (2000) evaluated Nd, Sr, and Pb isotopic signatures of the Voisey's Bay intrusion and a relatively unmineralized intrusion, the Mushuau intrusion, both part of the Nain Plutonic Suite. The Voisey's Bay intrusion is characterized by initial isotopic compositions most similar to mantle values, suggesting derivation from a mantle magma that underwent a small amount of crustal interaction at mid-crustal levels (magma defined by ε_{Nd} = –1 to –2, $^{87}Sr/^{86}Sr$ = 0.7034 to 0.7038, and $^{206}Pb/^{204}Pb$ = 15.34 to 15.54, $^{207}Pb/^{204}Pb$ = 15.10 to 15.18 and $^{208}Pb/^{204}Pb$ = 35.24 to 35.56). The amount of mid-level contamination was probably not sufficient to cause sulfide segregation at that point, and sulfide saturation was probably not reached until the magma was contaminated by the Tasiuyak gneisses at a higher level, resulting in ore deposition. Nearby intrusions, such as Mushuau, contain only minor sulfide mineralization and have the following isotopic signatures: ε_{Nd} = –3 to –10, $^{87}Sr/^{86}Sr$ = 0.7034 to 0.7052, and $^{206}Pb/^{204}Pb$ = 14.21 to 14.55, $^{207}Pb/^{204}Pb$ = 14.63 to 14.77, and $^{208}Pb/^{204}Pb$ = 34.36 to 34.65 (Amelin and others, 2000). The enriched Nd (more negative) and elevated Sr signatures are consistent with substantial contamination by Archean gneisses (likely 15–35 percent), which likely caused the magma to reach early sulfur saturation at mid-crustal levels and resulted in residual magmas that were depleted in Ni-Cu-PGE upon reaching the upper crust (Amelin and others, 2000). From an assessment/exploration perspective, mantle-derived magmas that experience only limited crustal contamination in mid-crust would be less likely to experience early sulfur saturation and would be more likely to be prospective for economic concentrations of sulfides when emplaced at shallow depths.

Likewise, at the Insizwa deposit, the basal picrite, basal gabbro, and Central Zone gabbros each have different initial $^{87}Sr/^{86}Sr$ and initial $^{143}Nd/^{144}Nd$ values, which indicate that they each represent different batches of magma not directly related to one another (Lightfoot and others, 1984). At Insizwa, only the basal gabbro and picritic units are mineralized and are characterized by ε_{Nd} = –2.4 to –4.8 and $^{87}Sr/^{86}Sr$ = 0.7071 to 0.7086, suggesting some contamination, likely at depth. Overlying unmineralized granophyres likely are crustal melts (ε_{Nd} = about 5.4 and $^{87}Sr/^{86}Sr$ >0.710) (Lightfoot and others, 1984).

The effect of hydrothermal alteration on intrusions also can be evaluated using radiogenic isotopes. Marcantonio and others (1994) combined Sr, Nd, and Os isotopes to conclude that hydrothermal alteration played an important role in the Wellgreen deposit, but whether such alteration occurred during or at some time after the deposit formed is uncertain. Although both the Sr and Os isotope systematics appear to have been disturbed significantly, there is no correlation between Sr and Os with Nd isotope ratios, reflecting the relative immobility of Nd during low-grade metamorphism. Post-ore metamorphism also has affected the Os, Pb, and Sr isotopic systems at the Jinchuan deposit, preferentially causing disruptions in the isotopic signatures of disseminated ores rather than of the massive ores (Yang and others, 2008).

10. Petrology of Associated Igneous Rocks

Rock Names

Magmatic sulfide-rich Ni-Cu±PGE deposits are associated spatially with and hosted by a wide variety of mafic and ultramafic igneous rock types generally classified on the basis of varying amounts mostly of olivine, pyroxene, and plagioclase, as well as their textural relations (fig. 10–1). Common rock types include peridotite, pyroxenite, olivine gabbro, troctolite, gabbro, leucogabbro, and picrite (table 10–1). However, the use of rock names is complicated by a number of problems including changes in rock nomenclature over time, inconsistent use of rock names (gabbro, gabbronorite, and monzogabbro, for example), variable bases for naming rocks (cumulus minerals versus modal mineralogy), and use of local terminology (for example, Russian taxitic gabbro and picritic gabbrodolerite).

Forms of Igneous Rocks and Rock Associations

Magmatic sulfide-rich Ni-Cu±PGE deposits generally are found in association with small- to medium-sized mafic and/or ultramafic dikes, sills, chonoliths (tens to a few hundreds of meters thick, tens to a few thousand meters wide, and hundreds of meters to several kilometers in length), and plug-like intrusions (generally <10-km diameter). Hypabyssal dike- and sill-like intrusions may show significant changes in dip and width along their strike length and may be surrounded by intense metamorphic and metasomatic aureoles that can extend outwards into the country rocks for as much as 400 m. The intrusions generally appear to have formed as the plumbing system to large-scale emplacements of mafic magmas in LIPs (Ernst and Buchan, 2001).

Mineralogy

The mafic and ultramafic igneous rocks spatially associated with sulfide-rich Ni-Cu±PGE deposits dominantly are composed of varying amounts of olivine, orthopyroxene, clinopyroxene, and plagioclase (table 10–1). Common primary

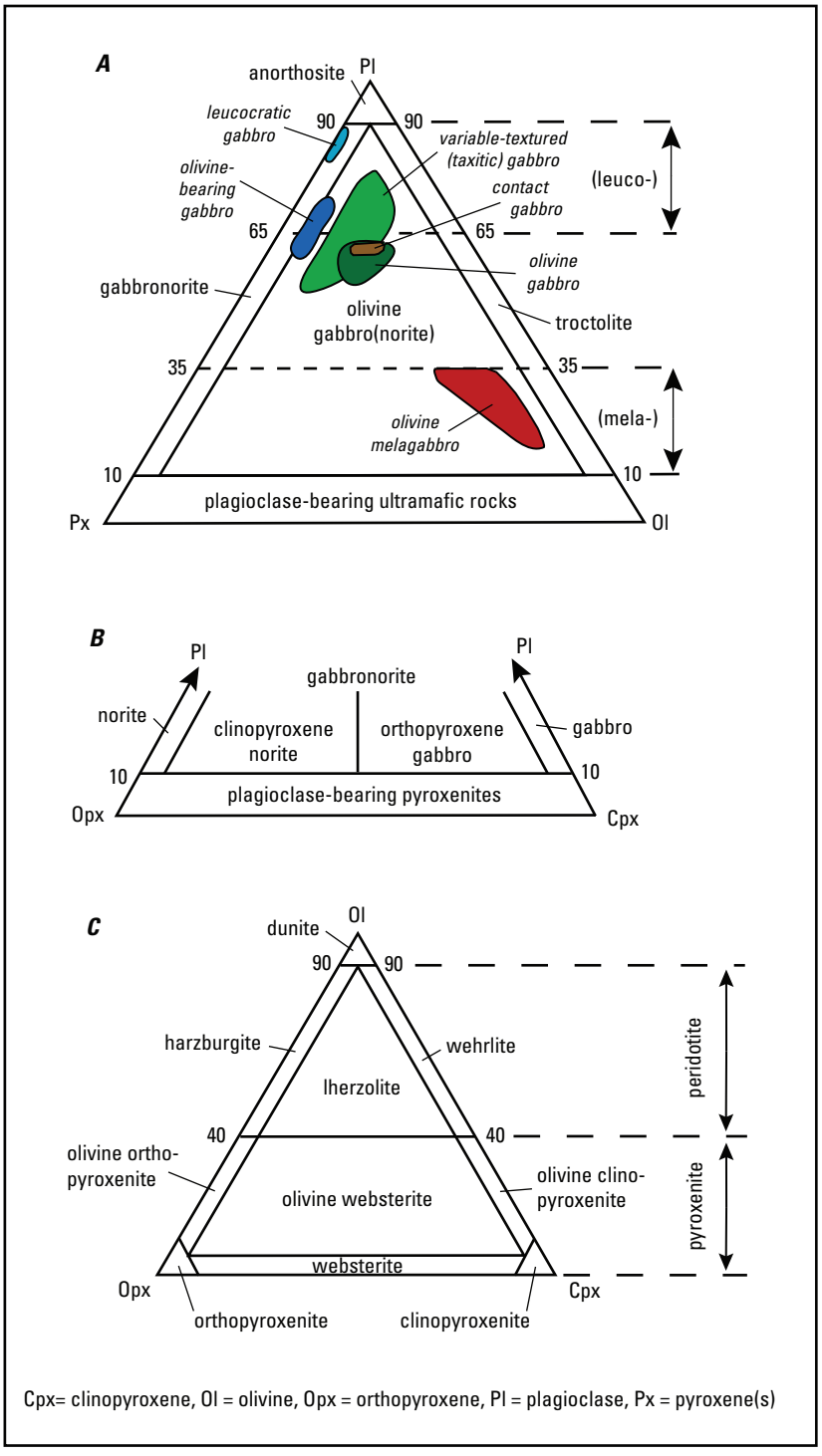

Figure 10–1. The International Union of Geological Sciences (IUGS) classification and nomenclature of gabbroic and ultramafic rocks based on the proportions of olivine, orthopyroxene, clinopyroxene, and plagioclase (from Le Maitre, 1989). Fields in *A* show rock types that compose the Noril'sk-type (Russia) ore-bearing intrusions. Modified from Czamanske and others (1995).

Table 10–1. Lithology, mineralogy, and texture of rocks that host sulfide-rich Ni-Cu±PGE mineralization at Voisey's Bay, Canada (Li and others, 2000) and at Noril'sk, Russia (Czamanske and others, 1995).

[Abbreviations: cum, cumulate; intercum, intercumulate; Ap, apatite; Bt, biotite; Cpx, clinopyroxene; Gn/incl, gneiss inclusions; Hb, hornblende; Hy, hypersthene; Mt, magnetite; Ol, olivine; Opx, orthopyroxene; Pl, plagioclase; %, percent]

Intrusion	Intrusive phase	Lithodemic unit	Minearology	Texture
Voisey's Bay	Phase I	Chilled margin gabbro	cum Pl (<10%) intercum Pl, Cpx, Opx, Hb, Bt, Mt	Ophitic
		Feeder olivine gabbro	cum Pl (<10%), Ol (<10%) intercum Pl, Ol, Hy, Hb, Bt, Mt, Ap	Subophitic
		Ferrodiorite	cum Pl (<5%) intercum Pl, Cpx, Hb, Bt, Mt, Ap	Massive
		Leucotroctolite	cum Pl (60–70%), Ol (15–25%) intercum Pl overgrowth, <15% Cpx+Bt	Massive
	Intermediate	Olivine gabbro	cum Pl (60–70%), Ol (5–10%)	Lamination
		Basal breccia	Gn/incl (>25%), cum Pl (<10%), Ol (<10%) intercum Opx, Pl, Hb, Bt, Mt, sulfides	Breccia
		Feeder breccia	Gn/incl (>25%), cum Pl (<10%), Ol (<10%) intercum Opx, Pl, Hb, Bt, Mt, sulfides	Breccia
	Phase II	Variable troctolite	cum Pl (50%), Ol (20–30%), Gn/incl (5–15%) intercum Cpx, Hb, Bt, Mt, sulfides	Variable
		Leopard troctolite	cum Pl (40–50%), Ol (20–40%) intercum Cpx, Bt, sulfides	Leopard
		Normal troctolite	cum Pl (40–60%), Ol (20–40%) intercum Pl overgrowth, <15% Cpx+Bt+Mt	Lamination
Ore-Bearing Noril'sk		Contact	Pl + Cpx + Ol (10–17%)	Fine grained
		Variable olivine gabbro	Pl + Ol (7–18%) + Cpx + Mt + Bt + sulfide	Variable
		Olivine melagabbro	Ol (40–80%) + Pl + Cpx + Bt + sulfide	Fine to medium grained
		Olivine gabbro	Pl + Cpx + Ol (10–27%) + Bt + Mt	Subophitic, fine to medium grained
		Olivine-bearing gabbro	Pl + Cpx + Ol (3–7%) + Mt	Fine to medium grained, trachytic
		Leucogabbro	Pl + Cpx + Ol (0–3%) + Mt + sulfide	Coarse grained

accessory phases include chromite, ilmenite, titanomagnetite, apatite, and sulfides. Hornblende, biotite, and/or phlogopite are common accessory minerals in some rocks, particularly near interstitial sulfide minerals. Zircon and/or baddeleyite may be present as accessory phases, particularly in coarser grained mafic rocks, and are useful for age determination (Heaman, 2009). Mafic minerals generally have relatively high MgO contents but often show zoning to more Fe-rich compositions. Plagioclase generally is relatively anorthitic with zoning to more albitic compositions. For both mafic minerals and plagioclase, compositional zoning may be varied and complex. With metamorphism and alteration, olivine generally is replaced by tremolite and/or serpentine (± magnetite); pyroxenes by talc, amphibole, and chlorite; and plagioclase by saussurite, epidote, and chlorite.

Because olivine generally is the first phase to crystallize from mafic and ultramafic magmas, its composition can be particularly useful in estimating liquid compositions at various stages during crystallization of mafic/ultramafic intrusions (Naldrett, 2004). In particular, the forsterite (Fo) content of olivine can indicate the FeO/MgO ratio of the magma from which it crystallized (Roeder and Emslie, 1970), while anomalously low Ni content can be an indication of prior sulfide saturation and fractionation of a sulfide liquid (Naldrett, 2004).

Textures, Structures, and Grain Size

Textures of the igneous rocks spatially associated with sulfide-rich Ni-Cu±PGE deposits are widely variable, ranging from aphanitic to diabasic, porphyritic, ophitic, skeletal-acicular, coarse-grained equigranular, and pegmatitic (table 10–1). Many such rocks, however, are characterized by hypidiomorphic-granular textures. In many cases, the rocks are composed of accumulations of minerals and show cumulate textures (Irvine, 1982). Grain size varies from aphanitic to coarse to pegmatitic, although many rocks are fine to medium grained. Grain size, mineralogy, and crystal form can vary at all scales, from centimeters to tens of meters, resulting in varied-textured (taxitic) rocks, such as at Noril'sk and Nebo-Babel. Textures indicative of chilling, unidirectional growth, and magma flow also may be present. Magmatic

breccias locally are present, particularly at the base and sometimes at the upper contact of intrusions, such as at Noril'sk and Voisey's Bay. Breccias may contain fragments of country rock and "exotic" lithologies, such as the ultramafic rocks not present in the host intrusion at Voisey's Bay, and commonly are mineralized. Texture and grain size are products of a number of factors that include depth of emplacement, magma composition, cooling rate, volatile content, magma mixing, contamination, and subsequent metamorphism.

Host intrusions commonly show some form of mineralogical and/or compositional layering, although layering is generally not as well developed nor of the same type as in larger layered mafic intrusions like the Stillwater or Bushveld complexes. In undeformed terranes, igneous layers generally are subhorizontal, but they also can be parallel to the margins of dikes and to the roof of intrusions. The presence in some intrusions of abrupt transitions between rock types, variations in major and trace element concentrations, reversals in (zoned) mineral compositions, and the discontinuous distribution of lithologies indicate that multiple, distinct magma pulses were emplaced into these intrusions (for example, Noril'sk, Czamanske and others, 1995; Voisey's Bay, Li and others, 2000; Uitkomst, de Waal and others, 2001; Eagle, Ding and others, 2010; Kabanga, Maier and others, 2010). These intrusions cannot be viewed as the product of in situ fractional crystallization and differentiation of a single crystal-free magma nor of the single input of a crystal- and sulfide-bearing magma. Because of the complexities that can result from multiple injections of magma in conduit systems, the oldest layers may not be at the base nor the youngest near the top of the intrusions.

Petrochemistry

The igneous rocks spatially associated with sulfide-rich Ni-Cu±PGE deposits range in composition from ultramafic to mafic to highly evolved (granophyric). Commonly the rocks have cumulate textures and do not represent magmatic liquid compositions. Most sulfide deposits and their host intrusions, however, appear to have been the product of primitive mantle-derived magmas including ferropicrite (Pechenga, Eagle), tholeiitic picrite (Noril'sk-Talnakh), high-Mg basalt (Jinchuan), and siliceous high-Mg basalt (Uitkomst, Kabanga) (table 10–2). Possible exceptions include the Voisey's Bay deposits, which appear to be related to a distinct high-Al-type basaltic magma (Scoates and Mitchell, 2000), although Li and others (2000) concluded that the geochemistry of the troctolitic intrusions at Voisey's Bay is consistent with derivation from picritic basalts similar in composition to those from Noril'sk and West Greenland. There are no known deposits associated with mid-ocean ridge basalts (MORB) or alkaline rocks (Barnes and Lightfoot, 2005). Subduction-related igneous rocks also typically do not host sulfide-rich Ni-Cu±PGE deposits, although some Ni sulfide occurrences in the Svecofennian terrane of Finland and the Aguablanca Ni-Cu sulfide deposit in Spain are inferred to have developed in Andean-type continental magmatic arcs from calc-alkaline magmas (Peltonen, 2004; Piña and others, 2010).

A large body of literature exists describing the geochemistry and petrogenesis of LIP-related igneous rocks and those hosting sulfide-rich Ni-Cu±PGE deposits (Mahoney and Coffin, 1997; Ernst and Buchan, 2001; Foulger and Jurdy, 2007; Zhang and others, 2008). Picrites, primitive and near-primitive high-Mg tholeiites (those with Mg numbers [Mg/(Mg+Fe)] ≥0.65 and/or MgO >9 weight percent) occur as a minor component of most LIP sequences, generally at the base. However, the picrites and tholeiites appear more abundant in those LIPs that host sulfide-rich Ni-Cu±PGE deposits (Zhang and others, 2008). In general, the sequences that host major sulfide deposits are more depleted in basaltic components such as Al_2O_3 and Na_2O than those that are barren.

One of the best-studied volcanic-intrusive sequences associated with sulfide-rich Ni-Cu±PGE deposits is the Siberian Traps region in the Noril'sk area of Russia. Eleven volcanic suites have been recognized in 3,500 m of vertical thickness of extrusive rocks (Naldrett and others, 1992) (fig. 10–2). The lower part of the sequence (Lower Series or assemblage) consists of mostly alkaline volcanic rocks with compositions ranging from ferropicrite to basalt and basanite to trachybasalt. The middle of the sequence (Middle Series) consists of tholeiitic basalts and picrites of the Tuklonsky Suite and the crustal-contaminated basalts of the lower part of the Nadezhdinsky Suite. The upper part of the sequence (Upper Series) consists of a compositionally relatively uniform series of moderately contaminated and evolved tholeiitic basalts. The lithologic and geochemical characteristics of the Noril'sk volcanic suites are summarized in table 10–3.

The intrusions of the Noril'sk region are mostly comagmatic with the volcanic rocks and have been classified into three general groups on the basis of field relations, age, petrography, geochemistry, and isotopic composition, with those synchronous with the main phase of tholeiitic volcanism distinguished from those that intruded earlier or later (Diakov and others, 2002). The pre-tholeiite intrusions, such as the Ergalakh complex and North Kharaelakh intrusion, are linked to the Lower Series alkaline volcanism, whereas those emplaced after flood-basalt volcanism include both mafic intrusions, such as Oganer and Daldykan, and more-felsic intrusions. All Ni-Cu±PGE sulfide ore deposits are related to the syn-tholeiite intrusive group that is further subdivided into (1) differentiated mafic-ultramafic ore-bearing or Noril'sk-type intrusions; (2) weakly mineralized, differentiated, mafic-ultramafic Lower Talnakh-type intrusions; and (3) a variety of other intrusions ranging from homogeneous to differentiated, mostly barren or with weak, disseminated mineralization (Diakov and others, 2002). The Noril'sk ore-bearing intrusions have petrologic and geochemical characteristics similar to the Morongovsky-Mokulaevsky volcanic suites (Fedorenko and others, 1996). These magmas are interpreted to have formed through crustal contamination of a tholeiitic picrite magma (see table 10–2)

Table 10–2. Compositions of inferred parental magmas to selected worldwide sulfide-rich Ni-Cu±PGE deposits. Sources are Pechenga, Russia, Lammas intrusion, Hanski and Smolkin (1995); Noril'sk, Russia, Tukllonsky (Tk) picrite, Naldrett (2004); Jinchuan, China, Chai and Naldrett (1992); Uitkomst, South Africa, Barnes and Maier (2002); Voisey's Bay, Canada, Scoates and Mitchell (2000).

[Abbreviations: $^{87}Sr/^{86}Sri$, initial strontium 87/86 ratio; $^{206}Pb/^{204}Pb$, lead 206/204 ratio; εNd, epsilon neodymium, relative Nd isotope-ratio deviation from the chondritic uniform reservoir value; γOs, gamma osmium, relative Os deviation from the chondritic upper mantle value; %, percent; ppm, parts per million; ppb, parts per billion; FeOt, total iron as ferrous (+2) iron oxide]

	Pechenga	Noril'sk Jinchuan	Uitkomst		Voisey's Bay
	Ferropicrite (Lammas)	Tholeiitic picrite (Tk)	High-Mg basalt	High-Si-Mg basalt	High-Al basalt
SiO_2 wt.%	45.49	48.23	50.8	55.87	48.26
TiO_2	2.02	0.77	1.0	0.37	0.96
Al_2O_3	6.45	12.82	12.5	12.55	17.22
FeOt	15.18	11.21	12.1	9.15	10.74
MnO	0.21	0.18	—	0.21	0.15
MgO	20.03	15.69	11.5	12.65	9.25
CaO	9.33	9.44	10.3	7.29	9.19
Na_2O	0.39	1.23	1.3	1.53	2.52
K_2O	0.15	0.35	1.8	0.77	0.44
P_2O_5	0.21	0.0	—	0.10	0.17
Rb ppm	6	8.75	30	27	2
Sr	—	157	200	180	461
Ba	76	141	—	310	288
Th	1.63	0.512	1.4	3.8	—
U	0.30	0.129	—	0.75	—
V	295	186	240	179	137
Sc	40.0	28	35	41	17
Cr	1,638	707	—	958	90
Y	—	12	20	—	12
Ta	1.26	0.136	—	0.16	—
Nb	—	—	8	—	—
Zr	111	56	100	74	36
Hf	—	1.426	2	—	—
La	19.9	4.7	12	13.2	6.70
Ce	37.0	10.91	26	26.6	14.4
Nd	20.7	6.44	15	15.9	8.44
Sm	4.81	1.82	3.5	2.57	1.95
Eu	1.40	0.709	0.9	0.71	1.13
Gd	—	2.210	—	—	1.87
Tb	0.54	0.345	0.4	0.32	—
Yb	0.98	1.279	1.5	1.06	0.74
Lu	0.14	0.199	0.25	0.14	0.094
Ni	822	288	400	257	177
Co	—	72	—	73	—
Cu	176	69	—	61	52
Os ppb	0.62	—	—	0.5	—
Ir	0.37	—	—	0.32	—
Ru	1.24	2.35	—	2	—
Rh	0.25	—	—	1.1	—
Pt	4	11.2	—	18	—
Pd	5	8.24	—	11	—
Au	—	—	—	3.05	—
$^{87}Sr/^{86}Sri$	—	0.7057	—	0.7032–0.7057	~0.7033
$^{206}Pb/^{204}Pb$	—	16.912	—	—	—
ε_{Nd}	+1.4	–2.03	–8	–4.59 to –6.31	~ +2.0
γ_{Os}	+6.0	+4.68	—	—	—

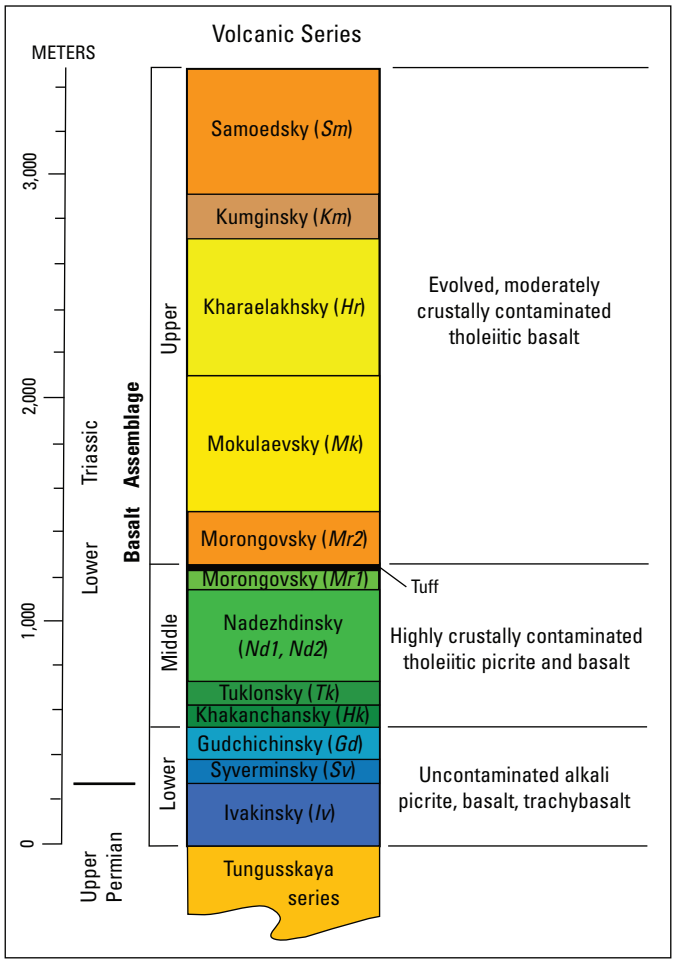

Figure 10–2. Volcanic rock stratigraphy of the Noril'sk region, Russia. Figure modified from Czamanske and others (1995). Note that volcanic-unit abbreviations are appended to the unit names in the stratigraphic sequence depiction (colored column).

like that found in the Tuklonsky Suite (Wooden and others, 1993; Lightfoot and others, 1994; Naldrett, 2004). In contrast, the slightly older Lower Talnakh-type intrusions share many geochemical features with the volcanic rocks of the Nadezhinsky Suite (Arndt, 2005).

In contrast to the picrite-related ore-bearing intrusions at Noril'sk, the Voisey's Bay Ni-Cu±PGE deposits are associated with troctolitic rocks related to a high-Al-type basaltic magma (Scoates and Mitchell, 2000). This is reflected in the abundance of high-Al compositions controlled by proportions of cumulate plagioclase, olivine, and trapped silicate liquid (Li and others, 2000). Until the discovery of the Voisey's Bay deposits in 1993, such troctolitic-anorthositic intrusions were not considered permissive for the occurrence of significant Ni-Cu±PGE sulfide mineralization because the rocks generally lack major accumulations of ferromagnesian silicate minerals (olivine, pyroxene), have intermediate mineral compositions ($An_{40–60}$; $Fo_{40–60}$), and have relatively low Ni and Cr abundances.

Table 10–3. Lithological and geochemical characteristics of volcanic series at Noril'sk, Russia. Modified from Arndt (2005).

[Abbreviations: %, percent; ε_{Nd}, epsilon neodymium, relative Nd isotope-ratio deviation from the chondritic uniform reservoir value]

	Suites	Rock types	Geochemical characteristics	Origin
Upper Series	Samoedsky, Kumginsky, Kharaelakhsky, Mokulaevsky, Upper Morongovsky (Mr2)	Tholeiitic basalt of remarkably uniform composition	Evolved, moderately siliceous basalt (SiO_2 = 48.4–50%; MgO = 6.3–8.1%). Moderate enrichment of incompatible trace elements; negative Nb-Ta anomalies; ε_{Nd} ~ 0	Moderate crustal contamination of high-degree mantle melts
Middle Series	Lower Morongovsky (Mr1), Nadezhdinsky	Lavas and tuffs of tholeiitic basalt	Siliceous basalt (SiO_2 = 52–55%; MgO = 6.3–8.1%). Moderate to strong enrichment of incompatible trace elements; large negative Nb-Ta anomalies; ε_{Nd} ~ 0 to –11	Highly contaminated tholeiitic magma
	Tuklonsky	Basalt and picrite	Basalt (SiO_2 = 49–50 %; MgO = 8–9%); picrite (SiO_2 = 47–49%; MgO = 10–17%). Moderate enrichment of incompatible trace elements; negative Nb-Ta anomalies; ε_{Nd} ~ –1 to –4.5	Moderately contaminated, more primitive magmas
Lower Series	Gudchikhinsky	Lavas and tuffs of alkali picrite and basalt	Basalt (SiO_2 = 49–52%; MgO =5.5–9%); picrite (SiO_2 = 46–51%; MgO = 10–21%). Moderate enrichment of incompatible trace elements; no Nb-Ta anomalies; ε_{Nd} ~ –2 to +4.6	Relatively uncontaminated moderate-degree mantle melts
	Syverminsky, Ivakinsky	Lavas and tuffs of alkali trachybasalt and basalt	Variable compositions (SiO_2 = 47–55%; MgO = 2.8–7.5%). Variable enrichment of incompatible trace elements; variable Nb-Ta anomalies; ε_{Nd} ~ 0 to –4	Relatively uncontaminated low-degree mantle melts

Trace-Element Geochemistry

Magmas parental to the intrusions that host magmatic sulfide-rich Ni-Cu±PGE sulfide deposits are themselves relatively enriched in Ni, Cu, and PGE (Keays, 1995; Arndt and others, 2005). In addition, the magmas are variably enriched in most of the strongly incompatible elements such as K, P, Ba, Sr, Pb, Th, and light REE (fig. 10–3; Zhang and others, 2008). In contrast, abundances of these same elements in primitive basalts from sequences without Ni-Cu±PGE sulfide deposits generally are lower (Zhang and others, 2008). Rare earth element patterns are variable but typically contain enriched light REE ($[La/Yb]_n$—chondrite-normalized ratio—as much as 60), with depleted to flat middle and heavy REE. Low-Yb samples also are depleted in Al_2O_3 and have high CaO/Al_2O_3 ratios, all features reflecting the role of residual garnet in the source region. Depletion of high-field-strength elements, such as Nb, Ta, and Ti, is common, and the majority of samples have Ba/Nb (as large as 300) and La/Nb (as large as 18.5) ratios much greater than ratios of primitive mantle (9 and 0.9, respectively) and ocean floor basalts (Zhang and others, 2008).

Primitive continental flood basalts tend to have higher PGE abundances than MORB but similar abundances to average ocean island basalts (fig. 10–4; Crocket, 2002). Continental flood basalts typically show systematically greater PGE abundances than their oceanic counterparts, both showing a broad trend of decreasing Pt and Pd with decreasing Mg number, with a proportion of samples exhibiting strong PGE depletion indicative of sulfide fractionation (Fiorentini and others, 2010). Zhang and others (2008) suggest that LIPs hosting Ni-Cu±PGE sulfide deposits (fertile) tend to have enriched PGE contents (for example, Os ≥ 0.03 to 10 ppb) and low Re/Os (typically < 0) relative to barren LIPs. In contrast, Fiorentini and others (2010) found no PGE-based evidence to support anomalous chalcophile-element enrichment in LIPs that host Ni-Cu±PGE sulfide deposits. Fiorentini and others (2010) suggest that the higher average Os contents of ore-associated LIP magmas are a consequence of greater abundance of primitive high-MgO magmas, which typically are characterized by higher Os contents owing to the strongly compatible behavior of Os. All LIP-related samples (fig. 10–4) tend to show fractionation between PPGE (Pt, Pd, and Rh) and IPGE (Os, Ir, and Ru), with supra-chondritic Pd/Ir (ratios ≥2.6).

Isotope Geochemistry

The LIP basalts show a large range of Sr and Nd isotopic ratios with $\varepsilon_{Sr(i)}$ values (epsilon strontium, the relative strontium isotope-ratio deviation from a primitive (initial) mantle $^{87}Sr/^{86}Sr$ value) between –18 and +180 and $\varepsilon_{Nd(i)}$ values (initial epsilon neodymium, the relative Nd isotope-ratio deviation from the value of the chondritic uniform Nd reservoir) between +9 and –16 (Zhang and others, 2008). In general, LIP basalts lack the depleted MORB-type Sr-Nd isotopic signatures, and many samples also plot far outside the field for oceanic island basalts (see figs. 5*A* and *B* in Zhang and others, 2008). With respect to Pb isotopes, most samples plot above the present-day Northern Hemisphere Reference Line (NHRL; Hart, 1984) on both $^{207}Pb/^{204}Pb$ versus $^{206}Pb/^{204}Pb$ and $^{208}Pb/^{204}Pb$ versus $^{206}Pb/^{204}Pb$ diagrams, whereas $^{206}Pb/^{204}Pb$ ratios range from 15.4 to 22.7, with most samples clustering between 17.4 and 19.2 (see figs. 5*C* and *D* in Zhang and

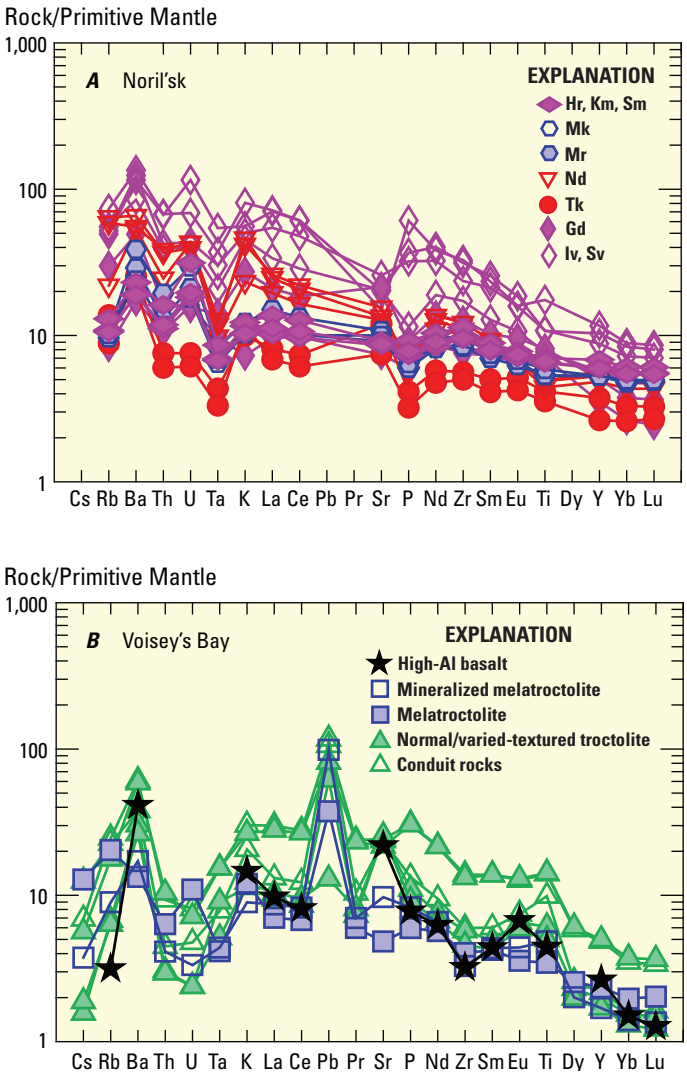

Figure 10–3. Primitive mantle-normalized trace-element patterns for volcanic rocks of *A*, the Noril'sk region, Russia, and *B*, intrusive rocks of the Voisey's Bay district, Canada. Also included in *B* is a high-Al basalt proposed as a parental composition for the Voisey's Bay troctolites (see table 11–2 in Scoates and Mitchell, 2000). Data from Naldrett (2004); Voisey's Bay data from Li and others (2000). Primitive mantle values from Sun and McDonough (1989). [Stratigraphic abbreviations in *A*, same as figure 10–2 for volcanic-series units: Sm, Samoedsky; Km, Kumginsky; Hr, Kharaelakhsky; Mk, Mokulaevsky; Mr, Morongovsky; Nd, Nadezhdinsky; Tk, Tuklonsky; Gd, Gudchichinsky; Sv, Syverminsky; and Iv, Ivakinsky.]

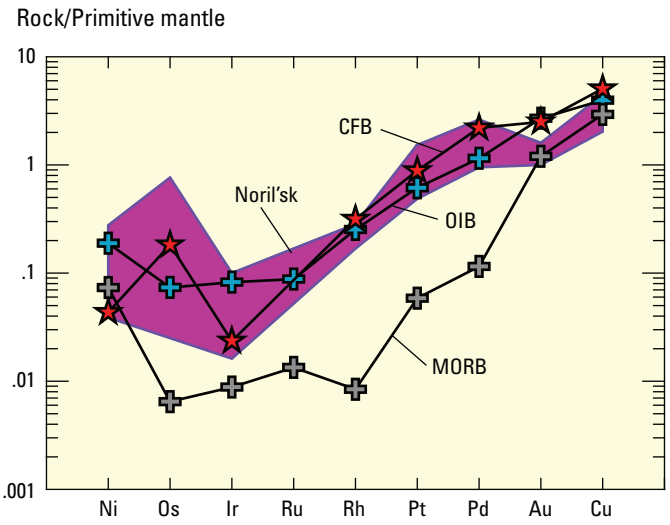

Figure 10–4. Primitive mantle-normalized chalcophile element patterns for average continental flood basalt (CFB), ocean island basalt (OIB), and mid-ocean ridge basalt (MORB). Also shown is the field for Noril'sk basalts and picrites. Basalt data from Crocket (2002); values for primitive mantle from Barnes and Lightfoot (2005).

others, 2008). The $^{187}Re/^{188}Os$ ratios of LIP basalts also show a large range of 0.04 to 1,800, with a time-integrated $^{187}Os/^{188}Os$ variation of 0.124 to 5.2. Positive correlations between $^{187}Re/^{188}Os$ and $^{187}Os/^{188}Os$ for basalts from some LIP provinces, however, produce "isochron" ages in close agreement with the age of magmatism determined by other methods and initial $^{187}Os/^{188}Os$ ratios close to chondritic, lower than ratios observed in most ocean island basalts and MORB ($\gamma_{Os(i)} \geq 2.4$; Shirey and Walker, 1998, where γ_{Os} is gamma osmium, relative Os deviation from the chondritic upper mantle value) and continental crustal rocks.

One distinctive isotopic feature of LIP basalts is that, despite considerable scatter in the data, correlations between Sr-Nd-Pb ratios for individual provinces appear to converge toward a common end-member composition, FOZO (focal zone; Zindler and Hart, 1986). In addition, neither continental nor oceanic LIP basalts show the HIMU-type (high μ-mantle; $\mu = {}^{238}U/{}^{204}Pb$) isotopic signatures common in oceanic island basalts (Zhang and others, 2008). In detail, basalts from individual LIPs define distinct Sr-Nd-Pb isotopic trends with varying slopes extending from a depleted (FOZO-like) source to varying enriched fields.

11. Petrology of Related Sedimentary and Metamorphic Country Rocks

Magmatic sulfide-rich Ni-Cu±PGE deposits range in age from Archean to Mesozoic and have been emplaced into a broad spectrum of country rock and basement terranes (table 11–1). However, as noted by Hoatson and others (2006), the presence of Ni-Cu±PGE mineralization shows no obvious correlation with the composition or metamorphic grade of basement lithologies. Thus, the importance of the country rocks that host magmatic Ni-Cu±PGE deposits lies not in their chemical composition but in whether the rocks may contribute to sulfur saturation of magma and to the physical controls that country rocks may exert on intrusion dynamics.

In a closed system, fractional crystallization of magma with low sulfur content will produce only a small volume of sulfide minerals late in the crystallization sequence. To produce sufficient sulfide to form a deposit, an external mechanism generally is needed to induce sulfur saturation early in the crystallization process (Lightfoot and others, 1984; Arndt, 2005). Two possible external mechanisms have been identified: (1) addition of sulfur to a magma either by bulk assimilation of sulfide- or sulfate-bearing country rocks (for example, Noril'sk: Naldrett, 1997; Voisey's Bay: Ripley and others, 2002) or by selective uptake by magma of externally derived sulfur as a vapor or fluid phase from surrounding country rocks (Ripley, 1981); and (2) assimilation of felsic wall rocks during magmatic ascent, thus increasing the silica content of the magma and thereby reducing sulfur solubility and inducing sulfur saturation (for example, Duluth Complex: Li and Naldrett, 1993; Nebo-Babel: Hoatson and others, 2006; Seat and others, 2009). For some deposits, both mechanisms may have played a role. Li and others (2009) have suggested that addition of external sulfur, as well as addition of siliceous material to drive sulfur saturation, were crucial for the development of the sulfide deposits at Noril'sk.

The sulfur content of crustal reservoirs plays an important role in determining whether a mafic-ultramafic magmatic system will produce sulfide mineralization. Keays and Lightfoot (2010) compared the unmineralized Deccan flood basalt system to the Siberian flood basalts which host the Noril'sk deposits and determined that simply having significant crustal contamination of the magmatic system was not sufficient to produce large Ni-Cu±PGE sulfide deposits. Although a wide variety of sedimentary and metamorphic rock types may interact with a S-undersaturated magma (table 11–1), unless a threshold level of sulfur is present within the crustal contaminant, the magmatic system likely will not reach early sulfur saturation and produce significant mineralization (Keays and Lightfoot, 2010). Where a magmatic system may be only slightly undersaturated with respect to sulfur, however, additional silica contributed by crustal contamination may be enough to trigger sulfide saturation, regardless of the sulfur content of the contaminant (Seat and others, 2009).

The effect of metamorphism and deformation on magmatic sulfide deposits can be manifested in several ways. First, metamorphism of the country rocks due to emplacement of intrusions may result in development of skarns and contact aureoles, such as at Noril'sk and Uitkomst. Post-emplacement cataclastic metamorphism may remobilize, and possibly disperse, sulfide ores, as in the development of matrix-brecciated sulfides at Pechenga (Naldrett, 2004) or the remobilization of sulfides along shear zones as at the Kabanga deposit (Maier and

Table 11–1. Comparison of exposed sedimentary and metamorphic country rocks associated with magmatic Ni-Cu±PGE sulfide deposits.

[Ma, Mega-annum]

Deposit/age Ma	Related sedimentary rocks	Related metamorphic rocks	Metamorphic grade
Wellgreen (Canada) (232 Ma)	Carbonates, volcaniclastic and clastic sedimentary rocks	None	Unmetamorphosed
Noril'sk-Talnakh (Russia) (251 Ma)	Dolomites, limestones, argillites, evaporites, coal seams	Hornfels (100–400 m thick)	Contact metamorphism
Jinchuan (China) (827 Ma)	Shales, limestones	Marbles, gneisses, schists	Upper amphibolite facies (basement rocks), greenschist facies (cover rocks)
Nebo-Babel (Australia) (1,078 Ma)	None	Orthogneisses	Amphibolite to granulite facies
Eagle (United States) (1,107 Ma)	Quartzites, cherts, graywackes, slates	Gneisses, metasedimentary rocks	Regional greenschist facies
Kabanga (Tanzania) (1,275 Ma)	Sulfide-bearing pelitic rocks (footwall); quartzites, immature clastic rocks, shales (hanging wall)	Muscovite-staurolite-biotite ± garnet schists	Contact metamorphism; country rocks are mid-amphibolite facies
Voisey's Bay (Canada) (1,334 Ma)	None	Orthogneisses, paragneisses	Amphibolite-granulite facies
Pechenga (Russia) (1,977 Ma)	Sandstones, siltstones, tuffs	Phyllites	Greenschist to amphibolite facies
Uitkomst (South Africa) (2,054 Ma)	Shales, quartzites, dolomites, chert-conglomerates	Archean granitic gneisses, quartzites	Contact metamorphism; skarn near dolomites
Radio Hill (Australia) (2,892 Ma)	None	Metavolcanic rocks, gneisses, migmatites	Variable, mostly high

others, 2010). High-grade metamorphism can be accompanied by recrystallization and an increase in grain size in both the host intrusion and the related sulfide zones. Equigranular granoblastic textures may be present in the intrusion, and a coarsening in the grain size of the sulfides can have a positive effect with respect to grinding requirements during mineral processing. The intensity and style of deformation may have a significant impact on the morphology of sulfide lenses that may be thickened in pressure shadows or conversely may be dismembered and/or attenuated.

The physical nature of country rocks also may influence intrusion emplacement styles (Naldrett, 2004). Continental crust typically is stratified with a lower layer of dense granulite-facies rocks, an intermediate layer of lower density granitoid and metamorphic rocks, and, in many cases, an upper layer of still less-dense sedimentary rocks. This crustal structure helps control the formation of magma chambers as ascending magma tends to become trapped at each density discontinuity (Arndt, 2005). When magma reaches horizontally bedded sedimentary strata in the upper crust, horizontal intrusions and sills tend to form, such as at Noril'sk (Naldrett, 2004), Kabanga (Maier and others, 2010), Uitkomst (Li and others, 2002), and Wellgreen (Marcantonio and others, 1994). Horizontal flow through upper crustal sill complexes can augment the period of interaction between magma and wall rocks, thereby increasing the extent of contamination and likelihood of sulfur saturation (Arndt, 2005). Differences in metamorphic grade between packages of rocks also may provide a structural contrast or weakness that can allow emplacement of an intrusion along such structural breaks. The deposit at Jinchuan is an example of an intrusion that likely was emplaced along a disconformity between marbles and felsic gneisses (Lehmann and others, 2007).

12. Theory of Deposit Formation

The formation of magmatic sulfide-rich Ni-Cu±PGE deposits is a consequence of the crystallization of mafic and ultramafic magmas. Separation of an immiscible sulfide liquid is a normal product in the crystallization of most mafic and ultramafic systems. Typically only a small quantity of sulfide is formed relatively late in the crystallization history because of limitations on abundance of sulfur in most magmas and because sulfur saturation and separation of a sulfide liquid generally occur late in the crystallization history when silicate

minerals are abundant. The common result is a small amount of disseminated sulfide minerals among more abundant silicate minerals; the sulfide minerals typically are insufficient both in quantity and metal tenor to be economic. In addition, because olivine commonly is the first phase to crystallize from most mafic and ultramafic magmas upon cooling, the late-forming disseminated sulfides exhibit relatively low Ni contents and Ni/Cu ratios because olivine removes Ni from the silicate melt as it crystallizes (Barnes and Lightfoot, 2005). Therefore, formation of sulfide-rich Ni-Cu±PGE deposits requires that sulfur saturation occurs relatively early in the crystallization history of the magmas. For this to occur typically requires incorporation of crustal sulfur (Li and others, 2001b, 2009).

Formation of magmatic sulfide-rich Ni-Cu±PGE deposits can be viewed as the outcome of several stages in the evolution of mafic-ultramafic magmatic systems (fig. 12–1; Naldrett, 2010). In the first stage, a metal-bearing primitive mafic or ultramafic parental magma is formed through partial melting in hotter-than-normal parts of the mantle. That magma typically represents the product of relatively high degrees of partial melting (≥20 to 25 percent), has large MgO content (>12 weight percent), is relatively enriched in Ni and PGE, and is sulfur-undersaturated during ascent from the mantle and emplacement into the crust (Keays, 1995; Naldrett, 2010). Such primitive magmas are a common component in most LIPs and are particularly prevalent early in a LIP's magmatic history.

Naldrett (2010) modeled the melting of a representative mantle composition at low (15 kb) pressure. For that mantle composition, the modeling showed that by 11 percent melting, all sulfide present in the source had dissolved into the silicate liquid. Therefore, as the percentage of mantle melting increases above 11 percent, Pt, Pd, and Cu, originally contained in mantle sulfide minerals, are diluted in the melt and decrease in concentration, whereas the Ni content, originally contained both in mantle sulfide and in olivine, continues to increase in the melt. Further, although the melt may be sulfur-saturated at the source, because of the negative effect of pressure on sulfur solubility (Wendlandt, 1982) as the magma rises, it will become undersaturated in sulfide upon emplacement into the crust. The degree of sulfide undersaturation of the magma as it enters the crust and begins to cool, however, has an important influence on capacity of the magma to form an economic sulfide deposit. If the magma composition is close to sulfide saturation upon emplacement, then sulfide liquid may segregate deep in the crust, leaving ore metals at depth and the remaining magma depleted in chalcophile metals. Alternatively, strongly sulfide-undersaturated magmas may rise to shallower levels in the crust but will require access to large external amounts of sulfur to achieve sulfide saturation (Arndt and others, 2005).

Sulfide-undersaturated magmas may interact with crustal wall rocks during ascent and staging in subcrustal magma chambers. Such interactions can form hybrid or contaminated magmas with higher silica contents and also may result in incorporation of crustal sulfur. Both processes can drive a magma to sulfur saturation and cause the formation of an immiscible sulfide liquid (Li and others, 2001b). The common derivation of sulfur from country rock is supported by the sulfur isotope composition of ores from a number of sulfide-rich Ni-Cu±PGE deposits, including those at Noril'sk, Pechenga, Voisey's Bay, and Eagle. For the efficient accumulation of massive sulfide, it is important that sulfide saturation and resultant sulfide liquid segregation occur early in the crystallization sequence, before abundant silicate minerals crystallize and trap the sulfides. In addition, early sulfide saturation is necessary because significant olivine crystallization prior to formation of an immiscible sulfide liquid will deplete a silicate liquid in Ni, thus limiting the quantity of Ni available to a sulfide liquid (Barnes and Lightfoot, 2005; Naldrett, 2010).

Once a sulfide liquid has formed, chalcophile metals are concentrated. Campbell and Naldrett (1979) have shown that, in a closed system, the concentration of a metal in a sulfide liquid (C_s) is a function of the concentration of the metal in the initial silicate liquid (C_L), the partition coefficient between the sulfide and silicate liquids (D), and the ratio of the mass of silicate magma to the mass of sulfide that reached equilibrium together, expressed as R:

$$C_s = C_L D(R + 1)/(R + D) \quad (1)$$

The effect of R is most pronounced for PGE, such that at low R values, in the range of 100 to 2,000, the Ni and Cu contents of the sulfides may be in the range typical of most Ni-Cu-sulfide ores, but Pt and Pd contents will be relatively low. In contrast, when R is in the range of 10,000 to 100,000, Ni and Cu contents will not be much higher than contents at lower R, but Pt and Pd contents will be much higher and in the range of concentrations found in some Noril'sk deposits and in "reefs" in layered intrusions, such as at the Merensky Reef in the Bushveld Complex, South Africa.

Because of their very high partition coefficients, PGE are extremely sensitive to removal of sulfides from silicate melt. Thus, whereas a small amount of early crystallization of olivine or sulfides will not lower the Ni content of the magma significantly, removal of even small amounts of sulfide will sharply deplete the PGE content and mildly deplete Cu (Barnes and Lightfoot, 2005). Lightfoot and Keays (2005) attribute early separation of a sulfide liquid for the exceptionally low PGE abundances observed in basaltic lavas overlying the Noril'sk deposits. In addition, any sulfide liquid that forms subsequently to an initial sulfide loss in such magmas will be depleted in PGE relative to Ni and Cu contents. This may explain why some deposits with comparable Ni contents have very different PGE contents, such as Noril'sk with high PGE versus Voisey's Bay with low PGE (Barnes and Lightfoot, 2005).

The resulting immiscible sulfide liquid may interact dynamically with a larger mass of silicate magma, thereby increasing the tenors of the ore metals, particularly for the strongly chalcophile elements that have very large partition coefficients between sulfide liquid and silicate magmas

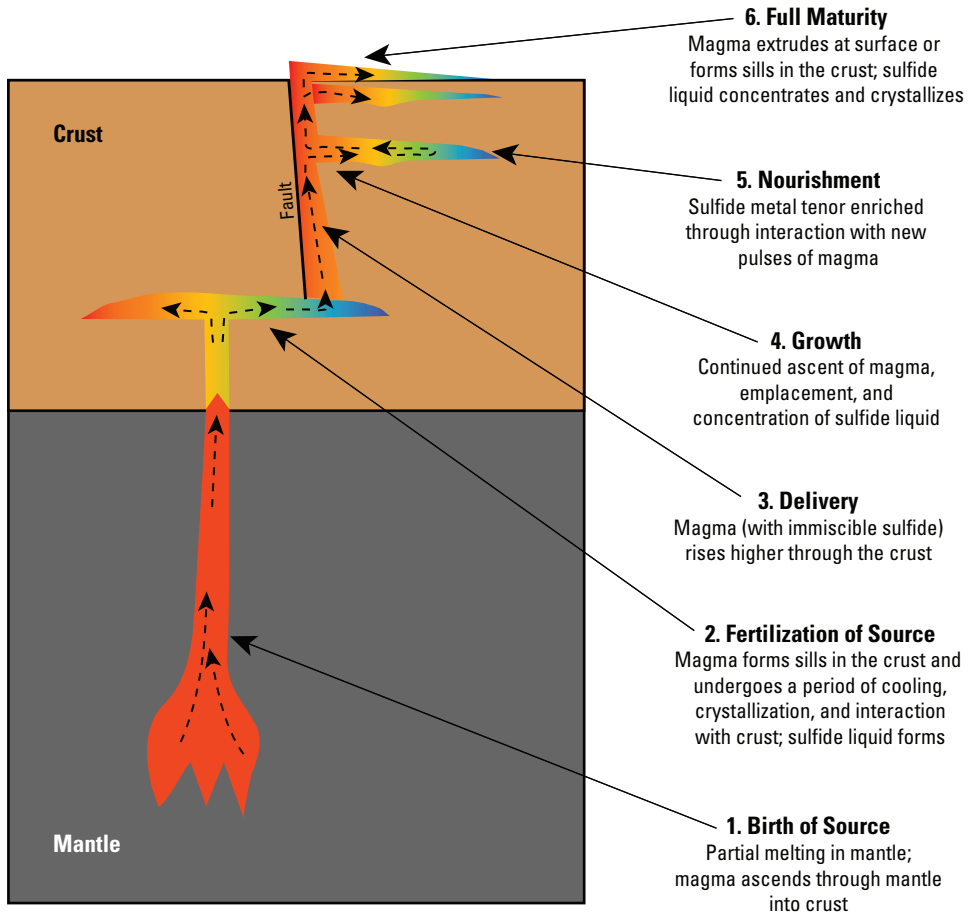

Figure 12–1. Stages in the formation of magmatic sulfide-rich Ni-Cu±PGE deposits (modified from Naldrett, 2010).

(Mungall, 2005). The Ni, Cu, and PGE contents of many ores are higher than would be expected of sulfide that had separated from the relatively small quantity of magma represented by their host intrusions (Campbell and Naldrett, 1979). Therefore, the sulfide liquid must have interacted with, and extracted ore metals from, a larger volume of silicate magma. Such upgrading is enhanced in magma conduit systems where previously formed sulfide can interact with new pulses of undepleted magma (Maier and others, 2001). Exactly how sulfide liquid and new pulses of magma interact is not clear, however, and may vary from deposit to deposit. Kerr and Leitch (2005) noted that new pulses of undepleted magma likely would be undersaturated in sulfide and, as a result, could be expected not only to contribute chalcophile elements to the sulfides but also to dissolve and remove sulfide. Because PGE, Ni, and Cu are much more chalcophile in nature than Fe, the bulk of the dissolved sulfide would be FeS, with the more chalcophile metals remaining with the original sulfide. Modeling of such upgrading with accompanying dissolution shows a much steeper increase in the metal content of the sulfide (high R factors) than would result from simple batch equilibration (Kerr and Leitch, 2005; Naldrett, 2010). Based on estimates of the diffusivities of the elements concerned, it appears that simple passage of undepleted magma over a pool of massive sulfide would not result in significant interaction and upgrading of metal tenors (Mungall, 2002). Thus, upgrading of metal tenors likely requires the intimate mixing of silicate magma and sulfide liquid on a droplet scale.

To form an economic Ni-Cu±PGE sulfide deposit, a sufficient quantity of metal-rich sulfide liquid must become concentrated in a restricted locality (Maier and others, 2001). Because the densities of sulfide liquids (about 4 to 5 g/cm^3) are greater than that of silicate magmas within which they develop (about 2.8 to 3.4 g/cm^3; table 6–2), sulfide droplets will tend to settle in a silicate melt unless impeded by such factors as the presence of phenocrysts, melt viscosity, surface tension, or melt transport velocity (Mungall and Su, 2005; Chung and Mungall, 2009). Because of density differences, sulfides can be transported vertically in a silicate melt if a magma's upward velocity is greater than the sulfide settling rate; modeling suggests that mafic magma moving upwards at 0.1 m/s could effectively transport 1-cm-diameter sulfide droplets (Lesher and Groves, 1986; de Bremond d'Ars and others, 2001). Further, the sulfide droplets are unlikely to coalesce during

transport because they will be armored from each other by a coating of silicate melt (de Bremond d'Ars and others, 2001). Any decrease in upward velocity, however, could cause the sulfide droplets to settle and pond. Therefore, structural traps, where the flow velocity of magma is reduced, are important sites for collection of sulfides. This includes embayments in the footwall, where dense sulfide liquid can migrate downward along the axis of the embayment and down the flanking sides (as at Noril'sk-Talnakh; Diakov and others, 2002), and where a narrow feeder conduit enters a larger intrusion, resulting in a decrease in flow velocity and preferential concentration of sulfide droplets (for example, Voisey's Bay; Li and others, 2000). If deformation occurs before the sulfide liquid has completely solidified, then residual sulfide liquid may migrate or be injected into dilatant structures in the footwall (Barnes and Lightfoot, 2005).

In most cases, sulfide liquids have lower solidus temperatures than silicate melts and can fractionate as crystallization proceeds with decreasing temperature (Naldrett, 2004). On cooling, the first phase generally to crystallize from a sulfide liquid is monosulfide solid solution (MSS, the Ni-bearing, high-temperature equivalent of pyrrhotite). Experimental studies of the partitioning of chalcophile metals between MSS and sulfide liquid (Mungall and others, 2005, and references therein) and observations on natural ores both show that fractionation of a sulfide liquid results in enrichment of Cu, Pt, Pd, and Au in residual liquid. If the resulting Cu-enriched liquid escapes from the crystallizing MSS, then it can form veins in dilatant structures in the footwall, such as at Noril'sk and Eagle.

13. Exploration and Resource Assessment Guidelines

A variety of geological, geochemical, and geophysical guides can be used in mineral exploration and resource assessment for magmatic sulfide-rich Ni-Cu±PGE deposits. In addition, some guides apply more at the regional scale and others at a local scale. A number of regional and local guides are outlined below along with typically used exploration methods.

Geological Guides for Regional Mineral Exploration and Resource Assessment

1. A Large Igneous Province (LIP) with evidence of primitive Mg-rich melts and large volumes of sulfur-undersaturated tholeiitic magmatic rocks occurring on or near the edges of ancient cratons.
2. Cratonic margins, rifts, and deeply penetrating faults that can allow for efficient transport of magma through the crust.
3. Presence of small- to medium-sized differentiated mafic and/or ultramafic dikes, sills, chonoliths, and plug-like intrusions. Deposits generally are not hosted in large, thick, layered intrusions.
4. Presence of sulfur-bearing (sulfide and/or sulfate) crustal rocks.

Geological Guides for Local Mineral Exploration and Resource Assessment

1. Clusters of small to medium-sized, generally mafic-dominated tholeiitic intrusions with ultramafic rocks, if present, typically concentrated at or near the base. Intrusions related to picrites, however, may be wholly or dominantly ultramafic, whereas intrusions related to high-Al basalts will tend to be dominantly plagioclase-rich troctolites and anorthosites.
2. Massive or layered intrusions with variably textured rocks and/or magmatic breccias along the margins. These features may be evidence for multiple injections of magma. Intrusions can exhibit changes in texture and mineralogy on a variety of scales (a few centimeters to tens of meters) with cumulus-, equigranular-, intergranular-, and/or subophitic-textured rocks.
3. Laterally extensive contact metamorphism, particularly above intrusions, and/or metasomatism of country rocks near intrusions.
4. Local geochemical evidence of crustal contamination and/or chalcophile-element depletion in intrusions and/or related volcanic rocks. Widespread evidence of contamination and/or chalcophile-element depletion may reflect source characteristics or prior magma contamination and sulfide fractionation in the lower crust, thus suggesting a less favorable environment for the presence of a major Ni-Cu±PGE sulfide deposit at shallow depths.
5. Significant changes in dip and width along the strike of an intrusion indicating sites of possible changes in magma flow dynamics. Changes in the dynamics of magma flow (whether slow, fast, or turbulent flow) and conduit geometry (changes from narrow vertical conduits to broad, subhorizontal magma chamber; physical traps) are important factors for the precipitation and accumulation of massive sulfide.

6. Evidence for a dynamic, open, periodically replenished magmatic system, such as sharp and cross-cutting lithologic contacts, magmatic breccias, reversals in fractionation indicators, and changes in chalcophile-element contents within intrusions and/or associated volcanic rocks.

7. Presence of massive, matrix, and disseminated Fe-Ni-Cu-Co-bearing sulfide minerals in the lower parts of intrusions and Cu-Pd-Pt-Au-enriched sulfide minerals either stratigraphically above Cu-poor sulfides or as footwall dikes and veins that provide evidence of remobilized and fractionated sulfide liquid. Massive sulfides typically are confined to structural embayments and depressions along the basal contacts of intrusions or in feeder conduits. Therefore, determination of the base of a given intrusion is an important criterion in exploration targeting, particularly in deformed terranes.

8. Because massive sulfides are incompetent and concentrate stress during deformation, they may be displaced significant distances (≥1 km) from their host intrusions. Therefore, country rocks surrounding sulfide-bearing intrusions also should be investigated in strongly deformed terranes.

Exploration Methods

1. Exploration using geophysics needs to be tailored to a study area based on factors such as the maximum depth of detection and physical properties of the overburden, intrusions, host lithologies, and mineralization. Regional aerial magnetic and gravity surveys are used to identify prospective areas of LIPs showing the regional characteristics noted above, and to determine the extent, geometry, and basal contacts of intrusions. At district to local scales, ground magnetics are used to delineate lithologic layering and to identify small-scale structural embayments and depressions along the basal contact of intrusions. Airborne and ground electromagnetics and induced polarization are used to identify and delineate conductive sulfides.

2. Stream-sediment and soil geochemistry for Ni, Cu, Cr, and PGE may be useful if intrusions are exposed or are in subcrop. Gossans, if present, are generally strongly leached of Ni and Cu but may have elevated PGE contents.

3. Lithogeochemical study of prospective intrusions for S, Cu, Ni, PGE contents, as well as for Cu/Pd ratio and Mg-number helps to determine stratigraphic variations and the occurrence of sulfur-saturation events.

4. Composition of olivine (Ni content versus Mg-number) can be used as an indicator of nickel depletion in magmas from which the olivine has crystallized.

5. Evidence for crustal contamination and/or sulfur addition can be determined from S, O, Sr, Nd, Pb, and Os isotopes; from high Th/Nb and La/Nb ratios and enriched light REE and alkali contents; from hybrid rocks; and from xenoliths of country rock and/or xenocrysts.

6. Evidence of depleted chalcophile elements, particularly PGE, such as shown by high Cu/Pd ratios (>10,000) and Pt and Pd contents near or below detection levels (<1 ppb). On a local scale, such values indicate the presence of sulfides stratigraphically below the depleted horizon, or up the magmatic flow direction from it, and provide a vector for focusing exploration.

7. Unusual gossan chemistry and mineralogy, such as high Bi, Pt, Pd, and Ir or the presence of chalcopyrite stringers and Ni-carbonates, can distinguish unmineralized pyritic gossans from gossans developed on Ni-Cu±PGE deposits.

8. Close-spaced drilling, particularly of basal contacts and feeder conduits, as well as downhole geophysics, such as time-domain electromagnetics and radio-imaging methods, can help direct exploration toward the most mineralized parts of an intrusion.

14. Geoenvironmental Features

Weathering Processes

Modern weathering processes operating on mine wastes from sulfide deposits result in acid generation and mobility of metals. Acid-mine drainage can be one of the most significant issues related to sulfide-rich Ni-Cu deposits because of an abundance of pyrrhotite and a general lack of any significant neutralizing potential or alkalinity. The geochemistry of acid-mine drainage was reviewed by Nordstrom and Alpers (1999), and additional aspects of the weathering of a variety of ore and gangue minerals were discussed by Plumlee (1999). Foose and others (1995) reviewed the geoenvironmental characteristics of magmatic sulfide deposits. Whereas the magmatic Ni-Cu±PGE deposits related to the Sudbury structure in Ontario represent a unique geologic phenomenon and therefore do not fall within this strict deposit classification, the overall geological and

geochemical characteristics of the Sudbury ores nevertheless generally conform to other magmatic Ni-Cu±PGE sulfide deposits. Therefore, environmental geochemical case studies of the Sudbury district should have broader relevance to other, similar sulfide deposits. Likewise, komatiite-hosted Ni deposits also represent a subclass of magmatic Ni-Cu sulfide deposits that is distinct from basaltic dike- and sill-related deposits but may offer some general environmental insights which may be useful.

Geochemical aspects of the formation of acid-mine drainage and its burden of metals and other elements of concern can be divided into three broad topics: (1) sulfide-oxidation, acid-generation, and acid-neutralization processes; (2) metal cycling associated with efflorescent secondary sulfate salts; and (3) secondary precipitation of hydroxides and hydroxysulfates and their sorption of metals.

Sulfide-Oxidation, Acid-Generation, and Acid-Neutralization Processes

The abundance of pyrrhotite in magmatic Ni-Cu±PGE sulfide deposits dominates most aspects of the environmental behavior of these deposits and their mine wastes. Acid generated by oxidative weathering of pyrrhotite can aggressively attack other ore and gangue minerals, thereby liberating a variety of potentially toxic elements, including metals from sulfides and Al from silicates. Metal-laden acid-sulfate waters can adversely affect surrounding surface water and groundwater. Within the hydrologic system of mine workings or mine wastes, minerals and other compounds, such as lime used in flotation circuits, can neutralize acid generated by the oxidative weathering of sulfide minerals. Thus, the chemistry of drainage from a mine site is the result of the competing processes of acid generation and acid neutralization.

The oxidation of pyrrhotite and other sulfide minerals proceeds with either dissolved oxygen (O_2) or dissolved ferric iron (Fe^{3+}) as the oxidizing agent. Dissolved oxygen is the most important oxidant at pH values above ≈4, whereas ferric iron dominates below pH values ≈4 (Williamson and others, 2006). The aqueous oxidation of pyrrhotite by dissolved oxygen is described by Reaction 1:

$$Fe_{1-x}S + (2-x/2)\ O_2 + x\ H_2O \rightarrow (1-x)\ Fe^{2+} + SO_4^{2-} + 2x\ H^+ \quad (1)$$

where x ranges from 0.000 to 0.125. Pyrrhotite oxidation by ferric iron is described by Reaction 2:

$$Fe_{1-x}S + (8-2x)\ Fe^{3+} + 4\ H_2O \rightarrow (9-3x)\ Fe^{2+} + SO_4^{2-} + 8\ H^+ \quad (2)$$

Reactions 1 and 2 actually represent the mass action of numerous intermediate reactions. In the oxidative weathering of pyrrhotite, a common initial reaction is the oxidation of pyrrhotite to either pyrite or marcasite as described by Reaction 3:

$$2Fe_{1-x}S + (1/2-x)\ O_2 + (2-4x)\ H^+ \rightarrow FeS_2 + (1-2x)\ Fe^{2+} + (1-2x)\ H_2O \quad (3)$$

Textural evidence of marcasite replacement of pyrrhotite is common in pyrrhotitic mine wastes (Jambor, 1994, 2003; Hammarstrom and others, 2001).

Although pyrite is not ubiquitous in mine waste from magmatic Ni-Cu±PGE deposits, its oxidation reactions are pertinent to understanding the behavior of wastes from this deposit type. The aqueous oxidation of pyrite by dissolved oxygen is described by Reaction 4:

$$FeS_2 + 7/2\ O_2 + H_2O \rightarrow Fe^{2+} + 2\ SO_4^{2-} + 2\ H^+ \quad (4)$$

The aqueous oxidation of pyrite by ferric iron is described by Reaction 5:

$$FeS_2 + 14\ Fe^{3+} + 8\ H_2O \rightarrow 15\ Fe^{2+} + 2\ SO_4^{2-} + 16\ H^+ \quad (5)$$

For reactions 2 and 5 where ferric iron is the oxidant, ferrous iron (Fe^{2+}) must be oxidized to ferric iron as described by Reaction 6:

$$Fe^{2+} + ¼\ O_2 + H^+ \rightarrow Fe^{3+} + ½\ H_2O \quad (6)$$

The rate of the oxidation of ferrous iron to ferric iron is strongly dependent on pH, and can be greatly enhanced by the iron-oxidizing bacterium *Acidithiobacillus ferrooxidans*. Singer and Stumm (1970) observed that *A. ferrooxidans* increased the rate of oxidation of ferrous iron to ferric iron by a factor of 100,000 compared to the abiotic rate. In the reactions for pyrrhotite (Reactions 1 and 2) and pyrite (Reactions 4 and 5), additional acid is generated by the oxidation and hydrolysis of the aqueous ferrous iron as described by Reaction 7:

$$Fe^{2+} + ¼\ O_2 + 5/2\ H_2O \rightarrow Fe(OH)_3 + 2\ H^+ \quad (7)$$

This also produces the orange and brown iron-oxide precipitates that typify acid-mine drainage.

Weathering of chalcopyrite and pentlandite also contributes metals, sulfate, and acidity to waters. The oxidative weathering of chalcopyrite by dissolved oxygen, which does not generate acid, can be described by Reaction 8:

$$CuFeS_2 + 4\ O_2 \rightarrow Cu^{2+} + Fe^{2+} + 2\ SO_4^{2-} \quad (8)$$

However, the continued oxidation and hydrolysis of ferrous iron, as described by Reaction 7, will generate acid. The oxidative weathering of chalcopyrite by ferric iron can be described by Reaction 9:

$$CuFeS_2 + 16\,Fe^{3+} + 8\,H_2O \rightarrow Cu^{2+} + 17\,Fe^{2+} + 2\,SO_4^{2-} + 16\,H^+ \quad (9)$$

As stated previously, continued oxidation of ferrous iron will generate additional acid.

Likewise, the oxidative weathering of pentlandite, approximated by the formula $(Fe_{0.5}Ni_{0.5})_9S_8$, by dissolved oxygen can be described by Reaction 10:

$$(Fe_{0.5}Ni_{0.5})_9S_8 + 15.5\,O_2 + H_2O \rightarrow 4.5\,Fe^{2+} + 4.5\,Ni^{2+} + 8\,SO_4^{2-} + 2\,H^+ \quad (10)$$

The oxidative weathering of pentlandite by ferric iron can be described by Reaction 11:

$$(Fe_{0.5}Ni_{0.5})_9S_8 + 66\,Fe^{3+} + 32\,H_2O \rightarrow 70.5\,Fe^{2+} + 4.5\,Ni^{2+} + 8\,SO_4^{2-} + 64\,H^+ \quad (11)$$

The continued oxidation and hydrolysis of ferrous iron produced by Reactions 10 and 11 will generate additional acid.

Pyrrhotite and other sulfides, such as chalcopyrite, can also undergo nonoxidative dissolution under anoxic conditions when exposed to acid, as described by the respective Reactions 12 and 13:

$$Fe_{1-x}S + (2-2x)\,H^+ + x\,H_2 \rightarrow (1-x)\,Fe^{2+} + H_2S \quad (12)$$

$$CuFeS_2 + 4\,H^+ \rightarrow Cu^{2+} + Fe^{2+} + 2\,H_2S \quad (13)$$

These reactions effectively decouple iron and sulfur oxidation and both reactions consume acid.

Gangue minerals in host rocks and surrounding lithologies can react and consume some of the acid generated by the oxidation of sulfide minerals. Silicate minerals commonly found with magmatic Ni-Cu±PGE sulfide deposits, such as olivine, orthopyroxene, and plagioclase, can neutralize minor amounts of acid generated by the oxidation of sulfide minerals as described by the respective idealized Reactions 14–16:

$$Mg_2SiO_4 + 4\,H^+ \rightarrow 2\,Mg^{2+} + H_4SiO_{4(aq)} \quad (14)$$

$$MgSiO_3 + 2\,H^+ + H_2O \rightarrow Mg^{2+} + H_4SiO_{4(aq)} \quad (15)$$

$$CaAl_2Si_2O_8 + 2\,H^+ + H_2O \rightarrow Ca^{2+} + Al_2Si_2O_5(OH)_{4(s)} \quad (16)$$

Solid solution of ferrous iron for magnesium in olivine and orthopyroxene can partially counteract the acid neutralization potential of Reactions 14 and 15 because of the continued oxidation and hydrolysis of ferrous iron (Reaction 7). Olivine is one of the most reactive silicate minerals with respect to acid neutralization (Jambor and others, 2002, 2007). Carbonate minerals, such as calcite, may also be present in country rocks surrounding magmatic sulfide deposits. Calcite can consume acid as described by Reaction 17:

$$CaCO_3 + H^+ \rightarrow Ca^{2+} + HCO_3^- \quad (17)$$

The influence of minor amounts of calcite is most prominent in the anoxic portions of tailings piles where it can effectively neutralize acid (Blowes and others, 2003).

Metal Cycling Associated with Efflorescent Sulfate Salts

Evaporative concentration of sulfate-rich mine drainage can produce a series of highly soluble secondary sulfate salts. Evaporative processes can operate during hot, arid conditions, within mine workings or other sheltered areas, or in tailings piles beneath snow packs. Common secondary sulfate salts in mining environments associated with magmatic Ni-Cu sulfide deposits include melanterite $[Fe^{2+}(SO_4)\cdot 7(H_2O)]$, rozenite $[Fe^{2+}(SO_4)\cdot 4(H_2O)]$, halotrichite $[Fe^{2+}Al_2(SO_4)_4\cdot 22(H_2O)]$, alunogen $[Fe^{2+}Al_2(SO_4)_4\cdot 22(H_2O)]$, copiapite $[Fe^{2+}Fe^{3+}{}_4(SO_4)_6(OH)_2\cdot 20(H_2O)]$, morenosite $[Ni(SO_4)\cdot 7(H_2O)]$, and chalcanthite $[Cu(SO_4)\cdot 5(H_2O)]$ (Jambor, 1994; Jambor and others, 2000; Hammarstrom and others, 2001). Gypsum $[Ca(SO_4)\cdot 2(H_2O)]$ is another common secondary sulfate, which can contribute dissolved solids to drainage, but does not store acidity or metals. Metal-sulfate salts offer a means of temporarily sequestering acidity and metals for later dissolution during rain events or snowmelt (Jambor and others 2000; Hammarstrom and others, 2001; Jambor, 2003). The effects of salt dissolution events can be dramatic, cycling through a watershed in a matter of hours.

Secondary Precipitation of Hydroxides and Hydroxysulfates

The oxidation of dissolved ferrous iron and neutralization of mine drainage produces a wide variety of secondary Fe or Al hydroxides and hydroxysulfates significantly less soluble than efflorescent sulfate salts. These phases range from nearly amorphous compounds to others that are well crystallized. Important Fe minerals include ferrihydrite [nominally $Fe_5HO_8\cdot 4H_2O$], schwertmannite $[Fe_8O_8(SO_4)(OH)_6]$, jarosite $[KFe_3(SO_4)_2(OH)_6]$, and goethite [α-FeO(OH)]. Important Al phases include amorphous Al hydroxide $[Al(OH)_3]$, gibbsite [γ-$Al(OH)_3$], and basaluminite $[Al_4(SO_4)(OH)_{10}\cdot 4H_2O]$. In mine-drainage environments, neutralization and hydrolysis are the main processes leading to the precipitation of the aluminum phases, whereas oxidation is additionally important for the precipitation of the iron phases. Jarosite tends to form in low-pH (1.5 to 3.0), high-sulfate (>3,000 mg/L) environments, schwertmannite in moderately acidic (pH = 3.0 to 4.0),

moderate-sulfate (1,000 to 3,000 mg/L) environments, and ferrihydrite in near-neutral (pH >5.0) environments (Bigham, 1994; Bigham and Nordstrom 2000; Stoffregen and others, 2000). Aluminum-bearing phases commonly precipitate at pH values above 4.5 (Nordstrom and Alpers, 1999). An important aspect of the secondary iron hydroxides is their ability to sorb significant quantities of trace metals and remove them from solution. Sorption behavior is pH-dependent. Metal cations, such as Ni^{2+}, Cu^{2+}, Zn^{2+}, and Cd^{2+}, generally sorb to a greater extent with increasing pH (Smith, 1999). Thus, secondary ferric hydroxides and hydroxysulfates can effectively remove metals from solution.

In the Sudbury Camp, Durocher and Schindler (2011) identified iron phases associated with acidic historical tailings ponds and a natural lake surrounded by waste rock. They found pH values ranging from 2.5 to 3.2 in the tailings ponds, and a pH of 6.2 in the lake. Total dissolved base metals (Cu + Co + Ni + Pb + Zn) in these water bodies ranged from 10.9 to 43.5 mg/L in the tailings ponds and 3.4 mg/L in the lake. Under these conditions, the secondary iron mineralogy was dominated by goethite, ferrihydrite, schwertmannite, and jarosite.

Pre-Mining Baseline Signatures in Soil, Sediment, and Water

Mine permitting and remediation require an estimate of pre-mining natural background conditions, particularly in regulated media such as groundwater, surface water, soil, and sediment, to serve as a goal for post-mining reclamation. Detailed baseline geochemical characterization prior to the onset of mining is essential. However, when baseline characterization was not done prior to mining, as is the case for many abandoned mines, a variety of methods have been used to estimate pre-mining backgrounds (Runnells and others, 1992, 1998; Alpers and others, 1999; Alpers and Nordstrom 2000).

In terms of pre-mining geochemical baselines, geochemical anomalies from magmatic Ni-Cu±PGE sulfide deposits can express themselves in groundwater, surface waters, and soils. The elemental suite and magnitude of these anomalies depend upon a number of factors, including extent of exposed outcrop, thickness and nature of overburden, climate, and topography. For example, the geochemical signatures in deflation lag and soil samples in the vicinity of the outcropping Babel and Nebo Ni-Cu±PGE sulfide deposits in central Australia have elevated and anomalous concentrations of Ni, Cu, Pt, Pd, and Au (Baker and Waugh, 2005).

Pre-mining geochemical data for groundwater and surface water near the Eagle deposit in northern Michigan and the Raglan deposit in northern Quebec were acquired during their respective permitting processes. The ultramafic intrusion hosting the Eagle deposit is buried beneath glacial outwash and till. Groundwater near the deposit has maximum concentrations of Fe (190 µg/L), Ni (59 µg/L), and Zn (88 µg/L) that may reflect the influence of mineralized rock; maximum concentrations of Cu (<5 µg/L) and Co (<10 µg/L) are below detection limits. Concentrations of Cu, Ni, and other trace elements in nearby surface waters are indistinguishable from concentrations in regional surface-water samples (Kennecott Eagle Minerals, 2006). Baseline characterization of surface waters near the Raglan Ni-Cu deposit in northern Quebec has been conducted by Nicholson and others (2003). Nickel concentrations in the Deception River prior to mining reached a maximum of 11 µg/L. Other surface-water samples near the deposit reached maximum Ni concentrations of 14.5 µg/L and sulfate concentrations of 5.25 mg/L.

Past and Future Mining Methods and Ore Treatment

Mining methods and ore-beneficiation techniques significantly influence the potential environmental impacts of massive sulfide deposits. Both open-pit and underground methods have been used to mine magmatic Ni-Cu±PGE sulfide deposits in historical and modern operations. The hydrologic differences between underground and open-pit mines are significant, particularly at abandoned mines. Evaporative concentration is prominent in open pits, particularly pits in semiarid to arid settings.

Mineral processing causes a number of physical and chemical changes to the ore during the production of metal concentrates. Most magmatic Ni-Cu±PGE sulfide deposits contain an excess of iron-sulfide minerals, such as pyrrhotite, relative to valuable base-metal sulfide minerals. The nature of ore processing and the method of disposal of the sulfide tailings and waste rocks are critical parameters that influence the scope of environmental impacts associated with mining magmatic Ni-Cu±PGE sulfide deposits. Some modern mines discharge fine-grained sulfide-rich tailings into tailings ponds underlain by impermeable linings, but historical tailings impoundments lack impermeable barriers at the base. Thus, many historical mining operations discharged tailings in a manner that has resulted in significant contamination of surface water and shallow groundwater.

Base-metal sulfide minerals, such as chalcopyrite and pentlandite, are typically separated by froth flotation. Some surfactants used in the process are toxic, but most are recycled and only relatively minor amounts are discharged to tailings facilities. The flotation properties of various sulfide minerals are affected by pH. Thus, base addition, typically in the form of lime [CaO] or sodium carbonate [Na_2CO_3], is a common practice to produce various sulfide-mineral concentrates; other additives to flotation circuits include potassium amyl xanthate, alcohols, ethers, pine oil, sodium cyanide [NaCN], and cupric sulfate [$CuSO_4 \cdot nH_2O$], all of which affect the flotation properties of various minerals (Biswas and Davenport, 1976). Most of these chemicals leave the sites as the tailings piles dewater. However, some may remain and continue to influence drainage chemistry.

The fine grain size, the typically large size of tailings piles, and the addition of a variety of chemicals establish distinct geochemical environments in tailings piles. The fine grain size enhances the reactivity of sulfide and gangue minerals by increasing surface area but also facilitates the formation of hardpan layers that can act as semipermeable to impermeable barriers to oxygen diffusion, thus limiting sulfide oxidation (Blowes and others, 1991, 2003). Numerous studies of tailings from a variety of mineral deposit types indicate that the pH of pore waters in the unsaturated and saturated zones of tailings piles is generally buffered by a predictable series of solid phases. Commonly, pore waters show a step-decrease in pH from 6.5–7.5, to 4.8–6.3, to 4.0–4.3, and finally to <3.5, which corresponds to buffering by calcite, siderite, $Al(OH)_3$, and $Fe(OH)_3$, respectively (Blowes and Ptacek, 1994; Jurjovec and others, 2002; Blowes and others, 2003). Thus, despite being a minor component of many of these mineralized systems, carbonate minerals exert an important control on the geochemistry of anoxic pore waters in tailing piles.

Smelter slag is another important type of mine waste, and the reactivity of slags is significant (Parsons and others, 2001; Piatak and others, 2004; Piatak and Seal, 2010). Leaching studies demonstrated that the suite of metals in leachates varies according to the compositional character of the ore (Piatak and others, 2004).

Airborne transport of contaminants has historically been a significant issue surrounding smelters lacking modern mitigation approaches such as scrubbers. The geochemistry of soils near magmatic Ni-Cu±PGE sulfide mining operations can reflect the combined influences of mining and smelting activities. In the Sudbury mining and smelting region, elevated concentrations of Cd (< 0.06 to 10.1 mg/kg), Co (0.9 to 113.3 mg/kg), Cu (11.4 to 1,891 mg/kg), Ni (5.3 to 2,149 mg/kg), and Zn (1.5 to 336 mg/kg) have been documented in soils, although modern methods have greatly reduced air emissions (Dudka and others, 1995). Residential soils in the Noril'sk mining district of Siberia have significant maximum concentrations of Co (1,229 mg/kg), Cu (16,000 mg/kg), Ni (2,915 mg/kg), and Zn (172.4 mg/kg) (Yakovlev and others, 2008).

Volume of Mine Waste and Tailings

Magmatic Ni-Cu±PGE sulfide deposits historically range in size from hundreds of thousands of tonnes to tens of millions of tonnes of sulfide ore. The largest district, Noril'sk-Talnakh, contains 1,903 million tonnes of ore, with Ni grades between 0.7 and 3 percent and Cu grades between 0.2 and 2 percent (Eckstrand and Hulbert, 2007). Because of the relatively low ore grades, the tonnage of tailings is similar to the tonnage of ore. However, the amount of waste rock will vary mostly based on the mining method. Open-pit mines may need to strip significant amounts of subeconomic, but potentially problematic, waste rock, whereas the amount of waste rock generated by underground mines is typically less.

Mine Waste Characteristics

Mineralogy

The environmental characteristics of these deposits are dominated by their significant acid-generating potential due to the abundance of pyrrhotite, and their limited acid-neutralizing potential due to the general absence or trace abundance of carbonate minerals in their mineralization, alteration, and host rock assemblages. Common sulfide minerals include pyrrhotite, pyrite, chalcopyrite, and pentlandite. Common gangue minerals include olivine, feldspar, pyroxene, quartz, chlorite, serpentine, and minor amounts of calcite or dolomite. Secondary phases include gypsum, magnetite, goethite, jarosite, native sulfur, covellite, marcasite, siderite, and clay (McGregor and others, 1998; Johnson and others, 2000).

Acid-Base Accounting

A series of static-test methods have been developed to predict the acid-generating potential of mine wastes as a tool to assist in waste disposal. These tests are known as acid-base accounting or ABA (Sobek and others, 1978; White and others, 1999), which is discussed in detail by Jambor (2003). The primary and secondary mineralogy of ores, their solid mine wastes, and associated rock types can affect ABA calculations. Acid-base accounting is based on the stoichiometric reaction:

$$FeS_2 + 2CaCO_3 + 3.75\ O_2 + 1.5H_2O \rightarrow Fe(OH)_3 + 2SO_4^{2-} + 2Ca^{2+} + 2CO_2(g) \quad (18)$$

which is simply the sum of Reactions 4 and 17 above to eliminate H^+ as a constituent. Reaction 18 describes acid generation through the oxidation of pyrite and subsequent neutralization by calcite (Sobek and others, 1978). For pyrrhotite, the dominant mineral of magmatic Ni-Cu±PGE sulfide deposits, acid-base accounting can be approximated by the simplified stoichiometric reaction:

$$FeS + CaCO_3 + 2.25\ O_2 + 1.5\ H_2O \rightarrow Fe(OH)_3 + SO_4^{2-} + Ca^{2+} + CO_2(g) \quad (19)$$

The net result of the proportion of $CaCO_3$ per unit of total S is the same as in Reaction 18, but the total S per unit of solid will be lower because pyrrhotite has approximately half of the S of pyrite.

Secondary metal-sulfate salts that commonly accumulate as intermediate products of sulfide oxidation also will contribute acidity (Alpers and others, 1994; Cravotta, 1994; Hammarstrom and others, 2001). For example, melanterite [$FeSO_4 \cdot 7H_2O$], rozenite [$FeSO_4 \cdot 4H_2O$], copiapite [$Fe^{2+}(Fe_4^{3+})(SO_4)_6(OH)_2 \cdot 20H_2O$], and halotrichite [$Fe^{2+}Al_2(SO_4)_4 \cdot 22H_2O$], are common and highly soluble; less soluble sulfate minerals, such as jarosite [$KFe^{3+}(OH)_6(SO_4)_2$] and schwertmannite

$[Fe_8O_8(OH)_6(SO_4)\cdot nH_2O]$, also are common in mining environments. Secondary metal-sulfate salts, such as chalcanthite $[CuSO_4\cdot 5H_2O]$, bonattite $[CuSO_4\cdot 3H_2O]$, morenosite $[NiSO_4\cdot 7H_2O]$, retgersite $[NiSO_4\cdot 6H_2O]$, and alunogen $[Al_2(SO_4)_3\cdot 17H_2O]$ may be important and act as highly soluble secondary sources of Ni, Cu, and Al. Modifications to the original ABA procedures attempt to accommodate these problems (White and others, 1999).

The dominance of pyrrhotite in mine tailings results in waste material with a high acid-generating potential; the minor presence of carbonate minerals in the ore assemblage and the lower reactivity of neutralizing minerals such as olivine or pyroxene offer minimal short-term acid neutralizing potential although some may be realized over longer time frames from olivine and pyroxene. However, much of the host rock surrounding these deposits can have very low acid-generating potential.

Despite genetic differences, the acid-base accounting characteristics of all types of magmatic Ni-Cu deposits share many features (fig. 14–1). Massive sulfide ore from the Eagle deposit is typified by a mean acidic net-neutralizing potential (NNP) of –1,111 kg $CaCO_3$ per tonne of waste; the mean NNP of semimassive sulfide ore at Eagle is –378 kg $CaCO_3$/t (Kennecott Eagle Minerals, 2006). The NNP of mineralogically similar tailings from Sudbury ores is similar (McGregor and others, 1998; Johnson and others, 2000). In contrast, NNP values from waste rock at the Raglan mine, Quebec, which is a komatiite-associated deposit, ranged from –106 to 62 kg $CaCO_3$/t; however, the samples with the highest (most alkaline) NNP values had total sulfur concentrations less than 0.5 weight percent (Rinker and others, 2003).

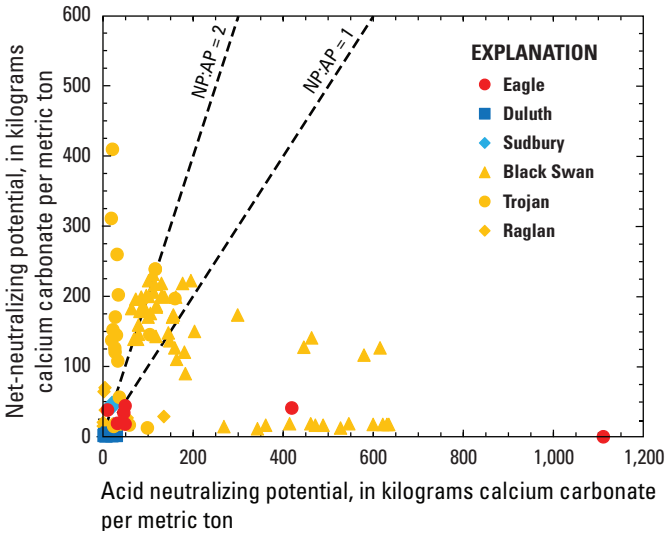

Figure 14–1. Acid-base accounting characteristics of magmatic Ni-Cu deposits. Basalt-related dike/sill-hosted deposits are shown in red (Kennecott Eagle Minerals, 2006); basal contact PGE-enriched, low-sulfide deposits are shown in dark blue (Lapakko and Antonson, 2006; Lapakko and others, 2003); astrobleme-associated deposits are shown in light blue (Tran and others, 2003); and komatiite-associated deposits are shown in yellow (Lupankwa and others, 2006; Lei and Watkins, 2005; Rinker and others, 2003). Samples with a net-neutralizing potential/acid-neutralizing potential ratio (NP:AP) greater than 2 generally are considered nonacid generating (NAG), and those with ratios less than 1 are considered probable acid generating (PAG). Those samples with ratios between 1 and 2 are uncertain.

Element Mobility Related to Mining in Groundwater and Surface Water

The quality of mine drainage is controlled by the geological characteristics of the mineral deposit modified by the combined effects of the mineralogy, mining and ore-beneficiation methods, the hydrologic setting of the mine workings and waste piles, and climate. Groundwater and surface-water data associated with magmatic Ni-Cu±PGE sulfide deposits and mines are limited. Johnson and others (2000) documented the generation of low pH (as low as 3) waters with high maximum dissolved concentrations of Fe (9.8 g/L), sulfate (24 g/L), Al (1,130 mg/L), and Ni (698 mg/L) in groundwater in the tailings pile at the Nickel Rim mine in the Sudbury district. Copper (3.5 mg/L) and Co (2.5 mg/L) also were important constituents. Similarly, for groundwater and surface-water in the vicinity of the Hitura Ni mine, western central Finland, Heikkinen and others (2002) found variable pH waters (2.8 to 8.7) with a range of dissolved Fe (<0.02 to 330 mg/L), Al (<0.01 to 20.4 mg/L), Mn (<0.01 to 19.5 mg/L), Cd (<0 .2 to 1,120 µg/L), Co (<0.03 to 2,610 mg/L), Cu (< 0.01 to 7.51 mg/L), Ni (<0.02 to 2,860 mg/L), Pb (<0.05 to 0.11 mg/L), Zn (<0.05 to 760 mg/L), and sulfate (<1 to 17,250 mg/L) concentrations.

Pit Lakes

Pit lakes are lakes formed as surface water and groundwater fill abandoned open pit mines. Studies of pit lakes associated with magmatic Ni-Cu sulfide deposits have not been undertaken.

Ecosystem Issues

The oxidative weathering of pyrrhotite is described above by Reactions 1 to 3. The low pH values generated by the oxidation of pyrrhotite enhance the solubility of base metals such as Cu, Ni, Zn, Cd, and Co, and the dissolution of silicate-gangue minerals, thus liberating Al and Mn. Most metals have greater solubility at lower pH values; however, Al and ferric iron have solubility minimums at circumneutral pH values, with greater solubility at both lower and higher pH. Once liberated, the metals and acidity can affect downstream

aquatic ecosystems. Metal contamination can also be dispersed downstream by the erosion and transport of tailings, which subsequently release metals to the water column.

The toxicity of Ag, Cd, Cr, Cu, Ni, Pb, and Zn to aquatic ecosystems is dependent on water hardness; toxicity limits of these metals are higher at higher hardness values (U.S. Environmental Protection Agency, 2006). Hardness is primarily a measure of the concentrations of Ca and Mg. The concentration of hardness is expressed in terms of an equivalent concentration of $CaCO_3$, typically in mg/L. The U.S. Environmental Protection Agency has presented hardness-dependent expressions for both acute (one-hour exposure) and chronic (four-day exposure) toxicity, and limits independent of hardness for cyanide, Al, As, Sb, Fe, Hg, Se, and Tl (U.S. Environmental Protection Agency, 2006; table 14–1). The metal concentrations described in the sections above locally exceed aquatic ecosystem guidelines.

Human Health Issues

Human-health impacts of magmatic Ni-Cu±PGE sulfide mining activities generally result from ingestion or inhalation of metals. Copper is an essential micronutrient for humans, whereas Ni is not. Human health effects of excessive Ni exposure can include contact dermatitis, lung fibrosis, cardiovascular and kidney disease, and cancer (nasal and lung); these effects are most notable among Ni refinery workers (Denkhaus and Salnikow, 2002; Cempel and Nikel, 2006).

Environmental guidelines protecting human health from drinking water and residential and industrial soils are summarized in table 14-1 for Ni and Cu, and a number of other contaminants commonly associated with mine sites in general. The U.S. Environmental Protection Agency has a drinking water standard for Cu (1,300 µg/L) but lacks one for Ni (U.S. Environmental Protection Agency, 2009). The World Health Organization has drinking water standards for both Cu (2,000 µg/L) and Ni (70 µg/L) (World Health Organization, 2008). Human-health vectors for metals include both drinking water and soils. The maximum concentrations in surface water and groundwater for Ni, Cu, Pb, and Zn all exceed drinking water guidelines. Likewise, the maximum concentrations of Cu and Ni exceed residential soil guidelines.

Climate Effects on Geoenvironmental Signatures

Climate plays a particularly important role in the potential environmental impact from mines that exploit magmatic Ni-Cu±PGE sulfide deposits. However, its effect is difficult to quantify systematically because insufficient data are available for this deposit type in a wide spectrum of climatic settings. Nevertheless, temperature and humidity are the prime variables which control evaporation. Evaporation can be expected to limit the amount of water in semiarid to arid climates. Evaporation can concentrate solutes in all climates. Acidity
and total metal concentrations in mine drainage in arid environments are typically several orders of magnitude greater than in more temperate climates because of the concentrating effects of the evaporation of mine effluent and the resulting "storage" of metals and acidity in highly soluble metal-sulfate mineral salts. Minimal surface-water flow in those areas inhibits generation of significant volumes of highly acidic, metal-enriched drainage. Concentrated release of these stored contaminants to local watersheds may be initiated by precipitation following a dry spell. In wet climates, high water tables may reduce exposure of abandoned ore bodies to oxidation and may continually flush existing tailings and mine dumps. Although metal-laden acidic mine water does form, it may be diluted to benign metal concentrations within several hundred meters of mixing with a higher order (larger flow) stream. Meldrum and others (2001) found that permafrost conditions,

Table 14–1. Environmental guidelines relevant to mineral deposits with respect to potential risks to humans and aquatic ecosystems from mine waste and mine drainage. Modified from U.S. Environmental Protection Agency (2006, 2009), World Health Organization (2008).

[Abbreviations: USEPA, U.S. Environmental Protection Agency; WHO, World Health Organization; mg/kg, milligrams per kilogram; µg/L, micrograms per liter; mg/L, milligrams per liter]

Element:	Human		Health		Aquatic	Ecosystem
Media:	Residential soil	Industrial soil	Drinking water	Drinking water	Acute toxicity	Chronic toxicity
Units:	mg/kg	mg/kg	µg/L	µg/L	µg/L	mg/L
Source:	USEPA	USEPA	USEPA	WHO	USEPA	USEPA
Al	77,000	990,000	200		750	87
As	23	160	10	10	340	150
Cd	70	810	5	3	2*	0.25*
Cu	3,100	41,000	1,300	2,000	13*	11*
Cr_{Total}			100	50		
Cr(III)	120,000	1,500,000**			570*	16*
Cr(VI)	0.29	5.6			74	11
Fe	55,000	720,000	300			1,000
Hg	6.7	28	2	6	1.4	0.77
Mn	1,800	23,000	50	400		
Mo	390	5,100		70		
Ni	1,600	20,000		70	470*	52*
Pb	400	800	15	10	65*	2.5*
Se	390	5,100	50	10		5
U	230	3,100		15		
Zn	23,000	310,000	5,000		120*	120*

*Hardness-dependent water-quality standards; value is based on a hardness of 100 mg/L $CaCO_3$.

**Values in excess of 1,000,000 mg/kg for some contaminants are used by U.S. Environmental Protection Agency for risk-screening purposes.

such as those found in Arctic Canada, can greatly reduce the oxidation rate of sulfide-rich mine wastes and the associated generation of acid drainage.

15. Knowledge Gaps and Future Research Directions

Much progress has been made in understanding the major factors controlling the formation of sulfide-rich Ni-Cu±PGE deposits and several recent publications provide useful overviews of recent developments (Naldrett, 2004; Barnes and Lightfoot, 2005; Eckstrand and Hulbert, 2007; Li and Ripley, 2009, 2011). However, important questions remain and require further study including the following.

1. What is the most important factor in triggering sulfide saturation in a given magma? A number of factors can lead to saturation of magmas in an Fe sulfide liquid including (Li and Ripley, 2005): (1) a rise in pressure, (2) a fall in temperature, (3) a change in magma composition (in particular a decrease in the Fe content or an increase in SiO_2, $Na_2O + K_2O$, or MgO), (4) an increase in fO_2 (fugacity of oxygen), and (5) a decrease in fS, (fugacity of sulphur). For the formation of sulfide-rich Ni-Cu±PGE deposits, the mechanisms commonly proposed to achieve saturation are assimilation of crustal rocks by the primary magma thereby changing the magma composition, or directly adding sulfur from sulfur-rich crustal rocks (Naldrett, 1966; Grinenko, 1985; Thériault and Barnes, 1998, Ripley and Li, 2003; Li and others, 2009). It remains unclear, however, which of these two mechanisms is the more important in producing sulfide saturation and ore formation. Recently, Keays and Lightfoot (2010) have suggested that crustal contamination without sulfur addition is insufficient to achieve sulfide saturation and the formation of magmatic Ni-Cu sulfide deposits.

2. Although there is considerable isotopic evidence supporting the addition of crustal sulfur in some deposits, such as Noril'sk, Pechenga, and Voisey's Bay, the mechanism by which sulfur is transferred from crustal rocks to the magma is still unclear. Initially, when the link between crustal sulfur addition and sulfide segregation was first proposed, it was assumed that the sulfur was volatilized from sulfur-rich country rocks (Naldrett, 1966). Subsequently, several ways were recognized as possible mechanisms for transferring sulfur from crustal rocks including (Arndt and others, 2005) (1) complete dissolution of all available sulfur by a hot and sulfide-understaturated magma; (2) wholesale melting, incongruent melting, or devolatilization from wall rocks, with or without other volatile and low-melting components, extracting some or all available sulfur; (3) extraction of sulfide from wall rocks to form blobs of "xenomelt" that mix with but never dissolve in a hot, already sulfide-saturated silicate melt; or (4) transfer of sulfur to the magma as a gas (Grinenko, 1985). One or more of these processes may have operated to varying degrees in different deposits (Lesher and others, 2001).

3. Although there is evidence that metal tenors of many ores are higher than would be expected of sulfide that had segregated from the quantity of magma represented by related small host intrusions (Campbell and Neldrett, 1979), exactly how magma interacts with sulfide is not clear and may vary from deposit to deposit. For example, in order to achieve large metal enrichments observed in the Noril'sk disseminated sulfides, large R factors (1,000 to 10,000) are required (Barnes and Lightfoot, 2005), implying an extremely dynamic, open, magmatic system. Droplets of sulfide have a large surface area-to-volume ratio that promotes scavenging of chalcophile elements as droplets are transported by flowing magma. Once sulfide droplets are deposited in a layer (which would have a low surface area-to-volume ratio), however, the droplets no longer would extract chalcophile elements efficiently from overlying silicate melt. This suggests that achieving high magma-to-sulfide ratios (high R factors) probably requires continued suspension and mixing of sulfide droplets with silicate melt. Alternatively, Kerr and Leitch (2005) suggest that the most effective way to significantly increase metal tenors is by resorption of sulfide liquid by new injections of sulfide-undersaturated silicate magma.

4. Massive or brecciated ores at several sulfide deposits, including Noril'sk, Jinchuan, Voisey's Bay, and Eagle, appear locally to transgress their host rocks and to have Cu/Pd ratios and PGE abundances different from associated disseminated mineralization. Those ores perhaps were injected as separate pulses of massive sulfide liquid or sulfide-rich breccia, generally along the base of host intrusions. It remains unclear, however, how a dense, low-viscosity sulfide liquid can be extracted from a site of initial accumulation, transported upward through much less-dense crustal rock, and subsequently injected along the base of the host intrusion. The transgressive relation may have resulted from mobilization of still-molten sulfide liquid during structural readjustments around the host intrusion; this alone, however, would not account for compositional differences from associated disseminated mineralization.

5. Are parental magmas to sulfide-rich Ni-Cu±PGE deposits typically enriched in ore metals, or do ore-forming processes depend more on the magmatic history of mantle-derived magmas, particularly the manner in which they interact with crustal rocks during their passage to the surface? Some studies concluded that the basaltic sequences that host major Ni-Cu±PGE sulfide deposits are enriched in chalcophile elements relative to barren sequences (Zhang and others, 2008). Other studies, however, contend that there is no difference in the chalcophile-element content between ore-hosting and barren sequences (Fiorentini and others, 2010). Komatiitic, tholeiitic, and alkaline mafic and ultramafic magmas all have sufficiently high metal contents to form deposits, yet only komatiites and tholeiitic picrites appear to host significant Ni-Cu±PGE sulfide deposits (Arndt and others, 2005). Arndt and others (2005) have suggested that the absence of deposits in alkaline sequences reflects the rapid ascent of alkaline magmas through the crust because of their volatile-rich, low-density character.

References Cited

Abzalov, M.Z., and Both, R.A., 1997, The Pechenga Ni-Cu deposits, Russia—Data on PGE and Au distribution and sulphur-isotope compositions: Mineralogy and Petrology, v. 61, p. 119–143.

Alpers, C.N., and Nordstrom, D.K., 2000, Estimation of pre-mining conditions for trace metal conditions for trace metal mobility in mineralized areas—An overview, *in* International Conference on Acid Rock Drainage, 5th, Denver, Colo., May 21–24, 2000, Proceedings: Littleton, Colo., Society for Mining, Metallurgy, and Exploration, p. 463–472.

Alpers, C.N., Blowes, D.W., Nordstrom, D.K., and Jambor, J.L., 1994, Secondary minerals and acid mine-water chemistry, *in* Jambor, J.L, and Blowes, D.W., eds., Short-course handbook on environmental geochemistry of sulfide mine-wastes: Mineralogical Association of Canada, v. 22, p. 247–270.

Alpers, C.N., Nordstrom, D.K., Verosub, K.L., and Helm, C.M., 1999, Paleomagnetic reversal in Iron Mountain gossan provides limits on long-term premining metal flux rates: Geological Society of America Abstracts with Programs, v. 31, p. 33.

Amelin, Y., Li, C., and Naldrett, A.J., 1999, Geochronology of the Voisey's Bay complex, Labrador, Canada, by precise U-Pb dating of coexisting baddeleyite, zircon, and apatite: Lithos, v. 47, p. 33–51.

Amelin, Y., Li, C., Valeyev, O., and Naldrett, A.J., 2000, Nd-Pb-Sr isotope systematics of crustal assimilation in the Voisey's Bay and Mushuau intrusions, Labrador, Canada: Economic Geology, v. 95, p. 815–830.

Ames, D.E., and Farrow, C.E.G., 2007, Metallogeny of the Sudbury mining camp, Ontario, *in* Goodfellow, W.D., ed., Mineral deposits of Canada—A synthesis of major deposit types, district metallogeny, the evolution of geological provinces, and exploration methods: Geological Association of Canada, Mineral Deposits Division, Special Publication no. 5, p. 329–350.

Arndt, N.T., 2005, The conduits of magmatic ore deposits, chap. 9, *in* Mungall, J.E., ed., Exploration for platinum-group element deposits: Mineralogical Association of Canada Short-Course Series, v. 35, p. 181–201.

Arndt, N.T., Czamanske, G.K., Walker, R.J., Chauvel, C., and Federenko, V.A., 2003, Geochemistry and origin of the intrusive hosts of the Noril'sk-Talnakh Cu-Ni-PGE sulfide deposits: Economic Geology, v. 98, p. 495–515.

Arndt, N.T., Lesher, C.M., and Czamanske, G.K., 2005, Mantle-derived magmas and magmatic Ni-Cu-(PGE) deposits, *in* Hedenquist, J.W., Thompson, J.F.H., Goldfarb, R.J., and Richards, J.P., eds., Economic Geology—One hundredth anniversary volume 1905–2005: Littleton, Colo., Society of Economic Geologists, p. 5–23.

Ash, M.R., Wheeler, M., Miller, H.G., Farquharson, C.G., and Dyck, A.V., 2006, Constrained three-dimensional inversion of potential field data from the Voisey's Bay Ni-Cu-Co deposit, Labrador, Canada: Annual Meeting, 76th, New Orleans, October 1–6, 2006, Society of Exploration Geophysicists [unpaginated poster].

Baker, P.M., and Waugh, R.S., 2005, The role of surface geochemistry in the discovery of the Babel and Nebo magmatic nickel-copper-PGE deposits: Geochemistry—Exploration, Environment, Analysis, v. 5, p. 195–200.

Balch, S.J., 1999, Ni-Cu sulphide deposits with examples from Voisey's Bay, *in* Lowe, C., Thomas, M.D., and Morris, W.A., eds., Geophysics in mineral exploration—Fundamentals and case histories: Geological Association of Canada Short-Course Notes, v. 14, p. 21–40.

Balch, S.J., 2005, The geophysical signatures of platinum-group element deposits, *in* Mungall, J.E., ed., Exploration for platinum-group element deposits: Mineralogical Association of Canada, Short-Course Series, v. 35, p. 275–286.

Balch, S.J, Mungall, J.E., and Niemi, J., 2010, Present and future geophysical methods for Ni-Cu-PGE exploration—Lessons from McFaulds Lake, Northern Ontario: Society of Economic Geologists, Special Publication 15, p. 550–572.

Barnes, Sarah-Jane, 1990, The use of metal ratios in prospecting for platinum-group element deposits in mafic and ultramafic intrusions: Journal of Geochemical Exploration, v. 37, p. 91–99.

Barnes, Sarah-Jane, and Maier, W.D., 2002, Platinum-group element distributions in the Rustenburg layered suite of the Bushveld Complex, South Africa, *in* Cabri, L.J., ed., The geology, geochemistry, mineralogy and mineral beneficiation of platinum-group elements: Canadian Institute of Mining, Metallurgy, and Petroleum, Special Volume 54, p. 431–458.

Barnes, Sarah-Jane, and Lightfoot, P.C., 2005, Formation of magmatic nickel sulfide deposits and processes affecting their copper and platinum-group element content, *in* Hedenquist, J.W., Thompson, J.F.H., Goldfarb, R.J., and Richards, J.P., eds., Economic Geology—One hundredth anniversary volume 1905–2005: Littleton, Colo., Society of Economic Geologists, p. 179–213.

Barnes, Sarah-Jane, Melezhik, V.A., and Sokolov, S.V., 2001, The composition and mode of formation of the Pechenga nickel deposits, Kola Peninsula, northwestern Russia: The Canadian Mineralogist, v. 39, p. 447–471.

Barnes, Sarah-Jane, Cox, R.A., and Zientek, M.L., 2006, Platinum-group elements, gold, silver and base metal distribution in compositionally zoned sulfide droplets from the Medvezky Creek Mine, Noril'sk, Russia: Contributions to Mineralogy and Petrology, v. 152, p. 187–200.

Barnes, Sarah-Jane, Couture, J-F., Sawyer, E.W., and Bouchaib, C., 1993, Nickel-copper occurrences in the Belleterre-Angliers Belt of the Pontiac subprovince and the use of Cu-Pd ratios in interpreting platinum-group element distributions: Economic Geology, v. 88, p. 1402–1418.

Barnes, Sarah-Jane, Makovicky, E., Karup-Moller, S., Makovicky, M., and Rose-Hagen, J., 1997, Partition coefficients for Ni, Cu, Pd, Pt, Rh, and Ir between monosulfide solid solution and sulfide liquid, and the implication for the formation of compositionally zoned Ni-Cu sulfide bodies by fractional crystallization of sulfide liquid: Canadian Journal of Earth Sciences, v. 34, p. 366–374.

Barnes, Sarah-Jane, Boyd, R., Korneliussen, A., Nilsson, L-P., Often, M., Pedersen, R-B., and Robins, B., 1988, The use of mantle normalization and metal ratios in discriminating between the effects of partial melting, crystal fractionation and sulphide segregation on platinum-group elements, gold, nickel, and copper—Examples from Norway, *in* Prichard, H.M., Potts, P.J., Bowles, J.F.W., and Cribb, S.J., eds., Geoplatinum 87 (Open University), London, Elsevier Applied Science, p. 113–143.

Barlow, A.E., 1906, On the origin and relations of the nickel and copper deposits of Sudbury, Ontario, Canada: Economic Geology, v. 1, p. 454–466.

Begg, G.C., Hronsky, J.A.M., Arndt, N.T., Griffin, W.L., O'Reilly, S.Y., and Hayward, Nick, 2010, Lithospheric, cratonic, and geodynamic setting of Ni-Cu-PGE sulfide deposits: Economic Geology, v. 105, p. 1057–1070.

Bell, Robert, 1891a, The nickel and copper deposits of Sudbury District, Canada: Geological Society of America Bulletin, v. 2, p. 125–137.

Bell, Robert, 1891b, On the Sudbury mining district: Geological Survey of Canada, Annual Report, New Series, v. 5, no. 1, p. 5F–95F.

Bigham, J.M., 1994, Mineralogy of ochre deposits formed by sulfide oxidation, *in* Jambor, J.L, and Blowes, D.W., eds., Short course handbook on environmental geochemistry of sulfide mine-wastes: Mineralogical Association of Canada, v. 22, p. 103–132.

Bigham J.M., and Nordstrom, D.K., 2000, Iron and aluminum hydroxysulfates from acid sulfate waters, *in* Alpers, C.N., Jambor, J.L., and Nordstrom, D.K., eds., Sulfate minerals—Crystallography, geochemistry, and environmental significance: Reviews in Mineralogy and Geochemistry, v. 40, p. 351–404.

Biswas, A.K., and Davenport, W.G., 1976, Extractive metallurgy of copper: New York, Pergamon, 438 p.

Blowes, D.W., Reardon, E.J., Jambor, J.L., and Cherry, J.A., 1991, The formation and potential importance of cemented layers in inactive sulfide mine tailings: Geochimica et Cosmochimica Acta, v. 55, no. 4, p. 965–978.

Blowes, D.W., and Ptacek, C.J., 1994, Acid-neutralization mechanisms in inactive mine tailings, *in* Jambor, J.L, and Blowes, D.W., eds., Short-course handbook on environmental geochemistry of sulfide mine-wastes: Mineralogical Association of Canada, v. 22, p. 271–292.

Blowes, D.W., Ptacek, C.J., and Jurjovec, J., 2003, Mill tailings—Hydrogeology and geochemistry, *in* Jambor, J.L., Blowes, D.W., and Ritchie A.I.M., eds., Environmental aspects of mine wastes: Mineralogical Association of Canada Short-Course Series, v. 31, p. 95–116.

Boerboom, T. J., 2009, Mineral endowment, *in* Boerboom, T. J., Geologic atlas of Carlton County and the southern portion of St. Louis County, Minnesota: University of Minnesota/Minnesota Department of Natural Resources, Division of Waters, County Atlas Series, Geologic Atlas C–19, part A, pl. 6, scale 1:200,000.

Boyd, Rognvald, and Nixon, Frank, 1985, Norwegian nickel deposits—A review: Finland Geological Survey, Bulletin 333, p. 363–394.

Brügmann, G.E., Hanski, E.J., Naldrett, A.J., and Smolkin, V.F., 2000, Sulfide segregation in ferropicrites from the Pechenga Complex, Kola Peninsula, Russia: Journal of Petrology, v. 41, p. 1721–1742.

Bryan, S.C., 2007, Silicic large igneous provinces: Episodes, v. 30, p. 20-31.

Bryan, S.C., and Ernst, R.E., 2008, Revised definition of large igneous provinces (LIPs): Earth-Science Reviews, v. 86, p. 175–202.

Cabri, L.J., 1973, New data on phase relations in the Cu-Fe-S system: Economic Geology, v. 68, p. 443–454.

Campbell, I.H., 2001, Identification of ancient mantle plumes, *in* Ernst, R.E., and Buchan, K.L., eds., Mantle plumes—Their identification through time: Geological Society of America Special Paper 352, p. 5–21.

Campbell, I.H., and Naldrett, A.J., 1979, The influence of silicate:sulfide ratios on the geochemistry of magmatic sulfides: Economic Geology, v. 74, p. 1503–1505.

Campbell, I.H., and Barnes, S.J., 1984, A model for the geochemistry of the platinum-group elements in magmatic sulphide deposits: Canadian Mineralogist, v. 22, p. 151–160.

Cempel, M., and Nikel, G., 2006, Nickel—A review of its sources and environmental toxicology: Polish Journal of Environmental Studies, v. 15, p. 375–382.

Chai, G., and Naldrett, A.J., 1992, Characteristics of Ni-Cu-PGE mineralization and genesis of the Jinchuan deposit, northwest China: Economic Geology, v. 87, p. 1475–1495.

Chevallier, L., and Woodford, A., 1999, Morpho-tectonics and mechanism of emplacement of the dolerite rings and sills of the western Karoo, South Africa: South African Journal of Geology, v. 102, p. 43–54.

Chung, Hye-Yoon, and Mungall, J.E., 2009, Physical constraints on migration of immiscible fluids through partially molten silicates, with special reference to magmatic sulfide ores: Earth and Planetary Science Letters, v. 286, p. 14–22.

Clowes, R.M., 2010, Initiation, development, and benefits of Lithoprobe—Shaping the direction of earth science research in Canada and beyond: Canadian Journal of Earth Sciences, v. 47, p. 291–314.

Coffin, M.F., and Eldholm, Olav, 1994, Large igneous provinces—Crustal structure, dimensions, and external consequences: Reviews in Geophysics, v. 32, p. 1–36.

Cogulu, E.H., 1993, Mineralogy and chemical variations of sulphides from the Crystal Lake intrusion, Thunder Bay, Ontario: Geological Survey of Canada, Open File 2749, 56 p.

Coleman, A.P., 1905, The Sudbury nickel region: Ontario Bureau of Mines, Report 14, part 3, 183 p.

Coleman, A.P., 1913, The nickel industry, with special reference to the Sudbury region, Ontario: Canada Department of Mines, Mines Branch, no. 170, 206 p.

Condie, K.C., 2001, Mantle plumes and their record in Earth history: Cambridge, Cambridge University Press, 306 p.

Courtillot, V.E., and Renne, P.R., 2003, On the ages of flood basalt events: Comptes Rendus Geoscience, v. 335, p. 113–140.

Craig, J.R., and Scott, S.D., 1974, Sulfide phase equilibria, *in* Ribbe, P.H., ed., Sulfide mineralogy: Mineralogical Society of America, Short-Course Notes, v. 1, p. CS-1 to CS-110.

Cravotta, C.A., III, 1994, Secondary iron-sulfate minerals as sources of sulfate and acidity—Geochemical evolution of acidic ground water at a reclaimed surface coal mine in Pennsylvania, *in* Alpers, C.N., and Blowes, D.W., eds., Environmental geochemistry of sulfide oxidation: American Chemical Society, Symposium Series 550, p. 345–364.

Crocket, J.H., 2002, Platinum-group element geochemistry of mafic and ultramafic rocks, *in* Cabri, L.J., ed., The geology, geochemistry, mineralogy and mineral beneficiation of platinum-group elements: Canadian Institute of Mining, Metallurgy, and Petroleum, Special Volume 54, p. 177–210.

Czamanske, G.J., Zen'ko, T.E., Fedorenko, V.A., Calk, L.C., Budahn, J.R., Bullok, J.H., Jr., Fries, T.L., King, B-S.W., and Siems, D.F., 1995, Petrographic and geochemical characterization of ore-bearing intrusions of the Noril'sk type, Siberia, *with* Discussion of their origin: Resource Geology, Special Issue 18, p. 1–48.

de Bremond d'Ars, Jean, Arndt, N.T., and Hallot, Erwan, 2001, Analog experimental insights into the formation of magmatic sulfide deposits: Earth and Planetary Science Letters, v. 186, p. 371–381.

Denkhaus, E., and Salnikow, K., 2002, Nickel essentiality, toxicity, and carcinogenicity: Critical Reviews in Oncology/Hematology, v. 42, p. 35–56.

de Waal, S.A., Maier, W.D., Armstrong, R.A., and Gauert, C.D.K., 2001, Parental magma and emplacement of the stratiform Uitkomst Complex, South Africa: Canadian Mineralogist, v. 39, p. 557–571.

de Wit, M.J., and Ashwal, L.D., eds., 1997, Greenstone belts: Oxford, Clarendon Press, 809 p.

Diakov, Sergei, West, Richard, Schissel, Don, Krisrtsov, Anatoly, Kochnev-Pervoukhov, Vladimir, and Migachev, Igor, 2002, Recent advances in the Noril'sk model and its application for exploration of Ni-Cu-PGE sulfide deposits, *in* Goldfarb, R.J., and Nielsen, R.L., eds., Integrated methods for discovery—Global exploration in the 21st century: Littleton, Colo., Society of Economic Geologists, Special Publication 9, p. 203–226.

Dickson, C.W., 1903, The ore deposits of Sudbury: American Institute of Mining Engineers, Transactions, v. 34, p. 1–67 [reprinted in 1913].

Dietz, R.S., 1964, Sudbury structure as an astrobleme: Journal of Geology, v. 72, p. 412–434.

Ding, Xin, Ripley, E.M., Li, Chusi, and Shirey, S.B., 2008, Re-Os isotopic study of the Eagle Ni-Cu sulfide deposit, northern Michigan, USA [abs.]: Geological Society of America, Abstracts with Programs, v. 40, no. 6, p. 386.

Ding, Xin, Ripley, E.M., and Li, Chusi, 2009, Multiple S isotopic study of the Eagle Ni-Cu-PGE magmatic deposit, northern Michigan, USA [abs.]: American Geophysical Union, Fall Meeting 2009, abstract #V21A-1971.

Ding, Xin, Li, Chusi, Ripley, E.M., Rossell, Dean, and Kamo, Sandra, 2010, The Eagle and Eagle East sulfide ore-bearing mafic-ultramafic intrusions in the Midcontinent rift system, upper Michigan—Geochronologic and petrologic evolution: Geochemistry, Geophysics, Geosystems, v. 11, 22 p.

Distler, V.V., 1994, Platinum mineralization of the Noril'sk deposits, *in* Lightfoot, P.E., and Naldrett, A.J., eds., Sudbury–Noril'sk Symposium, Sudbury, Oct. 3–6, 1992, Proceedings: Ontario Ministry of Northern Development and Mines/Ontario Geological Survey, Special Publication 5, p. 243–260.

Distler, V., Fillmonova, A., Grokhovskaya, T., and Laputina, I., 1990, Platinum-group elements in the copper-nickel ores of the Pechenga ore field: International Geology Review, v. 32, p. 70–83.

Durocher, J.L., and Schindler, M., 2011, Iron-hydroxide, iron-sulfate and hydrous-silica coatings in acid mine-tailings facilities—A comparative study of their trace-element composition: Applied Geochemistry, v. 26, p. 1337–1352.

Duchesne, J.-C., Liégeois, J.-P., Deblond, A., and Tack, L., 2004, Petrogenesis of the Kabanga–Musongati layered mafic-ultramafic intrusions in Burundi (Kibaran Belt)—Geochemical, Sr-Nd isotopic constraints and Cr-Ni behaviour, *in* Ennih, N., Liégeois, J.-P., and Thomas, R.J., eds., Key points on African geology: Amsterdam, Elsevier, Journal of African Earth Sciences, v. 39 [special issue], p. 133–145.

Dudka, S., Ponce-Hernandez, R., and Hutchinson, T.C., 1995, Current level of total element concentrations in the surface layers of Sudbury's soils: Science of the Total Environment, v. 162, p. 161–171.

Eckstrand, O.R., 1995, Magmatic nickel-copper sulfide, *in* Eckstrand, O.R., Sinclair, W.D., and Thorpe, R.I., eds., Geology of Canadian mineral deposit types: Geological Survey of Canada, Geology of Canada, v. 8, p. 584–605.

Eckstrand, O.R., and Hulbert, L.J., 1987, Selenium and the source of sulphur in magmatic nickel and platinum deposits: Geological Association of Canada–Mineralogical Association of Canada, Program with Abstracts, v. 12, p. 40.

Eckstrand, O.R., and Hulbert, L.J., 2007, Magmatic nickel/copper/platinum-group element deposits, *in* Goodfellow, W.D., ed., Mineral deposits of Canada—A synthesis of major deposit types, district metallogeny, the evolution of geological provinces, and exploration methods: Geological Association of Canada, Mineral Deposits Division, Special Publication 5, p. 205–222.

Elias, Mick, 2002, Nickel laterite deposits—Geological overview, resources and exploitation, *in* Cooke, D.R., and Pongratz, J., eds., Giant ore deposits—Characteristics, genesis, and exploration: University of Tasmania, Hobart Center for Ore Deposit Research, Special Publication, v. 4, p. 205–220.

Ernst, R.E., 2007, Mafic-ultramafic large igneous provinces (LIPs)—Importance of the pre-Mesozoic record: Episodes, v. 30, p. 108–114.

Ernst, R.E., and Buchan, K.L., eds., 2001, Mantle plumes—Their identification through time: Geological Society of America Special Paper 352, 593 p.

Evans-Lamswood, D.M., Butt, D.P., Jackson, R.S., Lee, D.V., Muggridge, M.G., and Wheeler, R.I., 2000, Physical controls associated with the distribution of sulfides in the Voisey's Bay Ni-Cu-Co deposit, Labrador: Economic Geology, v. 95, p. 749–769.

Fedorenko, V.A., Lightfoot, P.C., Naldrett, A.J., Czamanske, G.K., Zen'ko, T.E., Hawkesworth, C.J., Wooden, J.L., and Ebel, D.S., 1996, Petrogenesis of the flood-basalt sequence at Noril'sk, north-central Siberia: International Geology Review, v. 38, p. 99–135.

Fiorentini, M.L., Barnes, S.J., Lesher, C.M., Heggie, G.J., Keays, R.R., and Burnham, O.M., 2010, Platinum-group element geochemistry of mineralized and nonmineralized komatiites and basalts: Economic Geology, v. 105, p. 795–823.

Fleet, M.E., Chryssoulis, S.L., Stone, W.E., and Weisener, C.G., 1993, Partitioning of platinum-group elements and Au in the Fe-Ni-Cu-S system—Experiments on the fractional crystallization of sulfide melt: Contributions to Mineralogy and Petrology, v. 115, p. 36–44.

Fleet, M.E., Crocket, J.H., Liu, M., and Stone, W.E., 1999, Laboratory partitioning of platinum-group elements (PGE) and gold with application to magmatic sulfide-PGE deposits: Lithos, v. 47, p. 127–142.

Foose, M.P., Zientek, M.L., and Klein, D.P., 1995, Magmatic sulfide deposits, *in* du Bray, E.A., ed., Preliminary compilation of descriptive geoenvironmental mineral deposit models: U.S. Geological Survey, Open-File Report 95–0831, p. 28–38.

Ford, K., Keating, P., and Thomas, M.D., 2007, Overview of geophysical signatures associated with Canadian ore deposits, *in* Goodfellow, W.D., ed., Mineral deposits of Canada—A synthesis of major deposit types, district metallogeny, the evolution of geological provinces, and exploration methods: Geological Association of Canada, Mineral Deposits Division, Special Publication 5, p. 939–970.

Foulger, G.R., and Jurdy, D.M., eds., 2007, Plates, plumes, and planetary processes: Geological Society of America, Special Paper 430, 997 p.

Freyssinet, P., Butt, C.R.M., Morris, R.C., and Piantone, P., 2005, Ore-forming processes related to lateritic weathering, *in* Hedenquist, J.W., Thompson, J.F.H., Goldfarb, R.J., and Richards, J.P., eds., Economic Geology—One hundredth anniversary volume, 1905–2005: Littleton, Colo., Society of Economic Geologists, p. 681–722.

Genkin, A.D., and Evstigneeva, T.L., 1986, Associations of platinum-group minerals of the Noril'sk copper-nickel sulfide ores: Economic Geology, v. 81, p. 1203–1212.

Godel, B., Seat, Z., Maier, W.D., and Barnes, Sarah-Jane, 2011, The Nebo-Babel Ni-Cu-PGE sulfide deposit (West Musgrave Block, Australia)—Part 2, Constraints on parental magma and processes, with implications for mineral exploration: Economic Geology, v. 106, p. 557–584.

Gorbachev, N.S., 2006, Mineralogical and geochemical zoning and genesis of massive sulfide ores at the Oktyabr'sky deposit: Geology of Ore Deposits, v. 48, p. 473–488.

Grieve, R.A.F., 1994, An impact model of the Sudbury structure, *in* Lightfoot, P.C., and Naldrett, A.J., eds., Sudbury–Noril'sk Symposium, Sudbury, Oct. 3–6, 1992, Proceedings: Ontario Ministry of Northern Development and Mines/Ontario Geological Survey, Special Volume 5, p. 119–132.

Grinenko, L.N., 1985, Sources of sulfur of the nickeliferous and barren gabbro-dolerite intrusions of the northwest Siberian platform: International Geology Review, v. 28, p. 695–708.

Guo, W.W., and Dentith, M.C., 1997, Geophysical signature of the Jinchuan Ni-Cu-PGE deposit, Gansu Province, China: Exploration and Mining Geology, v. 6, p. 223–231.

Hammarstrom, J.M., Seal, R.R., II, Ouimette, A.P., and Foster, S.A., 2001, Sources of metals and acidity at the Elizabeth and Ely mines—Geochemistry and mineralogy of solid mine waste and the role of secondary minerals in metal recycling, *in* Hammarstrom, J.M., and Seal, R.R., II, eds., Environmental geochemistry and mining history of massive sulfide deposits in the Vermont copper belt: Society of Economic Geologists, Field Trip Guidebook Series, v. 35, pt. II, p. 213–248.

Hansen, D.M., Cartwright, J.A., and Thomas, D., 2004, 3D seismic analysis of the geometry of igneous sills and sill-junction relationships, *in* Davies, R.J., Cartwright, J.A., Stewart, S.A., Lappin, M., and Underhill, J.R., eds., 3D seismic technology—Application to the exploration of sedimentary basins: Geological Society of London, Memoirs, v. 29, p. 199–208.

Hanski, E.J., and Smolkin, V.F., 1995, Iron- and LREE-enriched mantle source for Early Proterozoic intraplate magmatism as exemplified by the Pechenga ferropicrites, Kola Peninsula, Russia: Lithos, v. 34, p. 107–125.

Hanski, E.J., Huhma, H., Smolkin, V.F., and Vaasjoki, M., 1990, The age of the ferropicritic volcanics and comagmatic Ni-bearing intrusions at Pechenga, Kola Peninsula, U.S.S.R.: Geological Society of Finland, Bulletin, v. 62, p. 123–133.

Hart, S.R., 1984, A large-scale isotope anomaly in the Southern Hemisphere: Nature, v. 309, p. 753–757.

Hawley, J.E., 1962, The Sudbury ores—Their mineralogy and origin: The Canadian Mineralogist, v. 6, p. 437–447.

Heaman, L.H., 2009, The application of U-Pb geochronology to mafic, ultramafic and alkaline rocks—An evaluation of three mineral standards: Chemical Geology, v. 261, p. 42–51.

Heikkinen, P.M., Korkka-Niemi, K., Lahti, M., and Salonen, V.-P., 2002, Groundwater and surface-water contamination in the area of the Hitura nickel mine, western Finland: Environmental Geology, v. 42, p. 313–329.

Hemly, H.M., Ballhaus, C., Berndt, J., Bockrath, C., and Wohlgemuth-Ueberwasser, C., 2007, Formation of Pt, Pd and Ni tellurides—Experiments in sulfide-telluride systems: Contributions to Mineralogy and Petrology, v. 153, p. 577–591.

Hoatson, D.M., Jaireth, Subhash, and Jaques, A.L., 2006, Nickel sulfide deposits in Australia—Characteristics, resources, and potential: Ore Geology Reviews, v. 29, p. 177–241.

Horan, M.F., Walker, R.J., Fedorenko, V.A., and Czamanske, G.K., 1995, Osmium and neodymium isotopic constraints on the temporal and spatial evolution of Siberian flood basalt sources: Geochimica et Cosmochimica Acta, v. 59, p. 5159–5168.

Howard-White, F.B., 1963, Nickel, an historical review: Princeton, D. Van Nostrand Company, 350 p.

Howell, D.A., and McDonald, I., 2010, A review of the behavior of platinum-group elements within natural magmatic sulfide ore systems: Platinum Metals Review, v. 54, p. 26–36.

Hunt, G.R., and Ashley, R.P., 1979, Spectra of altered rocks in the visible and near infrared: Economic Geology, v. 74, p. 1613–1629.

Irvine, T.N., 1982, Terminology for layered intrusions: Journal of Petrology, v. 23, p. 127–162.

Ivanov, A.V., 2007, Evaluation of different models for the origin of the Siberian Traps, *in* Foulger, G.R., and Jurdy, D.M., eds., Plates, plumes, and planetary processes: Geological Society of America, Special Paper 430, p. 669–691, doi: 10.1130/2007.2430(31).

Jambor, J.L., 1994, Mineralogy of sulfide-rich tailings and their oxidation products, *in* Jambor, J.L, and Blowes, D.W., eds., Short-course handbook on environmental geochemistry of sulfide mine wastes: Mineralogical Association of Canada, v. 22, p. 59–102.

Jambor, J.L., 2003, Mine-waste mineralogy and mineralogical perspectives of acid-base accounting, *in* Jambor, J.L., Blowes, D.W., and Ritchie A.I.M., eds., Environmental aspects of mine wastes: Mineralogical Association of Canada Short-Course Series, v. 31, p. 117–146.

Jambor, J.L., Nordstrom, D.K., and Alpers, C.N., 2000, Metal-sulfate salts from sulfide mineral oxidation, *in* Alpers, C.N., Jambor, J.L., and Nordstrom, D.K., eds., Sulfate minerals—Crystallography, geochemistry, and environmental significance: Reviews in Mineralogy and Geochemistry, v. 40, p. 303–350.

Jambor, J.L., Dutrizac, J.E., Groat, L.A., and Raudsepp, M., 2002, Static tests of neutralization potentials of silicate and aluminosilicate minerals: Environmental Geology, v. 43, p. 1–17.

Jambor, J.L., Dutrizac, J.E., and Raudsepp, M., 2007, Measured and computed neutralization potentials from static tests of diverse rock types: Environmental Geology, v. 52, no. 6, p. 1019–1031.

Johnson, R.H., Blowes, D.W., Robertson, W.D., and Jambor, J.L., 2000, The hydrogeochemistry of the Nickel Rim mine tailings impoundment, Sudbury, Ontario: Journal of Contaminant Hydrology, v. 41, p. 49–80.

Jurjovec, J., Ptacek, C.J., and Blowes, D.W., 2002, Acid neutralization mechanisms and metal release in mine tailings—A laboratory column experiment: Geochimica et Cosmochimica Acta, v. 66, no. 9, p. 1511–1523.

Keays, R.R., 1995, The role of komatiitic and picritic magmatism and S saturation in the formation of ore deposits: Lithos, v. 34, p. 1–18.

Keays, R.R., and Lightfoot, P.C., 2004, Formation of Ni-Cu-platinum-group element sulfide mineralization in the Sudbury impact melt sheet: Mineralogy and Petrology, v. 82, p. 217–258.

Keays, R.R., and Lightfoot, P.C., 2010, Crustal sulfur is required to form magmatic Ni-Cu sulfide deposits—Evidence from chalcophile element signatures of Siberian and Deccan Trap basalts: Mineralium Deposita, v. 45, p. 241–257.

Keays, R.R., Nickel, E.H., Groves, D.I., and McGoldrick, P.J., 1982, Iridium and palladium as discriminants of volcanic-exhalative, hydrothermal and magmatic nickel-sulfide mineralization: Economic Geology, v. 77, p. 1535–1547.

Kennecott Eagle Minerals, 2006, Eagle Project [Michigan, USA] Mining Permit Application [Jonathan C. Cherry, Marquette, Mich., February 20, 2006], *to* Lansing, Michigan Department of Environmental Quality: Kennecott Eagle Minerals Co., v. I [application and supporting documents], 126 p.

Kerr, Andrew, and Leitch, A.M., 2005, Self-destructive sulfide segregation systems and the formation of high-grade magmatic ore deposits: Economic Geology, v. 100, p. 311–332.

Kerr, Andrew, and Smith, J.L., 1997, The search for magmatic Ni-Cu-Co mineralization in northern Labrador—A summary of active exploration programs: Newfoundland [Canada] Department of Mines and Energy, Geological Survey, Current [c. 1997] Research Report 97–1, p. 73–91.

King, A., 2007, Review of geophysical technology for Ni-Cu-PGE deposits, *in* Milkereit, B., ed., Exploration 07—Exploration in the new millennium, 5th, Toronto, Sept. 9–12, 2007, Proceedings: Toronto, Decennial Mineral Exploration Conference, p. 647–665.

Knight, C.W., 1917, Geology of the Sudbury area and description of the Sudbury ore bodies: Toronto, Ontario, Royal Ontario Nickel Commission, Report, p. 104–211.

Kooistra, J., and Chesner, C.A., 2010, An ore-microscopy study of the Eagle massive sulfide Ni-Cu deposit, Upper Michigan [abs.]: Geological Society of America, Abstracts with Programs, v. 42, no. 2, p. 62.

Kuck, P.H., 2010, Nickel: U.S. Geological Survey, 2008 Minerals Yearbook, 29 p.

Kullerud, G., Yund, R.A., and Moh, G.H., 1969, Phase relations in the Cu-Fe-S, Cu-Ni-S and Fe-Ni-S systems: Economic Geology, v. 4, p. 323–343.

Kunilov, V.Ye., 1994, Geology of the Noril'sk region—The history of the discovery, prospecting, exploration and mining of the Noril'sk deposits, *in* Lightfoot, P.C., and Naldrett, A.J., eds., Sudbury–Noril'sk Symposium, Sudbury, Oct. 3–6, 1992, Proceedings: Ontario Ministry of Northern Development and Mines/Ontario Geological Survey, Special Volume 5, p. 203–216.

Lambert, D.D., Foster, J.G., Frick, L.R., Ripley, E.M., and Zientek, M.L., 1998, Geodynamics of magmatic Cu-Ni-PGE sulfide deposits—New insights from the Re-Os isotope system: Economic Geology, v. 93, p. 121–136.

Lambert, D.D., Foster, J.G., Frick, L.R., and Ripley, E.M., 1999a, Re-Os isotope geochemistry of magmatic sulfide ore systems: Reviews in Economic Geology, v. 12, p. 29–58.

Lambert, D.D., Foster, J.G., Frick, L.R., Li, Chusi, and Naldrett, A.J., 1999b, Re-Os isotopic systematics of the Voisey's Bay Ni-Cu-Co magmatic ore system, Labrador, Canada: Lithos, v. 47, p. 69–88.

Lambert, D.D., Frick, L.R., Foster, J.G., Li, Chusi, and Naldrett, A.J., 2000, Re-Os isotopic systematics of the Voisey's Bay Ni-Cu-Co magmatic ore system, Labrador, Canada—Part II, Implications for parental magma chemistry, ore genesis, and metal redistribution: Economic Geology, v. 95, p. 867–888.

Lapakko, K.A., and Antonson, D.A., 2006, Laboratory dissolution of Duluth Complex rock from the Babbitt and Dunka Road prospects—Status report: Minnesota Department of Natural Resources, unpublished report, 304 p.

Lapakko, K.A., Antonson, D.A., and Johnson, A.M., 2003, Duluth Complex tailings-dissolution experiments: Minnesota Department of Natural Resources, unpublished report, 28 p.

Lehmann, J., Arndt, N., Windley, B., Zhou, M.-F., Wang, C.Y., and Harris, C., 2007, Field relationships and geochemical constraints on the emplacement of the Jinchuan intrusion and its Ni-Cu-PGE sulfide deposit, Gansu, China: Economic Geology, v. 102, p. 75–94.

Lei, L., and Watkins, R., 2005, Acid-drainage reassessment of mine tailings, Black Swan mine, Kalgoorlie, Western Australia: Applied Geochemistry, v. 20, p. 661–667.

Le Maitre, R.W., ed., 1989, A classification of igneous rocks and glossary of terms—Recommendations of the International Union of Geological Sciences Subcommisssion on the Systematic of Igneous Rocks: Oxford, Blackwell Scientific, 193 p.

Lesher, C.M., 2004, Footprints of magmatic Ni-Cu-(PGE) systems, *in* Muhling, J., Goldfarb, R.J., Vielreicher, N., Bierlein, F., Stumfl, E., Groves, D.I., and Kenworthy, S., eds., SEG 2004—Predictive mineral discovery under cover [extended abstracts]: Society of Economic Geologists and The Center for Global Metallogeny (Australia), Society of Economic Geologists Conference Series, p. 117–120.

Lesher, C.M., and Groves, D.I., 1986, Controls on the formation of komatiite-associated nickel-copper sulfide deposits, *in* Friedrich, G.H., ed., Geology and metallogeny of copper deposits: Berlin, Springer Verlag, p. 63–90.

Lesher, C.M., and Keays, R.R., 2002, Komatiite-associated Ni-Cu-PGE deposits—Geology, mineralogy, geochemistry, and genesis, *in* Cabri, L.J., ed., The geology, geochemistry, mineralogy, and mineral beneficiation of platinum-group elements: Canadian Institute of Mining, Metallurgy, and Petroleum, Special Volume 54, p. 579–617.

Lesher, C.M., Barnes, S.J., and Hulbert, Larry, 2001, Trace-element geochemistry and petrogenesis of barren and ore-bearing komatiites: Canadian Mineralogist, v. 39, p. 673–696.

Li, Chusi, and Naldrett A.J., 1993, Sulfide capacity of magma—A quantitative model and its application to the formation of the sulfide ores at Sudbury: Economic Geology, v. 88, p. 1253–1260.

Li, Chusi, and Naldrett, A.J., 1999, Geology and petrology of the Voisey's Bay intrusion—Reaction of olivine with sulfide and silicate liquids: Lithos, v. 47, p. 1–31.

Li, Chusi, and Naldrett, A.J., 2000, Melting reactions of gneissic inclusions with enclosing magma at Voisey's Bay, Labrador, Canada—Implications with respect to ore genesis: Economic Geology, v. 95, p. 801–814.

Li, Chusi, and Ripley, E.M., 2005, Empirical equations to predict the sulfur content of mafic magmas at sulfide saturation and applications to magmatic sulfide deposits: Mineralium Deposita, v. 40, p. 218–230.

Li, Chusi, and Ripley, E.M., eds., 2009, New developments in magmatic Ni-Cu and PGE deposits: Beijing, Geological Publishing House, 290 p.

Li, Chusi, and Ripley, E.M., eds., 2011, Magmatic Ni-Cu and PGE deposits—Geology, geochemistry, and genesis: Society of Economic Geologists, Reviews in Economic Geology, v. 17, 370 p.

Li, Chusi, Maier, W.D., and de Waal, S.A., 2001a, The role of magma mixing in the genesis of PGE mineralization in the Bushveld Complex—Thermodynamic calculations and new interpretations: Economic Geology, v. 96, p. 653–662.

Li, Chusi, Maier, W.D., and de Waal, S.A., 2001b, Magmatic Ni-Cu versus PGE deposits—Contrasting genetic controls and exploration implications: South African Journal of Geology, v. 104, p. 309–318.

Li, Chusi, Ripley, E.M. and Naldrett, A.J., 2003, Compositional variation of olivine and sulfur isotopes in the Noril'sk and Talnakh intrusions, Siberia—Implications for ore-forming processes in dynamic magma conduits: Economic Geology, v. 98, p. 68–86.

Li, Chusi, Ripley, E.M., and Naldrett, A.J., 2009, A new genetic model for the giant Ni-Cu-PGE sulfide deposits associated with the Siberian flood basalts: Economic Geology, v. 104. p. 291–301.

Li, Chusi, Lightfoot, P.C., Amelin, Yuri, and Naldrett, A.J., 2000, Contrasting petrological and geochemical relationships in the Voisey's Bay and Mushuau intrusions, Labrador, Canada—Implications for ore genesis: Economic Geology, v. 95, p. 771–799.

Li, Chusi, Ripley, E.M., Maier, W.D., and Gomwe, T.E.S., 2002, Olivine and sulfur isotopic compositions of the Uitkomst Ni-Cu sulfide ore-bearing complex, South Africa—Evidence for sulfur contamination and multiple magma emplacements: Chemical Geology, v. 188, p. 149–159.

Lightfoot, P.C., and Hawkesworth, C.J., 1997, Flood basalts and magmatic Ni, Cu, and PGE sulfide mineralization—Comparative geochemistry of the Noril'sk (Siberian traps) and West Greenland sequences: American Geophysical Union, Monograph 100, p. 357–380.

Lightfoot, P.C., and Keays, R.R., 2005, Siderophile and chalcophile metal variations in flood basalts from the Siberian Trap, Noril'sk region—Implications for the origin of the Ni-Cu-PGE sulfide ores: Economic Geology, v. 100, p. 439–462.

Lightfoot, P.C., Naldrett, A.J., and Hawkesworth, C.J., 1984, The geology and geochemistry of the Waterfall Gorge Section of the Insizwa Complex with particular reference to the origin of the nickel sulfide deposits: Economic Geology, v. 79, p. 1857–1879.

Lightfoot, P.C., Hawkesworth, C.J., Hergt, J., Naldrett, A.J., Gorbachev, N.S., Fedorenko, V.A., and Doherty, W., 1993, Remobilization of the continental lithosphere by a mantle plume—Major-, trace-element, and Sr-, Nd-, and Pb-isotope evidence from picritic and tholeiitic lavas of the Noril'sk district, Siberian Traps, Russia: Contributions to Mineralogy and Petrology, v. 114, p. 171–188.

Lightfoot, P.C., Naldrett, A.J., Gorbachev, N.S., Fedorenko, V.A., Hawkesworth, C.J., Hergt, J., and Doherty, W., 1994, Chemostratigraphy of Siberian trap lavas, Noril'sk district, Russia—Implications for the source of flood basalt magmas and their associated Ni-Cu mineralization, *in* Lightfoot, P.C., and Naldrett, A.J., eds., Sudbury–Noril'sk Symposium, Sudbury, Oct. 3–6, 1992, Proceedings: Ontario Ministry of Northern Development and Mines/Ontario Geological Survey, Special Volume 5, p. 283–312.

Likhachev, A.P., 1994, Ore-bearing intrusions of the Noril'sk region, *in* Lightfoot, P.C., and Naldrett, A.J., eds., Sudbury–Noril'sk Symposium, Sudbury, Oct. 3–6, 1992, Proceedings: Ontario Ministry of Northern Development and Mines/Ontario Geological Survey, Special Publication 5, p. 185–201.

Lupankwa, K., Love, D., Mapani, B., Mseka, S., and Meck, M., 2006, Influence of the Trojan mine on surface-water quality, Mazowe Valley, Zimbabwe—Runoff chemistry and acid-generation potential of waste rock: Physics and Chemistry of the Earth, v. 31, p. 789–796.

Macheyeki, A.S., 2011, Application of lithogeochemistry to exploration for Ni-Cu sulfide deposits in the Kabanga area, NW Tanzania: Journal of African Earth Sciences, v. 61, p. 62–81.

Mahoney, J.J., and Coffin, M.F., eds., 1997, Large igneous provinces—Continental, oceanic, and planetary flood volcanism: American Geophysical Union, Geophysical Monograph 100, 438 p.

Maier, W.D., and Barnes, S.-J., 1999, The origin of Cu sulfide deposits in the Curaca Valley, Bahia, Brazil—Evidence from Cu, Ni, Se, and platinum-group element concentrations: Economic Geology, v. 94, p. 165–183.

Maier, W.D., and Barnes, S.-J., 2010, The Kabanga Ni sulfide deposits, Tanzania—II. Chalcophile and siderophile element geochemistry: Mineralium Deposita, v. 45, p. 443–460.

Maier, W.D., Barnes, S.-J., and Dewaal, S.A., 1998, Exploration for magmatic Ni-Cu-PGE sulphide deposits—A review of recent advances in the use of geochemical tools, and their application to some South African ores: South African Journal of Geology, v. 101, p. 237–253.

Maier, W.D., Li, Chusi, and de Waal, S.A., 2001, Why are there no major Ni-Cu sulfide deposits in large layered mafic-ultramafic intrusions?: Canadian Mineralogist, v. 39, p. 547–556.

Maier, W.D., Marsh, J.S., Barnes, S.-J., and Dodd, D.C., 2002, The distribution of platinum group elements in the Insizwa lobe of the Mount Ayliff Complex, South Africa—Implications for Ni-Cu-PGE sulfide exploration in the Karoo Igneous Province: Economic Geology, v. 97, p. 1293–1306.

Maier, W.D., Gomwe, T., Barnes, Sarah-Jane, Li, Chusi, and Theart, H., 2004, Platinum-group elements in the Uitkomst Complex, South Africa: Economic Geology, v. 99, p. 499–516.

Maier, W.D., Barnes, S.-J., Sarkar, Arindam, Ripley, E.M., Li, Chusi, and Livesey, Tim, 2010, The Kabanga Ni sulfide deposit, Tanzania—Geology, petrography, silicate rock geochemistry, and sulfur and oxygen isotopes, [part] I: Mineralium Deposita, v. 45, p. 419–441.

Mandel, R., 2009, Noront expands Eagle One with polymetallic finds: The Northern Miner, June 4, 2009.

Marcantonio, F., Reisberg, L., Zindler, A., Wyman, D., and Hulbert, L., 1994, An isotopic study of the Ni-Cu-PGE-rich Wellgreen intrusion of the Wrangellia Terrane—Evidence for hydrothermal mobilization of rhenium and osmium: Geochimica et Cosmochimica Acta, v. 58, p. 1007–1017.

Mariga, J., Ripley, E.M., and Li, Chusi, 2006, Oxygen isotopic studies of the interactions between xenoliths and mafic magma, Voisey's Bay Intrusion, Labrador, Canada: Geochimica et Cosmochimica Acta, v. 70, p. 4977–4996.

McClenaghan, M.B., Layton-Matthews, D., and Matile, G., 2011, Till geochemical signatures of magmatic Ni-Cu deposits, Thompson Nickel Belt, Manitoba, Canada: Geochemistry—Exploration, Environment, Analysis, v. 11, p. 145–159.

McConnell, J.W., 2003, Lake-sediment and soil surveys for platinum-group metals in central Labrador and the Voisey's Bay area: Newfoundland Department of Mines and Energy, Geological Survey, Current Research Report 03–1, p. 179–192.

McGregor, R.G., Blowes, D.W., Jambor, J.L., and Robertson, W.D., 1998, Mobilization and attenuation of heavy metals within a nickel mine-tailings impoundment near Sudbury, Ontario, Canada: Environmental Geology, v. 36, no. 3–4, p. 305–319.

Meldrum, J.L., Jamieson, H.E., and Dyke, L.D., 2001, Oxidation of mine tailings from Rankin Inlet, Nunavut, at subzero temperatures: Canadian Geotechnical Journal, v. 38, no. 5, p. 957–966.

Milkereit, B., Green, A., and the Sudbury Working Group, 1992, Deep geometry of the Sudbury structure from seismic reflection profiling: Geology, v. 20, p. 807–811.

Milkereit, B., Eaton, D., Wu, J., Perron, G., Salisbury, M., Berrer, E.K., and Morrison, G., 1996, Seismic imaging of massive sulfide deposits—Reflection seismic profiling [Part II]: Economic Geology, v. 91, p. 829–834.

Milkereit, B., Berrer, E.K., Watts, A., and Roberts, B., 1997, Development of 3-D seismic exploration technology for Ni-Cu deposits, Sudbury Basin, *in* Gubins, A.G., ed., Exploration 97—Geophysics and geochemistry at the Millennium, 4th, Toronto, Sept. 14–18, 1997, Proceedings: Toronto, Decennial Mineral Exploration Conference, GEO/FX, p. 439–448.

Milkereit, B., White, D., Adam, E. Boerner, D., and Salisbury, M., 1994, Implications of the Lithoprobe seismic reflection transect for Sudbury geology, *in* Lightfoot, P.C., and Naldrett, A.J., eds., Sudbury–Noril'sk Symposium, Sudbury, Oct. 3–6, 1992, Proceedings: Ontario Ministry of Northern Development and Mines/Ontario Geological Survey, Special Volume 5, p. 11–20.

Miller, R.L., 1945, Geology of the Katahdin pyrrhotite deposit and vicinity, Piscataquis County, Maine: Maine Geological Survey, Bulletin 2, 17 p.

Miller, W.R., Ficklin, W.H., and McHugh, J.B., 1992, Geochemical exploration for copper-nickel deposits in the cool humid climate of northeastern Minnesota: Journal of Geochemical Exploration, v. 42, p. 327–344.

Mungall, J.E., 2002, Kinetic controls on the partitioning of trace elements between silicate and sulfide liquids: Journal of Petrology, v. 43, p. 749–768.

Mungall, J.E., 2005, Magmatic geochemistry of the platinum-group elements, *in* Mungall, J.E., ed., Exploration for platinum-group element deposits: Mineralogical Association of Canada, Short-Course Notes, v. 35, p. 1–34.

Mungall, J.E., 2007, Crystallization of magmatic sulfides—An empirical model and application to Sudbury ores: Geochimica et Cosmochimica Acta, v. 71, p. 2809–2819.

Mungall, J.E., 2009, Uses of geophysical data in the discovery of the Eagle One, Eagle Two and Blackbird deposits, Toronto, March 1–4, 2009, Proceedings: Prospectors and Developers Association of Canada Trade Show and Convention, Technical Sessions. [Pagination unavailable].

Mungall, J.E., and Su, Shanguo, 2005, Interfacial tension between magmatic sulfide and silicate liquids—Constraints on kinetics of sulfide liquation and sulfide migration through silicate rocks: Earth and Planetary Science Letters, v. 234, p. 135–149.

Mungall, J.E., Ames, D.E., and Hanley, J.J., 2004, Geochemical evidence from the Sudbury structure for crustal redistribution by large bolide impacts: Nature, v. 429, p. 546–548.

Mungall, J.E., Andrews, D.R.A., Cabri, L.J., Sylvester, P.J., and Tubrett, M., 2005, Partitioning of Cu, Ni, Au, and platinum-group elements between monosulfide solid solution and sulfide melt under controlled oxygen and sulfur fugacities: Geochimica et Cosmochimica Acta, v. 69, p. 4349–4360.

Mungall, J.E., Harvey, J.D., Balch, S.J., Brownwyn, A., Atkinson, J., and Hamilton, M.A., 2010, Eagle's Nest—A magmatic Ni-sulfide deposit in the James Bay Lowlands, Ontario, Canada: Society of Economic Geologists, Special Publication 15, p. 539–557.

Naldrett, A.J., 1966, The role of sulphurization in the genesis of iron-nickel sulphide deposits of the Porcupine district, Ontario: Canadian Institute of Mining and Metallurgy, Transactions, v. 69, p. 147–155.

Naldrett, A.J., 1969, A portion of the system Fe-S-O between 900 ºC and 1080 ºC and its application to sulfide ore magmas: Journal of Petrology, v. 10, p. 171–201.

Naldrett, A.J., 1989, Magmatic sulfide deposits: Oxford, Oxford University Press, 186 p.

Naldrett, A.J., 1997, Key factors in the genesis of Noril'sk, Sudbury, Jinchuan, Voisey's Bay, and other world-class Ni-Cu-PGE deposits—Implications for exploration: Australian Journal of Earth Sciences, v. 44, p. 283–315.

Naldrett, A.J., 1999, World-class Ni-Cu-PGE deposits—Key factors in their genesis: Mineralium Deposita, v. 34, p. 227–240.

Naldrett, A.J., 2004, Magmatic sulfide deposits—Geology, geochemistry, and exploration: Berlin, Springer-Verlag, 727 p.

Naldrett, A.J., 2005, A history of our understanding of magmatic Ni-Cu-sulfide deposits: The Canadian Mineralogist, v. 43, p. 2069–2098.

Naldrett, A.J., 2010, Secular variation of magmatic sulfide deposits and their source magmas: Economic Geology, v. 105, p. 669–688.

Naldrett, A.J., and Li, Chusi, 2009, Ore deposits related to flood basalts, Siberia, *in* Li, Chusi, and Ripley, E.M., eds., New developments in magmatic Ni-Cu and PGE deposits: Beijing, Geological Publishing House, p. 141–179.

Naldrett, A.J., Craig, J.R., and Kullerud, G., 1967, The central portion of the Fe-Ni-S system and its bearing on pentlandite solution in iron-nickel sulfide ores: Economic Geology, v. 62, p. 826–847.

Naldrett, A.J., Lightfoot, P.C., Fedorenko, V.A., Gorbachev, N.S., and Doherty, W., 1992, Geology and geochemistry of intrusions and flood basalts of the Noril'sk region, USSR, with implications for the origin of the Ni-Cu ores: Economic Geology, v. 87, p. 975–1004.

Naldrett, A.J., Singh, J., Kristic, S., and Li, Chusi, 2000, The mineralogy of the Voisey's Bay Ni-Cu-Co deposit, northern Labrador, Canada—Influence of oxidation state on textures and mineral compositions: Economic Geologist, v. 95, p. 889–900.

Naldrett, A.J., Asif, M., Gorbachev, N.S., Kunilov, V.E., Stehkin, A.I., Fedorenko, V.A., and Lightfoot, P.C., 1994, The composition of the Ni-Cu ores of the Noril'sk region, *in* Lightfoot, P.C., and Naldrett, A.J., eds., Sudbury–Noril'sk Symposium, Sudbury, Oct. 3–6, 1992, Proceedings: Ontario Ministry of Northern Development and Mines/Ontario Geological Survey, Special Publication 5, p. 357–372.

Naldrett, A.J., Fedorenko, V.A., Lightfoot, P.C., Kunilov, V.I., Gorbachev, N.S., Doherty, W., and Johan, Z., 1995, Ni-Cu-PGE deposits of Noril'sk region, Siberia—Their formation in conduits for flood basalt volcanism: Institute of Mining and Metallurgy, Transactions [Section B, Applied Earth Sciences], v. 104, p. B18–B36.

Nicholson, R.V., Williams, G., Rinker, M.J., Venhuis, M.A., and Swarbrick, B., 2003, Implications of non-acid metal leaching on mine rock management at a nickel mine in permafrost terrain—2, Environmental baseline investigation, *in* Spiers, G., Beckett, P., Conroy, H., eds., Sudbury 2003—Mining and the Environment Conference, Sudbury, May 25–28, 2003, Proceedings: Canadian Land Reclamation Association, pagination unavailable.

Nordstrom, D.K., and Alpers, C.N., 1999, Geochemistry of acid mine waters, *in* Plumlee, G.S., and Logsdon, M.J., eds., The environmental geochemistry of mineral deposits—Part A, Processes, techniques, and health issues: Reviews in Economic Geology, v. 6A, p. 161–182.

Page, N.J., 1986a, Descriptive model of Stillwater Ni-Cu, *in* Cox, D.P., and Singer, D.A., Mineral deposit models: U.S. Geological Survey Bulletin 1693, p. 11–12.

Page, N.J., 1986b, Descriptive model of Duluth Cu-Ni-PGE, *in* Cox, D.P., and Singer, D.A., Mineral deposit models: U.S. Geological Survey Bulletin 1693, p. 16.

Page, N.J., 1986c, Descriptive model of Noril'sk Cu-Ni-PGE, *in* Cox, D.P., and Singer, D.A., Mineral deposit models: U.S. Geological Survey Bulletin 1693, p. 17.

Page, N.J., 1986d, Descriptive model of komatiitic Ni-Cu, *in* Cox, D.P., and Singer, D.A., Mineral deposit models: U.S. Geological Survey Bulletin 1693, p. 18–19.

Page, N.J., 1986e, Descriptive model of dunitic Ni-Cu, *in* Cox, D.P., and Singer, D.A., Mineral deposit models: U.S. Geological Survey Bulletin 1693, p. 24.

Page, N.J., 1986f, Descriptive model of synorogenic-synvolcanic Ni-Cu, *in* Cox, D.P., and Singer, D.A., Mineral deposit models: U.S. Geological Survey Bulletin 1693, p. 28.

Papunen, Heikki, 1991, Concepts of the genesis of sulfide nickel-copper deposits—A historical review, *in* Hutchinson, R.W., and Grauch, R.I., eds., Historical perspectives of genetic concepts and case histories of famous deposits: Economic Geology, Monograph 8, p. 3–19.

Parsons, M.B., Bird, D.K., Einaudi, M.T., and Alpers, C.N., 2001, Geochemical and mineralogical controls of trace element release from the Penn Mine base-metal slag dump, California: Applied Geochemistry, v. 16, p. 1567–1593.

Peach, C.L., and Mathez, E.A., 1993, Sulfide melt-silicate melt distribution coefficients for nickel and iron and implications for the distributions of other chalcophile elements: Geochimica et Cosmochimica Acta, v. 57, p. 3013–3021.

Peach, C.L., Mathez, E.A., and Keays, R.R., 1990, Sulfide melt-silicate melt distribution coefficients for noble metals and other chalcophile elements as deduced from MORB—Implication for partial melting: Geochimica et Cosmochimica Acta, v. 54, p. 3379–3389.

Peltonen, P., 2004, Mafic-ultramafic intrusions of the Svecofennian orogen, *in* Lehtinen, M., Nurmi, P.A., and Ramo, O.T., eds., Precambrian bedrock of Finland—A key to the evolution of the Fennoscandian Shield: Amsterdam, Elsevier, p. 413–417.

Piatak, N.M., and Seal, R.R., II, 2010, Mineralogy and the release of trace elements from slag from the Hegeler zinc smelter, Illinois (USA): Applied Geochemistry, v. 25, no. 2, p. 302–320.

Piatak, N.M., Seal, R.R., II, and Hammarstrom, J.M., 2004, Mineralogical and geochemical controls on the release of trace elements from slag produced by base- and precious-metal smelting at abandoned mine sites: Applied Geochemistry, v. 19, p. 1039–1064.

Pietruszka, A.J., and Garcia, M.O., 1999, Rapid fluctuation in the mantle source and melting history of Kilauea volcano inferred from geochemistry of its historical summit lavas (1790–1982): Journal of Petrology, v. 40, p. 1321–1342.

Piña, Rubén, Romeo, Ignacio, Ortega, Lorena, Lunar, Rosario, Capote, Ramón, Grevilla, Fernando, Tejero, Rosa, and Quesada, Cecilio, 2010, Origin and emplacement of the Aguablanca magmatic Ni-Cu-(PGE) sulfide deposit, SW Iberia—A multidisciplinary approach: Geological Society of America Bulletin, v. 122, p. 915–925.

Pirajno, Franco, 2007, Mantle plumes, associated intraplate tectono-magmatic processes and ore systems: Episodes, v. 30, p. 6–19.

Plumlee, G.S., 1999, The environmental geology of mineral deposits, *in* Plumlee, G.S., and Logsdon, M.J., eds., The environmental geochemistry of mineral deposits—Part A, Processes, techniques, and health issues: Reviews in Economic Geology, v. 6A, p. 71–116.

Prichard, H.M., Hutchinson, D., and Fisher, P.C., 2004, Petrology and crystallization history of multiphase sulfide droplets in a mafic dike from Uruguay—Implications for the origin of Cu-Ni-PGE sulfide deposits: Economic Geology, v. 99, p. 365–376.

Queffurus, M., and Barnes, Sarah-Jane, 2010, The use of S/Se ratios in magmatic Ni-Cu-PGE sulfide deposits—International Platinum Symposium, 11th, Sudbury, Ontario, June 21–24, 2010, Program Abstracts: Ontario Geological Survey, Miscellaneous Data, Release 269, pagination unavailable.

Reid, M.R., 2003, Timescales of magma transfer and storage in the crust, *in* Rudnick, R., ed., The crust—Treatise on geochemistry, v. 3, chap. 5, p. 167–193.

Rempel, G.G., 1994, Regional geophysics at Noril'sk, *in* Lightfoot P.C., and Naldrett, A.J., eds., Sudbury–Noril'sk Symposium, Sudbury, Oct. 3–6, 1992, Proceedings: Ontario Ministry of Northern Development and Mines/Ontario Geological Survey, Special Volume 5, p. 147–160.

Rinker, M.J., Nicholson, R.V., Venhuis, M.A., and Swarbrick, B., 2003, Implications of non-acid metal leaching on mine rock management at a nickel mine in permafrost terrain—1, Mine rock evaluation, *in* Spiers, G., Beckett, P., Conroy, H., eds., Sudbury 2003—Mining and the Environment Conference, Sudbury, Ontario, May 25–28, 2003, Proceedings: Canadian Land Reclamation Association, pagination unavailable.

Ripley, E.M., 1981, Sulfur isotopic abundances of the Dunka Road Cu-Ni deposit, Duluth Complex, Minnesota: Economic Geology, v. 76, p. 619–620.

Ripley, E.M., 1990, Se/S ratios of the Virginia Formation and Cu-Ni sulfide mineralization in the Babbitt area, Duluth Complex, Minnesota: Economic Geology, v. 85, p. 1935–1940.

Ripley, E.M., 1999, Systematics of sulphur and oxygen isotopes in mafic igneous rocks and related Cu-Ni-PGE mineralization, *in* Keays, R.R., Lesher, C.M., Lightfoot, P.C., and Farrow, C.E.G., eds., Dynamic processes in magmatic ore deposits and their application to mineral exploration: Geological Society of Canada, Short-Course Notes, v. 13, p. 133–158.

Ripley, E.M., and Li, Chusi, 2003, Sulfur isotope exchange and metal enrichment in the formation of magmatic Cu-Ni-(PGE) deposits: Economic Geology, v. 98, p. 635–641.

Ripley, E.M., Li, Chusi, and Shin, D., 2002, Paragneiss assimilation in the genesis of magmatic Ni-Cu-Co sulfide mineralization at Voisey's Bay, Labrador—$\delta^{34}S$, $\delta^{13}C$, and Se/S evidence: Economic Geology, v. 97, p. 1307–1318.

Ripley, E.M., Sarkar, A., and Li, Chusi, 2005, Mineralogic and stable isotope studies of hydrothermal alteration at the Jinchuan Ni-Cu deposit, China: Economic Geology, v. 100, p. 1349–1361.

Ripley, E.M., Park, Y-R., Li, Chusi, and Naldrett, A.J., 1999, Sulfur and oxygen isotopic evidence of country-rock contamination in the Voisey's Bay Ni-Cu-Co deposit, Labrador, Canada: Lithos, v. 47, p. 53–68.

Ripley, E.M., Park, Y-R., Li, Chusi, and Naldrett, A.J., 2000, Oxygen isotopic study of the Voisey's Bay Ni-Cu-Co deposit, Labrador, Canada: Economic Geology, v. 95, p. 831–844.

Ripley, E.M., Lightfoot, P.C., Li, Chusi, and Elswick, E.R., 2003, Sulfur isotopic studies of continental flood basalts in the Noril'sk region—Implications for the association between lavas and ore-bearing intrusions: Geochimica et Cosmochimica Acta, v. 67, p. 2805–2817.

Roeder, P.L., and Emslie, R.F., 1970, Olivine-liquid equilibrium: Contributions to Mineralogy and Petrology, v. 29, p. 275–289.

Rowan, L.C., Mars, J.C., and Simpson, C.J., 2005, Lithologic mapping of the Mordor, NT [Northern Territory], Australia, ultramafic complex by using the Advanced Spaceborne Thermal Emission and Reflection Radiometer (ASTER): Remote Sensing of the Environment, v. 99, p. 105–126.

Runnells, D.D., Shepherd, T.A., and Angino, E.E., 1992, Metals in water—Determining natural background concentrations in mineralized areas: Environmental Science & Technology, v. 26, p. 2316–2323.

Runnells, D.D., Dupon, D.P., Jones, R.L., and Cline, D.J., 1998, Determination of natural background concentrations of dissolved components in water at mining, milling, and smelting sites: Mining Engineering, v. 50, no. 2, p. 65–71.

Salisbury, M., and Snyder, D., 2007, Application of seismic methods to mineral exploration, *in* Goodfellow, W.D., ed., Mineral deposits of Canada—A synthesis of major deposit-types, district metallogeny, the evolution of geological provinces, and exploration methods: Geological Association of Canada, Mineral Deposits Division, Special Publication 5, p. 971–982.

Salisbury, M., Harvey, C., and Matthews, L., 2003, The acoustic properties of ores and host rocks in hardrock terranes, *in* Eaton, D., Milkereit, B., and Salisbury, M., eds., Hardrock seismic exploration: Society of Exploration Geophysicists, Developments in Geophysics Series, v. 10, p. 9–19.

Sarkar, A., Ripley, E.M., Li, Chusi, and Maier, W.D., 2008, Stable isotope, fluid inclusion, and mineral chemistry constraints on contamination and hydrothermal alteration in the Uitkomst Complex, South Africa: Chemical Geology, v. 257, p. 129–138.

Schmidt, J.M., and Rogers, R.K., 2007, Metallogeny of the Nikolai large igneous province (LIP) in southern Alaska and its influence on the mineral potential of the Talkeetna Mountains, *in* Ridgway, K.D., Trop, J.M., Glen, J.M.G., and O'Neill, J.M., eds., Tectonic growth of a collisional continental margin—Crustal evolution of southern Alaska: Geological Society of America, Special Paper 431, p. 623–648.

Schulz, K.J., Cannon, W.F., Nicholson, S.W., and Woodruff, L.G., 1998, Is there a "Voisey's Bay"-type Ni-Cu sulfide deposit in the Midcontinent rift system in the Lake Superior region?: Mining Engineering, August, p. 57–62.

Scoates, J.S., and Mitchell, J.N., 2000, The evolution of troctolitic and high-Al basaltic magmas in Proterozoic anorthosite plutonic suites and implications for the Voisey's Bay massive Ni-Cu sulfide deposit: Economic Geology, v. 95, p. 677–701.

Seat, Z., Beresford, S.W., Grguric, B.A., Gee, M.M.A., and Grassineau, N.V., 2009, Reevaluation of the role of external sulfur addition in the genesis of Ni-Cu-PGE deposits—Evidence from the Nebo-Babel Ni-Cu-PGE deposit, West Musgrave, Western Australia: Economic Geology, v. 104, p. 521–538.

Seat, Z., Beresford, S.W., Grguric, B.A., Waugh, R.S., Hronsky, J.M.A., Gee, M.M.A, Groves, D.I., and Charter, I.M., 2007, Architecture and emplacement of the Nebo-Babel intrusion, West Musgrave, Western Australia: Mineralium Deposita, v. 42, p. 551–581.

Sharma, P., 1997, Environmental and engineering geophysics: Cambridge, Cambridge University Press, 475 p.

Shirey, S.B., and Walker, R.J., 1998, The Re-Os isotope system in cosmochemistry and high-temperature geochemistry: Annual Review of Earth and Planetary Sciences, v. 26, p. 423–500.

Singer, D.A., 1993, Basic concepts in three-part quantitative assessments of undiscovered mineral resources: Natural Resources Research, v. 2, p. 69–81.

Singer, D.A., 2007, Short-course introduction to quantitative mineral resource assessments: U.S. Geological Survey Open-File Report 2007–1434, 13 p.

Singer, P.C., and Stumm, W., 1970, Acidic mine drainage—The rate-determining step: Science, v. 167, no. 3921, p. 1121–1123.

Smith, K.S., 1999, Metal sorption on mineral surfaces—An overview with examples relating to mineral deposits, *in* Plumlee, G.S., and Logsdon, M.J., eds., The environmental geochemistry of mineral deposits—Part A, Processes, techniques, and health issues: Reviews in Economic Geology, v. 6A, p. 161–182.

Smyk, M., 2010, The ring of fire—An overview of the geology, mineral deposits, and exploration history of the McFaulds Lake area: Institute on Lake Superior Geology, Proceedings, v. 56, Part 1, p. 63.

Sobek, A.A., Schuller, W.A., Freeman, J.R., and Smith, R.M., 1978, Field and laboratory methods applicable to overburdens and mine soils: Cincinnati, Ohio, U.S. Environmental Protection Agency, Protection Technology, [report] EPA-600/2-78-054, 203 p.

Souch, B.E., Podolsky, T., and Geological Staff, The International Nickel Company of Canada, Limited, 1969, The sulfide ores of Sudbury—Their particular relationship to a distinctive inclusion-bearing facies of the nickel irruptive, *in* Wilson, H.D.B., ed., Magmatic ore deposits: Economic Geology, Monograph 4, p. 252–261.

Stekhin, A.I., 1994, Mineralogical and geochemical characteristics of the Cu-Ni ores of the Oktyabr'sky and Talnakh deposits, *in* Lightfoot, P.C., and Naldrett, A.J., eds., Sudbury–Noril'sk Symposium, Sudbury, Oct. 3–6, 1992, Proceedings: Ontario Ministry of Northern Development and Mines/Ontario Geological Survey, Special Publication 5, p. 217–230.

Stoffregen, R.E., Alpers, C.N., and Jambor, J.L., 2000, Alunite-jarosite crystallography, thermodynamics, and geochronology, *in* Alpers, C.N., Jambor, J.L., and Nordstrom, D.K., eds., Sulfate minerals—Crystallography, geochemistry, and environmental significance: Reviews in Mineralogy and Geochemistry, v. 40, p. 454–480.

Sun, S.-S., and McDonough, W.F., 1989, Chemical and isotopic systematics of oceanic basalts—Implications for mantle composition and processes, *in* Saunders, A.D., and Norry, M.J., eds., Magmatism in the ocean basins: Geological Society of London, Special Publication 42, p. 313–345.

Thériault, R., and Barnes, Sarah-Jane, 1998, Compositional variations in Cu-Ni-PGE sulfides of the Dunka Road deposit, Duluth Complex, Minnesota—The importance of combined assimilation and magmatic processes: Canadian Mineralogist, v., 36, p. 869–886.

Thompson, J.F.H., Barnes, S.-J., and Duke, J.M., 1984, The distribution of nickel and iron between olivine and magmatic sulfides in some natural assemblages: Canadian Mineralogist, v. 22, p. 55–66.

Torgashin, A.S., 1994, Mineralogical and geochemical characteristics of the Cu-Ni ores of the Oktyabr'sky and Talnakh deposits, *in* Lightfoot, P.C., and Naldrett, A.J., eds., Sudbury–Noril'sk Symposium, Sudbury, Oct. 3–6, 1992, Proceedings: Ontario Ministry of Northern Development and Mines/Ontario Geological Survey, Special Publication 5, p. 217–241.

Tran, A.B., Miller, S., Williams, D.J., Fines, P., and Wilson, G.W., 2003, Geochemical and mineralogical characterization of two contrasting waste rock dumps—The INAP [International Network for Acid Prevention] waste-rock dump characterisation project, *in* International Conference on Acid-Rock Drainage—Application and Sustainability of Technologies, 6th, Cairns, Queensland, July 12–18, 2003, Proceedings: Australian Institute of Mining and Metallurgy, p. 939–947.

Trude, K.J., 2004, Kinematic indicators for shallow level igneous intrusions from 3D seismic data—Evidence of flow direction and feeder location, *in* Davies, R.J., Cartwright, J.A., Stewart, S.A., Lappin, M., and Underhill, J.R., eds., 3D seismic technology—Application to the exploration of sedimentary basins: Geological Society of London, Memoir, v. 29, p. 209–217.

U.S. Environmental Protection Agency, 2006, National Recommended Water Quality Criteria, accessed April 3, 2014, at *http://www.epa.gov/scitech/swguidance/standards/criteria/current/index.cfm*.

U.S. Environmental Protection Agency, 2009, National Primary Drinking Water Regulations: EPA 816-F-09-004, accessed July 9, 2009, at *http://www.epa.gov/safewater/consumer/pdf/mcl.pdf*.

Walker, R.J., Morgan, J.W., Naldrett, A.J., Li, C., and Fassett, J.D., 1991, Re-Os isotopic systematics of Ni-Cu sulfide ores, Sudbury igneous complex, Ontario—Evidence for a major crustal component: Earth and Planetary Science Letters, v. 105, p. 416–429.

Walker, R.J., Morgan, J.W., Hanksi, E.J., and Simolkin, V.R., 1997, Re-Os systematics of Early Proterozoic ferropicrites, Pechenga Complex, northwestern Russia—Evidence for ancient ^{187}Os-enriched plumes: Geochimica et Cosmochimica Acta, v. 61, p. 3145–3160.

Walker, R.J., Morgan, J.W., Horan, M.F., Czmanske, G.K., Krogstad, E.J., Fedorenko, V.A., and Kunilov, V.E., 1994, Re-Os isotopic evidence for an enriched mantle source for the Noril'sk-type ore-bearing intrusions, Siberia: Geochimica et Cosmochimica Acta, v. 58, p. 4179–4197.

Wandke, Alfred, and Hoffman, Robert, 1924, A study of the Sudbury ore deposits: Economic Geology, v. 19, p. 169–204.

Wang, C.Y., and Zhou, M-F., 2006, Genesis of the Permian Baimazhai magmatic Ni-Cu-(PGE) sulfide deposit, Yunnan, SW China: Mineralium Deposita, v. 41, p. 771–783.

Ware, A., Cherry, J., and Ding, X., 2008, Geology of the Eagle project: Institute on Lake Superior Geology, Proceedings, v. 54, part 2, p. 87–114.

Wendlandt, R.F., 1982, Sulfur saturation of basalt and andesite melts at high pressures and temperatures: American Mineralogist, v. 67, p. 877–885.

White, W.W., III, Lapakko. K.A., and Cox, R.L., 1999, Static test methods most commonly used to predict acid-mine drainage—Practical guidelines for use and interpretation, *in* Plumlee, G.S., and Logsdon, M.J., eds., The environmental geochemistry of mineral deposits—Part A, Processes, techniques, and health issues: Reviews in Economic Geology, v. 6A, p. 325–338.

Williamson, M.A., Kirby, C.S., and Rimstidt, J.D., 2006, Iron dynamics in acid mine drainage, *in* Barnhisel, R.I., ed., International Conference on Acid Rock Drainage, 7th, St. Louis, Missouri, USA, May 26–30, 2006, Proceedings: Lexington, Kentucky, American Society of Mining and Reclamation, p. 2411–2423.

Woodall, Roy, and Travis, G.A., 1969, The Kambalda nickel deposits, Western Australia, *in* Jones, M.J., ed., Commonwealth Mining and Metallurgical Congress, 9th, London, May 5–24, 1969, Proceedings: London, Institution of Mining and Metallurgy, v. 2, p. 517–533.

Wooden, J.L., Czamanske, G.K., Bouse, R.M., Likhachev, A.P., Kunilov, V.E., and Lyul'ko, V., 1992, Pb isotope data indicate a complex mantle origin for the Noril'sk-Talknakh ores, Siberia: Economic Geology, v. 87, p. 1153–1165.

Wooden, J.L., Czamanske, G.K., Fedorenko, V.A., Arndt, N.T., Chauvel, C., Bouse, R.M., Ling, B.W., Knight, R.J., and Siems, D.F., 1993, Isotopic and trace-element constraints on mantle and crustal contributions to Siberian continental flood basalts, Noril'sk area, Siberia: Geochimica et Cosmochimica Acta, v. 57, p. 3677–3704.

World Health Organization, 2008, Guidelines for drinking-water quality–volume 1–recommendations (3rd ed.): Geneva, Switzerland, World Health Organization Press, accessesd July 9, 2009, at *http://www.who.int/water_sanitation_health/dwq/gdwq3rev/en/index.html.*

Yakovlev, A.S., Plekhanova, I.O., Kudryashov, S.V., and Aimaletdinov, R.A., 2008, Assessment and regulation of the ecological state of soils in the impact zone of mining and metallurgical enterprises of Norilsk Nickel Company: Eurasian Soil Science, v. 41, no. 6, p. 648–659.

Yang, S., Qu, W., Tian, Y. Chen, J., Yang, G., and Du, A., 2008, Origin of the inconsistent apparent Re-Os ages of the Jinchuan Ni-Cu sulfide ore deposit, China—Post-segregation diffusion of Os: Chemical Geology, v. 247, p. 401–418.

Yinggui, L., Hangxin, C., Xuedong, Y., and Waisheng, X., 1995, Geochemical exploration for concealed nickel-copper deposits: Journal of Geochemical Exploration, v. 55, p. 309–320.

Zhang, Mingjie, Kamo, S.L., Li, C., Hu, Peiqing, Ripley, E.M., 2010, Precise U–Pb zircon–baddeleyite age of the Jinchuan sulfide ore-bearing ultramafic intrusion, western China: Mineralium Deposita, v. 45, p. 3–9.

Zhang, Ming, O'Reilly, S.Y., Wang, K-L., Hronsky, Jon, and Griffin, W.L., 2008, Flood basalts and metallogeny—The lithospheric mantle connection: Earth-Science Reviews, v. 86, p. 145–174.

Zhang, X., Pirajno, F., Qin, D., Fan, Z., Liu, G., and Nian, H., 2006, Baimazhai, Yunnan Province, China—A hydrothermally modified magmatic nickel-copper-PGE sulfide deposit: International Geology Review, v. 48, p. 725–741.

Zientek, M.L., Likhachev, A.P., Kunilov, V.E., Barnes, Sarah-Jane, Meir, A.L., Carlson, R.R., Briggs, P.H., Fries, T.L., and Adrian, B.M., 1994, Cumulus processes and the composition of magmatic ore deposits—Examples from the Talnakh district, Russia, *in* Lightfoot, P.C., and Naldrett, A.J., eds., Sudbury–Noril'sk Symposium, Sudbury, Oct. 3–6, 1992, Proceedings: Ontario Ministry of Northern Development and Mines/Ontario Geological Survey, Special Volume 5, p. 373–392.

Zindler, Alan, and Hart, S.R., 1986, Chemical geodynamics: Annual Review of Earth and Planetary Sciences, v. 14, p. 493–571.

Publishing support provided by:
Denver Publishing Service Center

For more information concerning this publication, contact:
Center Director, USGS Central Mineral and Environmental Resources Science Center

Box 25046, Mail Stop 973
Denver, CO 80225
(303) 236-1562

Or visit the Central Mineral and Environmental Resources Science Center Web site at:
http://minerals.cr.usgs.gov/

ISSN 2328-0328 (online)
http://dx.doi.org/10.3133/sir20105070I